

Hydrodynamics of the Newark Bay/Kills System

The New Jersey Toxics Reduction Workplan for New York-New Jersey Harbor

Study I-E

April 2006

Prepared by:

**Robert J. Chant, Ph.D.
Institute of Marine and Coastal Studies
Rutgers University
New Brunswick, New Jersey 08904**

**Prepared for: New Jersey Department of Environmental Protection
Division of Science, Research and Technology
New Jersey Toxics Reduction Workplan for NY-NJ Harbor**

Participants

Joel A. Pecchioli, NJ Department of Environmental Protection
Scott Douglas, NJ Department of Transportation

Rutgers University

| | |
|--------------------|------------------|
| Dr. Scott Glenn | Dr. Robert Chant |
| Dr. Richard Styles | Chip Haldeman |
| Elias Hunter | Liz Creed |

Stevens Institute of Technology

| | |
|-------------------|--------------------|
| Dr. Michael Bruno | Dr. Kelly Rankin |
| Brian Fullerton | Anne Pence |
| Pat Burke | Bethany McClanahan |
| Rob Miskewitz | Dr. Tom Herrington |

EXECUTIVE SUMMARY

NJ Toxics Reduction Workplan for NY-NJ Harbor Study I-E Hydrodynamic Studies

SIT and Rutgers University Components

The Newark Bay Complex, which is part of New York-New Jersey Harbor, consists of Newark Bay, the Arthur Kill and Kill van Kull tidal straits, and the Passaic and Hackensack Rivers. The presence of toxic chemicals in water and sediments throughout the harbor estuary has resulted in reduced water quality, fisheries restrictions/advisories, reproductive impairments in some species, and general adverse impacts to the estuarine and coastal ecosystems. In addition, problems associated with the management of contaminated dredged material have resulted in uncertainty regarding planned construction and future maintenance of the maritime infrastructure that supports shipping in the Harbor.

The New Jersey Toxics Reduction Workplan for NY-NJ Harbor (NJTRWP) includes a series of studies designed to provide the NJ Department of Environmental Protection with the information it needs to identify sources of the toxic chemicals of concern, and to prioritize these sources for appropriate action. As part of the NJTRWP, a comprehensive hydrodynamic study was completed between the years 2000 and 2002 to begin to understand the effects of tidal, meteorological, and freshwater forces on circulation patterns in the system. This was by far the most comprehensive deployment of hydrodynamic monitoring equipment of this type ever to occur in this economically important and complex estuarine system.

Study I-E of the NJTRWP, undertaken by Stevens Institute of Technology (SIT) and Rutgers University, focuses on the analysis of the hydrodynamics data collected from long-term instrument moorings deployed in the harbor during 2000-2002. In addition, because the data collected was not continuous enough in time or space to gain a complete understanding of the

system, a three-dimensional hydrodynamic model of the area has been developed by SIT. The model of the Newark Bay Complex developed for this study replicates the available water elevation, salinity, and current velocity data. Thus, the model may be utilized with confidence, along with the NJTRWP data, to investigate the hydrodynamics of the system.

Circulation Patterns

Although it is difficult to define a “normal” pattern of circulation in the Newark Bay Complex, this study and several prior studies have indicated that the circulation responds in a **complex event-driven fashion** to a combination of influences, both short-lived (winds and freshwater inflow) and longer term (classic estuarine gravitational circulation). The end result is that the identification of a long-term average circulation pattern is difficult. In light of this finding, it is best to examine the responses of the Newark Bay Complex to each of the possible primary influences.

Gravitational Circulation

Within the navigation channel of Newark Bay, classic estuarine gravitational circulation occurs, with daily averaged currents (the current averaged over several tidal cycles) directed seaward near the surface and landward near the bottom. The same estuarine circulation pattern occurs in the Kill van Kull and the southern portion of the Arthur Kill. However, in these tidal straights this pattern is not as pronounced during periods with a large range in tidal height (e.g., Spring tides). Figure 1 illustrates this classic estuarine circulation pattern in NY-NJ Harbor.

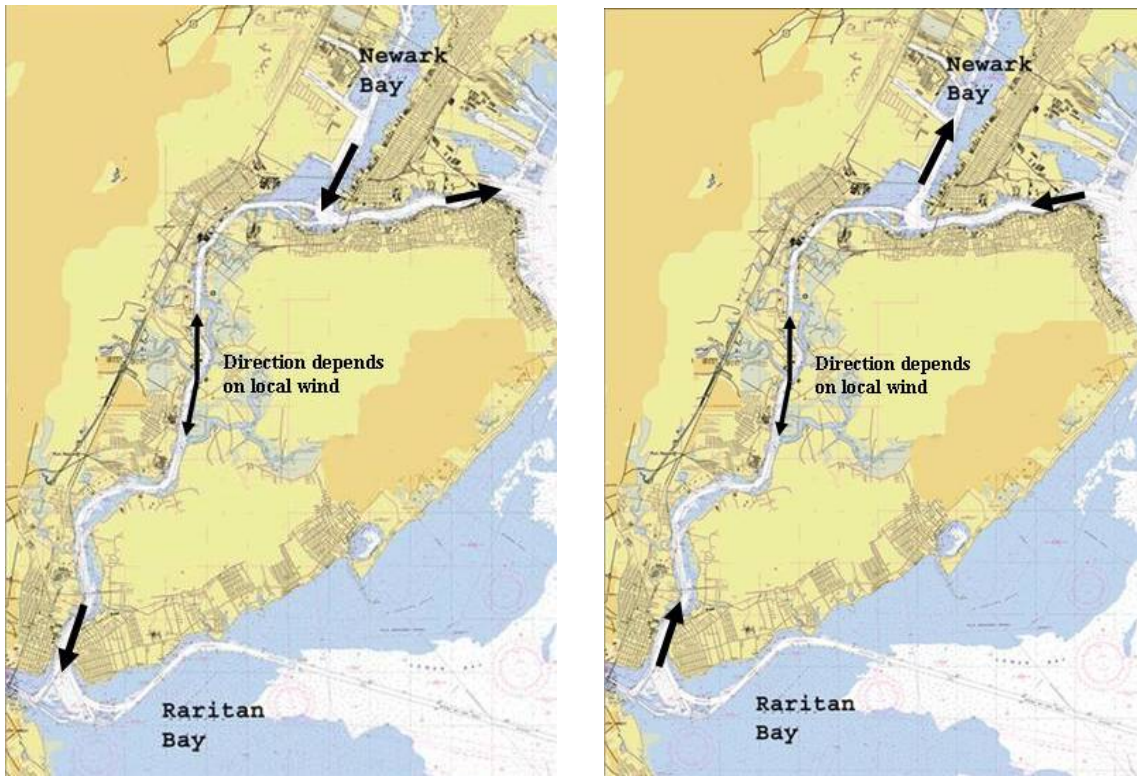


Figure 1: Daily Averaged Currents Associated with Estuary Gravitational Circulation, Near-Surface (left panel) and Near-Bottom (right panel).

The NJTRWP Study I-E data also suggests that while the mean depth-averaged flow in the main navigation channel of Newark Bay is landward, the net flow along the channel flanks is seaward.

This classic estuarine gravitational circulation pattern can be broken down – that is, the daily averaged currents become uniform throughout depth – during periods of very low freshwater discharge from the Passaic River. During these periods, the daily averaged currents in Newark Bay are directed largely landward (north) at all depths except near the surface.

An illustration of the effects of the competing influences of the tidal motion and gravitational circulation associated with the Passaic River freshwater inflow is shown in Figure 2, which presents the measured daily averaged currents at Newark Bay, the Kill van Kull and Perth Amboy during March, 2001. Days 66 to 68 were characterized as Spring Tide (large tidal range)

and very low freshwater inflow. Days 77 to 79 were characterized as Neap Tide (small tidal range) and high freshwater inflow. Days 87 to 89 were characterized as Spring Tide and moderately high freshwater inflow. During days 66 to 68, the daily averaged currents are nearly uniform throughout depth at all three locations, and are directed landward (north) in Newark Bay at all depths except very close to the water surface. By contrast, the periods during days 77 to 79 and 87 to 89, when the freshwater inflow was considerably higher, are characterized by daily averaged currents with considerable vertical variability: seaward directed currents in the upper layers and landward directed currents in the lower layers. The exception to this pattern is the Kill van Kull during days 87 to 89, which exhibited nearly uniform, seaward directed daily averaged currents. This is likely the result of very strong vertical mixing produced by the combination of the Spring Tide and the storm conditions that existed during this period. Thus, there is significant spring/neap tide variability in the vertical structure of the currents (and salinity), even during times of low Passaic River discharge.

Meteorological Events

Strong and persistent winds can have a major effect on water circulation in the Newark Bay Complex, and in the estuary as a whole. During periods of strong west winds acting synoptically over the New York Bight region (that is, including the coastal ocean area offshore of the harbor estuary), the water level in Raritan Bay is lowered, producing a strong pressure gradient from the Kills to the open ocean. Under this condition, the daily averaged currents are directed seaward (south) out of Newark Bay and through the Kill van Kull. During periods of strong east winds acting synoptically over the New York Bight region, the water level in Raritan Bay is raised, producing a strong pressure gradient from the open ocean toward the Kills. Under this condition, the daily averaged currents are directed landward in through the Kill van Kull and into Newark

Bay. The daily averaged currents in the Arthur Kill are strongly influenced by local (north/south) winds. The effects of these meteorological events are shown in Figure 3.

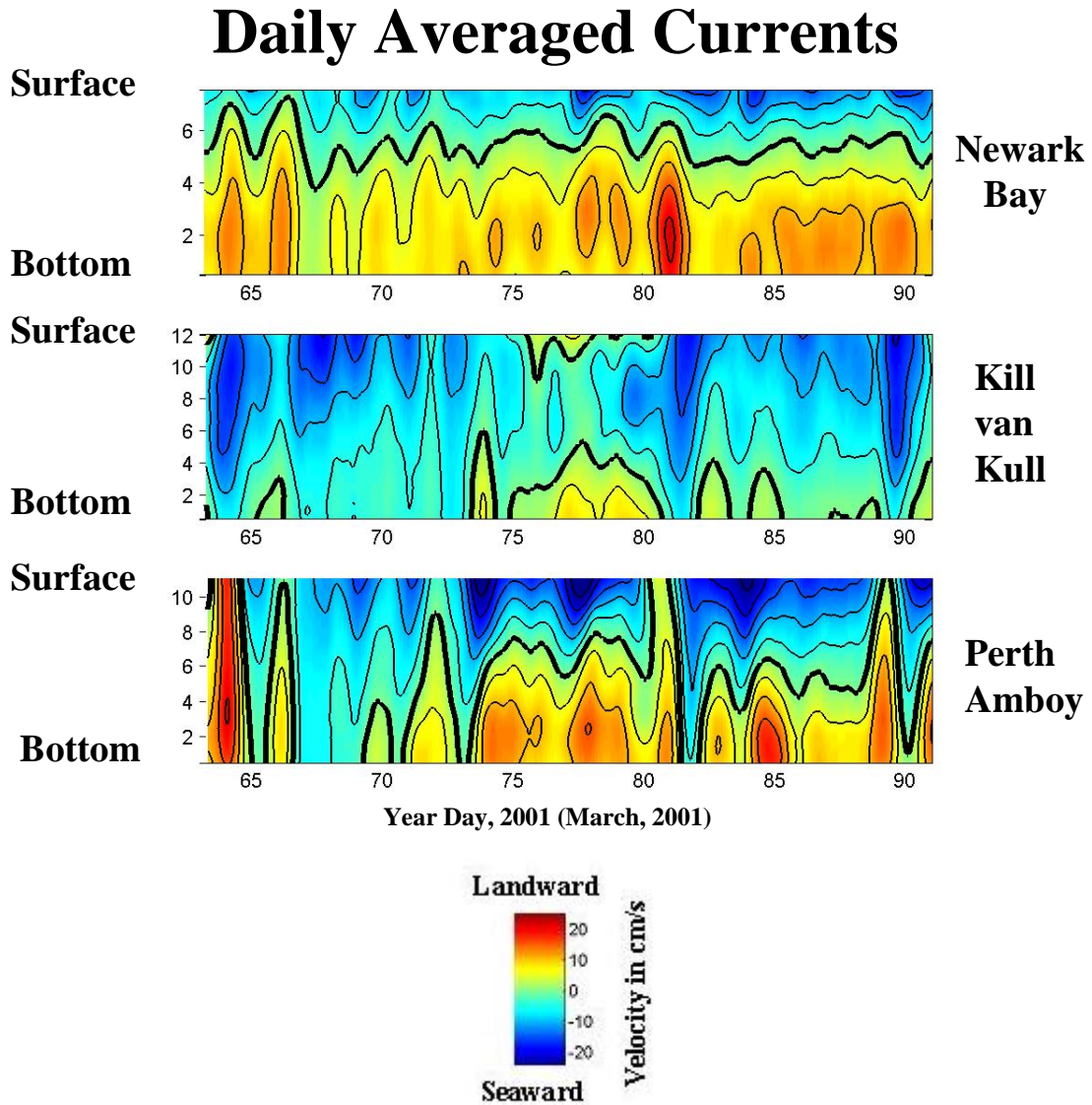


Figure 2: Daily Averaged Currents during March, 2001.

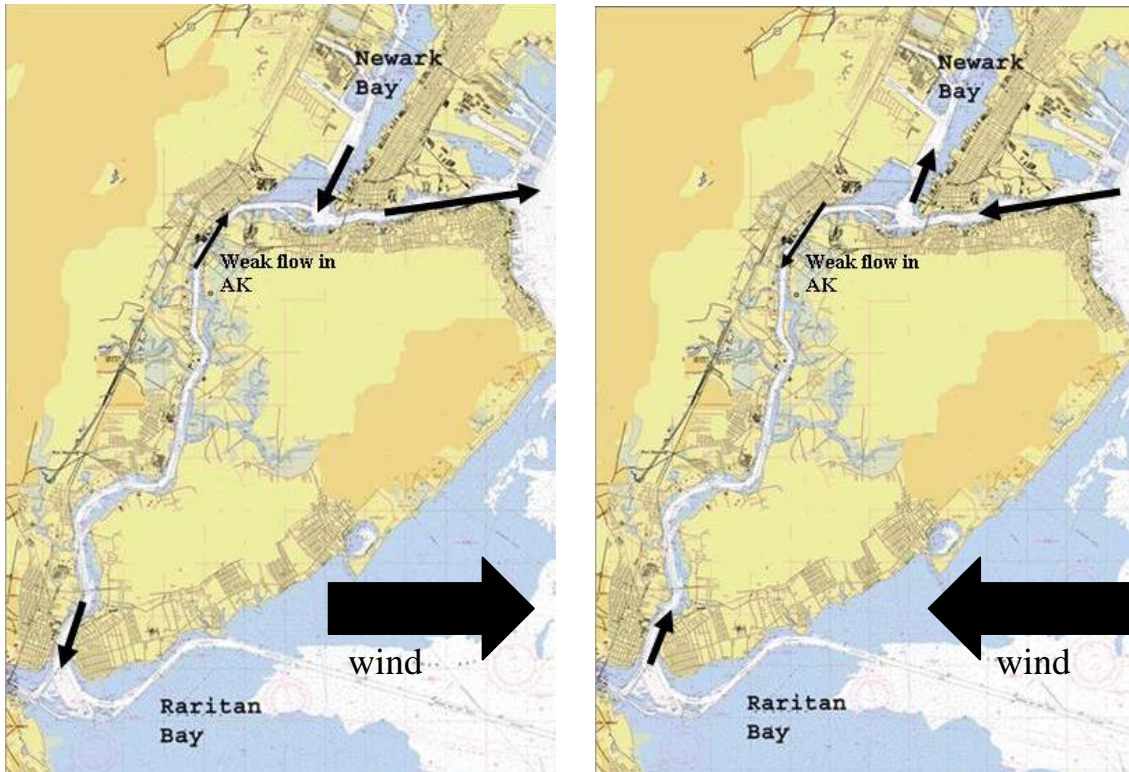


Figure 3: Tidal Residual Currents during Strong, Large-Scale Winds from the West (left panel) and the East (right panel).

Fate of Passaic River Suspended Sediment

Based on the NJTRWP Study I-E observations and the results from a simple sediment transport model developed by SIT, estuarine gravitational circulation plays a primary role in determining the fate of suspended sediment from the Passaic River. Large flow events from the Passaic River produce higher suspended sediment concentrations in Newark Bay. The fate of this suspended sediment load will depend on the settling rate of the suspended material. High discharge events increase both vertical stratification and the flow rate in the landward-flowing bottom layer in Newark Bay, and thus effectively trap material that rapidly settles to the lower layer. However, high flow events also increase the surface outflow and can transport slowly

settling material towards the Kill van Kull, where stronger tidal currents can easily carry this material into Upper New York Bay.

An initial estimate of the suspended sediment flux through the Kill van Kull completed by Rutgers University indicates that approximately 100,000 metric tons of suspended sediment (net) are transported from Upper New York Bay into Newark Bay each year. Finally, the partitioning of contaminants across sediment size and the settling velocity of the suspended sediment particles will significantly modify the fate and transport of contaminants in NY-NJ Harbor.

Effects of Navigation Channel Deepening

Computer model runs were performed by SIT to simulate future conditions in the Newark Bay Complex when navigation channels in the harbor are deepened to 50 feet. Deepening all of the navigation channels was shown to increase the tidal flux in the Arthur Kill and Kill van Kull by 17% and 2%, respectively. This may increase transport of sediment into (or out of) the system from Upper New York Bay and Raritan Bay. Tidal velocities would be reduced, which might result in increased sediment deposition in Newark Bay, and also limit the resuspension of sediment. Greater salt intrusion into the system could also result in the trapping of more sediment.

Summary and Main Findings

- **Circulation in the Newark Bay Complex responds to a combination of influences in a complex event-driven fashion, making the identification of a long-term average circulation pattern difficult.**
- **Within the navigation channel of Newark Bay, classic estuarine gravitational circulation occurs, with daily-averaged currents directed seaward near the surface and landward near the bottom. The same pattern also generally occurs in the Kill van Kull and lower Arthur Kill.**

- Larger Passaic River flows are associated with greater water column stratification and enhanced gravitational circulation. This produces higher daily averaged currents in the Newark Bay channel.
- This circulation pattern in Newark Bay can be broken down during periods of very low discharge from the Passaic River, such that daily averaged currents are largely directed landward throughout most of the water column.
- Persistent wind events can produce large “flow-through” flushing events in the Newark Bay Complex. During periods of strong, large-scale west winds over the region, the daily averaged currents are directed seaward out of Newark Bay and through the Kill van Kull. During periods of strong, large-scale east winds, the daily averaged currents are directed landward in through the Kill van Kull and into Newark Bay.
 - The daily averaged currents in the Arthur Kill are strongly influenced by local (north/south) winds.
- Large Passaic River flow events produce higher suspended sediment concentrations in Newark Bay. Such events also increase both vertical stratification and the current velocity in the landward-flowing bottom layer of the bay, and thus can trap material that rapidly settles to this layer. However, these events also increase the surface outflow and can transport slowly settling material towards the Kill van Kull, where stronger tidal currents can carry this material into Upper New York Bay. The fate of the suspended sediment will depend on the settling rate of the particles.
 - The partitioning of contaminants across sediment size and the settling velocity of the suspended sediment particles will significantly modify the fate and transport of contaminants in NY-NJ Harbor.
- An initial estimate of the suspended sediment flux through the Kill van Kull indicates that approximately 100,000 metric tons of suspended sediment (net) are transported from Upper New York Bay into Newark Bay each year.

Table of Contents

| | |
|---|-----------|
| Executive Summary | 2 |
| List of Figures | 11 |
| List of Tables | 12 |
| 1. Introduction | 13 |
| 2. Methods: Mooring Deployment | 15 |
| 3. Tributary River Flows | 17 |
| 4. Character of Raw Data and Analysis Techniques | 19 |
| 5. Tidal Motion | 20 |
| a) Sea Level | 20 |
| b) Depth Averaged Tidal Currents | 21 |
| c) Depth Dependent Tidal Motion | 23 |
| 6. Salinity | 25 |
| 7. Subtidal Circulation | 28 |
| 8. Meteorological Forcing | 30 |
| 9. Suspended Sediment | 33 |
| 10. Summary and Conclusions | 38 |
| 11. Suggested Future Work | 40 |
| 12. References | 41 |

List of Figures

- Figure 1** Schematic diagram depicting processes that drive estuarine sediment and contaminant transport.
- Figure 2a** Long-term mooring locations.
Figure 2b Mooring locations at Station KVK for 2000, 2001, and 2002.
- Figure 3** Mooring frame and instrumentation.
- Figure 4** Passaic River discharge and timing of mooring deployments.
- Figure 5** Discharge for the Passaic and Raritan Rivers.
- Figure 6a-e** Semidiurnal (M2) tidal ellipse for each mooring deployment.
- Figure 7a-e** Vertical structure of the semidiurnal tidal (M2) motion during spring and neap tides at each mooring location.
- Figure 8** Tidal range at Bergen Point during the mooring deployments for 2001 and 2002.
- Figure 9** Location of the turbidity maximum in the Arthur Kill.
- Figure 10** Near-bottom salinity at each mooring location and Passaic River discharge during 2001 and 2002.
- Figure 11** Near-bottom subtidal currents at each mooring location and Passaic River discharge during 2001 and 2002.
- Figure 12** Depth-dependent mean flow at Station NB1 for 2001 and 2002.
- Figure 13** Root mean square (rms) of subtidal velocity for all mooring deployments as a function of season.
- Figure 14a** Depth-averaged currents at Stations KVK and AK1 in 2002.
Figure 14b Depiction of depth-averaged currents in response to a north-westerly wind.
- Figure 15** Along channel currents and pressure at Station AK1 in 2002.
- Figure 16** Time-lagged correlation analysis between sea level change at Sandy Hook (dn/dt) and low frequency depth averaged flow at Stations PA1, AK1, and KVK1.

Figure 17 Scatter plot between measured SS and acoustic backscatter from the Sontek ADP; October 29, 2003 field calibration experiment.

Figure 18 Current speed and suspended sediment concentration during spring tide conditions at Station KVK1 during deployment 2 in 2002.

List of Tables

Table 1 Mooring Locations, time of deployment, and mean depths.

Table 2 Calculated tidal constituents at the mooring locations.

1. Introduction

The New York-New Jersey Harbor estuary system is of enormous and interdependent ecological and economic importance. However, the presence of toxic chemicals in the water and sediments results in reduced water quality, fisheries restrictions/advisories, reproductive impairments in some species, and general adverse impacts to the estuarine and coastal ecosystems. The Port of New York and New Jersey is the largest port on the East Coast of the United States and central to the economy of the region. However, problems associated with the management of contaminated dredged material, including high costs and the lack of suitable disposal/use alternatives, have resulted in uncertainty regarding planned construction and future maintenance of the maritime infrastructure that supports trans-ocean shipping in the harbor.

The New Jersey Toxics Reduction Workplan for NY-NJ Harbor (NJTRWP) includes a series of studies designed to provide the NJ Department of Environmental Protection (NJDEP) with the data and information it needs to meet the following primary objectives:

- to identify sources of the toxic chemicals of concern, and to prioritize these sources for appropriate action (management, regulatory, trackdown, clean-up).
- to identify selected contaminated sediments for future remediation and restoration activities.

NJTRWP Phase One Studies include monitoring studies of selected ambient water quality and suspended sediment parameters throughout various tributaries to the Newark Bay Complex, the Arthur Kill, and Raritan Bay (New Jersey Department of

Environmental Protection, 2001a). Consequently, it is important to characterize the processes that drive circulation and mixing in the Newark Bay/Kills System, with an emphasis on those processes that drive the exchange of dissolved and suspended matter between these systems and the coastal ocean. Figure 1 presents a schematic diagram that depicts the interaction between circulation and the transport of dissolved and suspended material, and the implications of these processes on contaminant transport.

This Project Report documents the methods, results, analyses, and conclusions of Study I-E (Rutgers University component) of the NJTRWP (New Jersey Department of Environmental Protection, 2001b), focusing on the hydrodynamics data collected from long-term (~30-day) instrument moorings implemented in NY-NJ Harbor during 2001 and 2002. A second report, prepared by Stevens Institute of Technology (SIT; Pence *et al.*, 2006), focuses on additional types of hydrodynamic measurements/data and modeling activities conducted as part of NJTRWP Study I-E (SIT component).

During the years 2000-2002 a series of mooring deployments were implemented in the Newark Bay/Kills system in order to characterize aspects of the tidal and subtidal flow, salinity, and the suspended sediment load. Tidal period motion occurs primarily at periods shorter than one day and is driven by the gravitational effects of the sun/earth/moon system. In Newark Bay, tidal period motion is dominated by the 12.42 hour semidiurnal (occurring twice a day) motion. Subtidal motion refers to motion at periods longer than one day, and is driven by both wind forcing in the estuary, and by wind forcing in the ocean that drives subtidal sea-level variability in the ocean (such as storm surges). This subtidal sea-level variability in the ocean propagates unattenuated

into estuaries such as the Newark Bay/Kills system. In the northeastern United States, subtidal motion is dominated by motion with periods in the 2-10 day range.

Previous work in the system has predominately been modeling efforts. Oey, Mellor and Hires (1985) developed the first hydrodynamic model of the region, but their focus was on the New York Bight Apex and the upper and lower harbor rather than the Newark Bay/Kills system. Blumberg *et al.* (1999) presented numerical simulations that suggested a counter-clockwise circulation around Staten Island that tended to drive fluid from Newark Bay out through the Arthur Kill. Analysis of 300 days of ADCP (acoustic Doppler current profile) data from the Kill van Kull by Chant (2002) was consistent with the findings of Blumberg *et al.* (1999). In contrast, tracer studies by Caplow *et al.* (2003) revealed that tidal pumping dominated the exchange between Newark Bay and Upper New York Bay, while dye studies by Richard Hires (personal communication) suggested that weak residual flows exist in the Arthur Kill. A more detailed discussion of previous studies can be found in Pence *et al.* (2006).

2. Methods: Mooring Deployment

Figures 2a and 2b show the locations where hydrodynamic monitoring equipment (i.e. “moorings”) were deployed, and Table 1 lists the timing of each mooring deployment. An initial “test” deployment occurred in June of 2000 in Newark Bay at Station NB1 only. All other deployments involved at least three moorings, with two of the moorings located at Stations NB1 and KVK1, and the third deployed in the Arthur Kill either at Station AK1 or Station PA1. In addition, there were two deployments at Station NB3 in 2001/2002. This is by far the most comprehensive deployment of

hydrodynamic monitoring equipment of this type ever to occur in this economically important and complex estuarine system.

A photograph of the equipment mooring frame with the hydrodynamic instrumentation is shown in Figure 3. Each equipment mooring contained strain gauge pressure sensors, a 1.5 kHz Sontek Acoustic Doppler Profiler (ADP), an optical backscatter sensor (model OBS3), a Seabird conductivity and temperature sensor (CT sensor SBE37si), and a Laser In-Situ Scattering and Transmissometry (LISST-100) instrument. The ADP measures vertical profiles of currents by transmitting and receiving acoustic pulses. The received signals, reflected off material suspended in the water column, is Doppler-shifted (changed in frequency) because the suspended material is moving with the current. Based on this Doppler shift, the ADP estimates the current speed. In addition, the intensity of the backscatter can be used as a proxy for the suspended sediment (SS) load, but this requires calibration with *in situ* SS samples. The OBS also provides estimates of suspended sediment through the backscatter of an optical signal. Like the ADP, it too needs to be calibrated with *in situ* SS samples. Unlike the ADP, which provides vertical profiles of SS, the OBS only provides estimates at a point in the water column. The CT sensor estimates salinity by measuring the temperature and the electrical conductivity of the water, from which salinity and density are estimated. Finally, the LISST provides estimates of the particle size distribution of material suspended in the water column by measuring the forward scattering of a laser as it is transmitted through the water. The forward scattering of the laser is measured by a series of concentric metal rings, from which algorithms provided by the manufacturer are used to estimate the particle size distribution.

This report focuses on measurements made by the current meters and CT sensors, with the objective of providing a benchmark for ongoing modeling studies in the harbor. Specifically, the analyses presented here provide estimates of the structure of the tidal and subtidal motion, as well as both qualitative and quantitative relationships between meteorological forcing and Passaic River discharge on the strength and nature of the subtidal flows in the Newark Bay/Kills System. Some aspects of the suspended sediment load, primarily based on the acoustic backscatter data from the ADP, were also investigated. Estimates of the suspended sediment load were based primarily on a calibration made in October 2003, when nearly 100 1-Liter pumped SS samples were taken while at anchor over a mooring at Station NB1 and profiling with the CTD/OBS and LISST instrument package. Together, this data and the following analyses provide targets to test the skill and quality of future hydrodynamic modeling studies of this system.

3. Tributary River Flows

Figure 4 depicts the locations and timing of the mooring deployments along with the discharge of the Passaic River (historically, discharge from the Hackensack River is over an order of magnitude smaller than the Passaic River, and thus it is not plotted in this figure). The discharge was moderately high during the two mooring deployments in 2001. After that, the region went into drought conditions that persisted for the second half of 2001 and throughout 2002. Dates for the mooring deployments are shown in Table 1.

Figure 5 shows the discharge for the Passaic (upper panel) and Raritan (lower panel) Rivers during 2001 and 2002 (blue and red lines, respectively), the mean flow for each day based on 100 years of data (thin black line), and the record high and low discharge for each day based on all available records for these rivers (gray envelope). While both of these rivers have similar discharge rates, it is the Passaic River that provides fresh water to the Newark Bay/Kills System, while the Raritan River provides fresh water to Raritan Bay. Discharge records for the Passaic River are continuous dating back to January 1, 1900. The record for the Raritan River begins on September 1, 1903, but contains a gap from 1909 to 1944. Mean discharge from the Raritan River over this period of record is 42.2 m³/sec, and the mean discharge for the Passaic River is 39.7 m³/sec. The largest discharge into the Raritan River occurred following Hurricane Floyd on September 17, 1999, with a daily mean discharge reported of 2,142 m³/sec. In the Passaic River, the maximum discharge occurred on October 10, 1903 during the “Great Flood of 1903”, with a mean discharge of 988 m³/sec.

Although one of the objectives of this study was to evaluate the potential effects of storm discharges on the mobility of sediment and contaminants, the study period coincided with a period of uncharacteristically low flow in both watersheds. The only time during the 2001 and 2002 mooring deployments that flow was above average in the Passaic River was during the first deployment in 2002 (initiated March 7, 2002). Otherwise, the discharge was always below daily mean flow rates. At no time during any of the mooring deployments did the Passaic River discharge ever approach a daily maximum. Thus, the results from this study are essentially a characterization of the hydrodynamics in the system during low flow conditions.

4. Character of Raw Data and Analysis Techniques

Raw data for the moored ADP, CTD, and OBS instruments were collected at 30 second intervals. The ADP transducers were located approximately 50 cm above the sea floor. The ADP collected data in 50-cm bins, with the center of the first bin approximately 0.75 meters above the transducer. The surface most reliable bin was located 85 percent of the local water column depth away from the instrument. The surface blanking interval existed because of interference with the side lobe of the acoustic beam, while the bottom blanking interval was due to ringing of the transducer following the transmission of the acoustic signal.

The data was screened for obvious outliers (defined as current speeds exceeding 3 m/sec) and averaged into 30 minute intervals. This screening removed a few data points with excessively high velocities that would have biased estimates of the mean values. Details of the criteria used for the velocity screening threshold had little impact on the 30 minute averages.

Once averaged, the tidal frequency motion was separated from the lower frequency subtidal period motion. This was done by applying a low-passed filter to the data using a Lancos window (Emery, 1998). The Lancos window had a cut-off period of 32 hours, and a half-window width of 51 hours. Both the tidal period and subtidal period motion were characterized in terms of their depth-averaged and depth-dependent structure, and these were characterized in terms of the tidal range, river flow, and meteorological forcing.

5. Tidal Motion

Tidal motion has been characterized for each mooring deployment by applying a least-squares fit to the tidal constituents for both the depth-averaged and depth-dependent tidal period motion. For the depth-averaged motion, the tidal ellipse characteristics are reported for the major diurnal (K1), semidiurnal (M2), and the first two over tides (the M4 and the M6; Knauss, 1996). The periods of these motions are 23.93 hours, 12.42 hours, 6.21 hours, and 3.1 hours, respectively. The tidal motion is described as a tidal ellipse with an amplitude of the major and minor axes, an orientation, and a phase. The phase is referenced to midnight on January 1, 2000. Currents and sea-level are phase-advanced (i.e. occur earlier) for smaller values of phase. A background description and discussion of these tidal constituents can be found in numerous physical oceanographic text books, such as Knauss (1996).

5a - Sea Level

Propagation of the M2 and K1 tidal constituents are apparent in both the sea-level and current meter data (see Table 2). Sea-level elevation is estimated with the pressure sensor data from the mooring records. High tide in the Kill van Kull at the semidiurnal frequency (M2) occurs 0.23 hours earlier than at Station NB1, indicating the propagation of the tidal motion from the KVK into Newark Bay. Phase for sea-level at the M2 tidal period at Perth Amboy (Station PA1) leads that in the upper Arthur Kill (Station AK1) by 0.73 hours. This is indicative of a northward propagation up the Arthur Kill at a speed of

approximately 22 km/h, which is nearly twice as fast as that predicted by a shallow water gravity wave (phase speed equals \sqrt{gh} , where g is acceleration due to gravity and h is the water depth.). While overtides are apparent at all of the sites, the ratio of the first two semidiurnal overtides (M4 and M6) to the M2 tidal constituent is less than 0.05 everywhere; the largest overtide is found at Station KVK1 where the M4/M2 ratio is 0.046. The phasing relationship between the M2 and M4 tidal constituents indicates that the Kill van Kull is slightly ebb-dominated, meaning that the time between high water and low water is longer than the time between low water and high water.

5b – Depth Averaged Tidal Currents

Tidal waves in estuaries can be classified as either purely progressive waves, standing waves, or a blend of the two. In a progressive wave, high tide and maximum current occur simultaneously, while in a standing wave slack current occurs at high and low water. In the latter case, we say that the current and sea level are in quadrature because their signals are a quarter of a period out of phase, with sea-level leading. In the case of the M2 tidal constituent, the tidal wave is purely standing when the current leads the sea level by 3.1 hours. Maximum current occurs at mid-tide, and slack water occurs at high tide.

Based on the observations made in this study, the tidal wave in NY-NJ Harbor is reasonably characterized as a standing wave (see Table 2) in the Kill van Kull and at both Newark Bay sites. In contrast to a progressive wave, standing waves do not drive a net transport of water. Consequently, the Stokes Drift in this system is relatively weak in the Kill van Kull and Newark Bay. However, since the length of the Kill van Kull is less

than the tidal excursion tidal currents will drive significant exchange between Newark Bay and New York Harbor. In contrast, the relationship between tidal sea-level and tidal currents varies in the Arthur Kill. At Station PA1 the maximum current occurs approximately 2 hours before high and low water, thus the tidal wave is closer to a standing wave than a progressive wave. At station AK1 sea-level and tidal currents are nearly in phase and this would be consistent with a progressive wave. However, since the phase propagation of sea-level and currents differ along the Arthur Kill, the tidal wave in this reach cannot be characterized by a standing or a progressive wave. Insights of the tidal dynamics in the Arthur Kill could be gained from existing numerical simulations or more detailed hydrographic measurements.

The M2 tidal ellipses for all of the mooring deployments are depicted on Figure 6(a-e). As expected, the tidal ellipses are highly rectilinear with the major axis oriented along the channel axis. At the Perth Amboy (Station PA1), Arthur Kill (Station AK1), and Newark Bay (Stations NB1 and NB3) sites there is little change in the tidal ellipse between the various mooring deployments. However, in the Kill van Kull, where the moorings had to be moved during the course of the study to avoid dredging operations (mooring deployments in 2001 occurred on the north side of the channel, while deployments were on the south side of the channel in 2002), there are significant variations in the ellipse structure (see Figure 6c). Stronger tidal currents are evident on the south side of the channel, and there is significant variation in the orientation of the tidal ellipse. With the possible exception of the September 4, 2001 deployment, the major axis of the M2 tidal ellipse is orientated with the nearby coastline. However, due to curvature in the channel, slight changes in the location of the mooring result in changes in

the orientation of the major axis. Furthermore, during ebb conditions, the flow entering the Kill van Kull must undergo significant curvature, and this can produce an eddying motion that will vary with tidal strength and stratification (Chant, 2002), and may also play a role in the deployment to deployment variability seen in Figure 6c.

5c - Depth Dependent Tidal Motion

Figure 7(a-e) presents the vertical structure of the semidiurnal motion from all of the mooring locations during neap and spring tide conditions. These estimates are made by a least-squares fit to the M2 tidal constituent for all available data. Furthermore, the data were divided into spring tide and neap tide conditions based on the tidal range at Bergen Point (see Figure 8). Neap tide is defined as those times when the tidal range is less than the mean tidal range, which is approximately 1.5 meters. Spring tide is defined as those times when the tidal range exceeds 1.5 meters.

At all of the mooring locations tidal currents are greater at the surface and exhibit strong vertical structure. Tidal currents are strongest at the KVK site, where surface currents during spring tides exceed 70 cm/sec. However, note that this estimate of tidal current amplitude is based on mooring deployments that occurred on both sides of the channel; peak surface tidal currents on the southern side of the channel during spring tides exceed 70 cm/sec, while those on the northern side will be less, as depicted by the depth-averaged tidal ellipses shown in Figure 6c. The phase of the tidal motion in the Kill Van Kull exhibits very little vertical structure, with no apparent phase difference during spring tides and a mere 0.1 hour phase advance at the bottom of the water column during neap tides.

Strong tidal currents are also apparent in the constricted channels at the Station AK1 and PA locations, where maximum tidal currents during spring tides are 55-60 cm/sec. As in the Kill van Kull, tidal period motion at Station AK1 exhibits only a small phase shift in the vertical, with bottom currents phase-advanced by 0.1 hours during neap tides and a nearly uniform phase during spring tides. Interestingly, however, tidal currents are phase-lagged at Station AK1 relative to Station KVK by approximately 2.0 hours, meaning that tidal currents begin flooding (or ebbing) in the Kill van Kull about 2 hours before they begin flooding (or ebbing) at Station AK1. At the Perth Amboy station, tidal current amplitude is similar to those at Station AK1, but there is significantly more vertical structure to the phase of the tidal currents. During neap tides, tidal currents at the bottom of the water column are advanced by over 1 hour relative to those at the surface. This is suggestive of greater water column stratification at Station PA1 compared to Stations KVK1 or AK1. In addition, this is consistent with CTD sections/transects taken along the length of the Arthur Kill that show a salt wedge that often penetrates northward from Perth Amboy up to the point where the channel makes a 90-degree turn in the vicinity of Fresh Kills (Figure 9). Tidal currents at Station PA1 are also phase advanced by approximately 2 hours from those at Station AK1, indicative of the propagation of the tidal wave up the Arthur Kill. Interestingly, while tidal currents exhibit a lag of 2 hours across the length of the Arthur Kill, with the tide turning first at Station PA1, sea-level only exhibits a 0.75 hour variation. This suggests that the tidal wave in the Arthur Kill cannot be simply characterized by a single northward propagating progressive wave.

At the Newark Bay sites, tidal currents are weaker and show a phase lag from those in the Kill van Kull, with peak currents at Stations NB3 and NB1 occurring

approximately 0.75 hours and 1 hour after peak currents in the KVK, respectively. Tidal currents are slightly stronger at Station NB1 relative to Station NB3, presumably due to the shoaling channel at Station NB1. Station NB1 also exhibits more vertical structure in phase than Station NB3, with bottom currents advanced by 0.5 hours during neap tides. This increase in vertical phase structure at Station NB1 is attributed to higher water column stratification at this site due to proximity to the Passaic River discharge.

6. Salinity

All salinity records from the 2001 and 2002 mooring deployments are plotted in Figure 10, along with discharge data for the Passaic River for these years. This figure emphasizes the inter-annual variability in river discharge between the two years, with 2001 showing approximately a one-month period of higher river discharge (greater than $100 \text{ m}^3/\text{sec}$). In contrast, the Passaic River discharge during 2002 was nearly zero during the entire period of the mooring deployments, with the exception of a weak discharge towards the end of the 2002 deployments (days 115 – 125).

Figure 10 (upper panel) depicts the 2001 near-bottom salinity at Stations PA1 (blue line), KVK1 (red line), and NB1 (black line), along with the Passaic River discharge (thick black line). Salinity during the deployments varied from a maximum exceeding 25 psu in the Kills to a minimum of less than 10 psu at Station NB1. The figure also emphasizes the quick response of the salt field to changes in Passaic River flow, particularly at Station NB1. This is most evident during the first 2001 deployment (initiated March 2, 2001) when the Passaic River discharge peaks at $150 \text{ m}^3/\text{sec}$ on day 80. Nearly coincident with this increased river flow is a drop in salinity at all three sites.

Also note the rise in salinity throughout the system as the Passaic River discharge drops off following day 100 in 2001. River discharge is low throughout the entire period of mooring deployments in 2002 (Figure 10, lower panel), and consequently salinity is significantly higher during 2002 compared to 2001.

The salinity record also shows evidence of clogging of the conductivity sensor; for example, see the Station KVK1 salinity line in 2001 after day 77 (Figure 10, upper panel). However, while it is obvious that tidal period salinity fluctuations are lost while the cell is clogged, it appears that the lower frequency salinity fluctuations are often captured. An exception to this is the second Station NB1 deployment of 2001 (initiated April 9, 2001), where salinity values became “pegged” after day 105. Clogging of the conductivity cell appears to have also occurred at Station NB1 between days 98 and 129 in 2001, and days 78-93, and 117-128 in 2002.

The largest Passaic River discharge events of the mooring deployment records occurred during the first and second deployments in 2001 (initiated March 2 and April 9, 2001). During these deployments, salinity at the bottom of the water column at Station NB1 became less than 10 psu, and dropped to nearly 10 psu at Station KVK1 during late ebb. Salinity at Perth Amboy was less responsive to the Passaic River discharge, but there is a clear dip in salinity during the peaks of Passaic River flow. However, this may also be due to coincident increases in the discharge from the Raritan River, which enters Raritan Bay a few kilometers south of Station PA1.

Time series of salinity during the drought of 2002 are plotted for Stations NB1 (black line), NB3 (green line), KVK1 (red line), and AK1 (blue line) in Figure 10 (lower panel). Salinity is higher during 2002 compared to 2001. Minimum salinity at Station

KVK1 during the 2002 deployments was over 22 psu, and maximum salinities exceeded 27 psu. In contrast, salinities at the KVK site in 2001 were as low as 11 psu and only exceeded 25 psu during the extreme neap tides around days 108 and 138 (see the upper panel of Figure 10). However, despite a persistent lack of Passaic River flow, there is low frequency variability to the salinity signal in 2002. Higher near-bottom salinities are evident during neap tides, which for the 2002 mooring deployments occur around days 68, 80, 95 and 110 (see Figure 8). This suggests that even during times of low Passaic River flow the estuary goes through neap/spring transitions, with the intrusion of saline water into the estuary during neap tides (when water column stratification presumably increases), and a decrease in near-bottom salinity during spring tides (when the water column becomes well-mixed). Spring-to-neap variations in vertical current shear in the Kill van Kull during both high and low Passaic river flow conditions have been previously reported by Chant (2002).

The spring/neap variability in near bottom salinity is consistent with the behavior of the salinity record at Stations NB1 and KVK1 in 2001 following the peak in Passaic River discharge, when the salinity rose rapidly as river discharge monotonically declined following day 100 (see upper panel of Figure 10). The peak in near bottom salinity at Stations NB1, KVK1, and PA1 again corresponds to neap tide conditions (see Figure 8), and suggests that salt water intrudes into the Newark Bay system under reduced tidal forcing during neap tides. This behavior has been observed in many other estuarine systems (Geyer *et al.*, 2000).

7. Subtidal Circulation

While tidal currents clearly dominate the current meter records and typically are an order of magnitude larger than the lower frequency subtidal flows, it is often the subtidal circulation that dominates the transport processes because of its persistence. Subtidal flows can be driven by gravitational circulation, local or remote meteorological forcing , or by non-linear tidal dynamics (Friedrichs and Hamrick, 1996).

Time series of near-bottom subtidal motion for all of the moorings deployments for 2001 and 2002 are plotted in Figure 11. Note that this low frequency motion represents the combined effects of tidally, gravitationally, and meteorologically forced motion. Nevertheless, we are able to isolate the relative importance of each. The higher frequency component of the sub-tidal motion apparent in Figure 11 occurs at the 2-5 day period and is driven by meteorological forcing. This is discussed in Section 8 of this report (“Meteorological Forcing”), together with the analysis of the depth-averaged subtidal motion.

At Station NB1, near-bottom subtidal velocities (thin black lines on Figure 11) are almost always directed northward/upstream, though there is a clear reduction in the subtidal velocity during the low discharge period in 2002. During 2001, near-bottom velocities are typically 5-10 cm/sec (upper panel of Figure 11), whereas in 2002 near-bottom velocities typically are 0-5 cm/sec (lower panel of Figure 11). Nevertheless, even during the low flow period in 2002, near-bottom velocities at Station NB1 are directed upstream. With the single exception of the March/April deployment during 2002 (days 100-108 and 115-119), the residual velocity at Station NB1 at all depths is to the north.

The persistent upstream velocity at Station NB1 is also apparent in the depth dependent mean flow for all of the mooring deployments at Station NB1 (see Figure 12).

While the vertical current shear is consistent with the density driven circulation, the mean velocity at the surface also tends to be upstream. Since the cross-sectional transport must be equal to the river flow - which is directed downstream - the observation that the mean flow at Station NB1 is directed upstream suggests that the flow over the navigation channel flanks is directed downstream. This inferred lateral structure to the flow - with inflow over the deep navigation channel and outflow over the shallow flanks - is consistent with the observations and theories presented by Friedrichs and Valle-Levinson (1998), and others. In addition, note that the annual mean Passaic River flow of $\sim 60 \text{ m}^3/\text{sec}$ would result in a cross-sectionally averaged outflow of approximately 1-2 cm/sec in Newark Bay.

During 2001, the near-bottom inflow at Station PA1 is of similar magnitude to that at Station NB1 (see the upper panel of Figure 11). Unfortunately, the failure of the current meter mooring during the second Station PA1 2002 deployment (days 100-125) precludes comparison with the second Station NB1 2002 deployment.

Weaker near-bottom flows are evident at Station KVK1 (red line) and Station PA1 (blue line) during 2002 (lower panel of Figure 11). This is likely due to the destruction of the two-layer flow by increased mixing caused by the enhanced tidal velocities within the tidal straights at these locations. However, during neap tides there is a clear increase in the near bottom flow at Station KVK1, such as on days 70-80 and 130-140 in 2001, and days 65-70, 95-100, and 110-115 in 2002. These inflows are coincident with the increased salinities observed at Stations KVK1 and NB3 (see Figure 10),

suggesting that increased salinities in Newark Bay have their source in Upper New York Bay.

At Station PA1 near-bottom salinity increases during neap tides following the reduction in Passaic River flow on day 100 in 2001. Similarly high salinities are observed at Station PA1 during neap tide conditions on day 135 in 2001. However, there is no evidence of increased salinities during neap tides at the Station AK1 site for any of the 2002 deployments (see Figure 10). This suggests that the neap tide salt intrusion into the Arthur Kill does not penetrate the entire length of this tidal straight. This is consistent with shipboard CTD sections/transects taken along the length of the Arthur Kill that show a salt front that penetrates from Perth Amboy into the Arthur Kill, but only up to the channel bends in the vicinity of the Fresh Kills landfill (Figure 9). It is likely that the sharp bends in the channel at this location drives strong mixing and arrests the advancement of the salt wedge (Seim and Greg, 1997).

The strong near-bottom southerly flows at Station AK1 on days 68 and 82 in 2002 (see lower panel of Figure 11) are associated with strong westerly winds that set down sea-level in the coastal ocean. Section 8 (“Meteorological Forcing”) discusses the correlation between wind forcing and circulation, and the variability within the system.

8. Meteorological Forcing

Oscillations in currents at periods of 2-5 days are apparent in all of the mooring deployments and stations in both the depth-averaged and depth-dependent motion. Estimates of the root mean square (rms) of the subtidal flow for the depth-averaged flows

for each mooring deployment are shown in Figure 13, and show a clear seasonal and spatial trend. Here the rms is calculated as $rms = \frac{1}{n} \sum_1^n v_s^2$, where v_s is the subtidal along channel velocity, and n is the number of subtidal current estimates. The rms is a measure of the energy in the subtidal flow. Energy is enhanced during the winter months, when wind forcing is stronger, and energy tends to be higher at the moorings in the Arthur Kill and Kill van Kull compared to currents in Newark Bay.

Time series of depth-averaged currents at Stations AK1 and KVK1 in 2002 (Figure 14a) show that there is a tendency for these meteorologically-induced flows to be characterized as a “through-flow” with circulation around Staten Island: inflow to (outflow from) the Kill van Kull is accompanied by an outflow (inflow) through the Arthur Kill. This is in contrast to a pumping mode of circulation whereby Newark Bay would be filled (emptied) by a simultaneous inflow (outflow) in both the Kill van Kull and Arthur Kill.

The most pronounced through-flow events occur during strong westerly/northwesterly winds (see Figure 14b) when sea level is depressed in the coastal ocean. Sea level set down is more pronounced at Perth Amboy due to the local effect of the wind on shallow Raritan Bay. This produces a pressure gradient whereby the sea-level slopes downward from New York Bay to Perth Amboy during strong westerly winds. This pressure gradient drives a pronounced through-flow circulation that can overcome tidal motion at Station PA1, such as depicted in the depth-averaged flows at Station AK1 during the first deployment in 2002 (initiated March 7, 2002; upper panel of Figure 15). During days 68-70 and 80-82 strong westerly winds set-down coastal sea

level (lower panel of Figure 15) and depth-averaged currents at Station AK1 ebb continuously for over 24 hours (upper panel of Figure 15).

Time-lagged cross-correlation analysis for depth-averaged along-channel currents at Stations KVK1, AK1 and PA1 (Figure 16) found a high correlation between depth averaged flows in the tidal straights and the rate of low frequency sea level change $\partial\eta/\partial t$ (where η is low passed sea level and t is time). In this analysis the time lag between the forcing (sea level or winds) and the response (currents) is determined by the time-lag that produces the largest correlation coefficient. Since the forcing must precede the response we reject lags that indicate currents leading the forcing. The correlation is positive at Stations AK1 and PA1, and negative at Station KVK1. This indicates that when sea level rises there is a flow into the Arthur Kill and out of the Kill van Kull, while as sea level falls the circulation is into the Kill van Kull and out of the Arthur Kill. For all mooring deployments the depth-averaged flow at both Stations PA1 and AK1 is positively correlated with rising sea-level at Sandy Hook, with a maximum correlation coefficient (r) between 0.7 and 0.8 at a lag of 5 hours. This means when sea-level begins to rise at Sandy Hook, 5 hours later an inflow begins in the Arthur Kill. In contrast, the depth-averaged flows in the Kill van Kull are negatively correlated with sea-level variability, but with a lower correlation coefficient ($r = -0.4$) and a longer lag time (~ 18 hours). Given the low correlation and long lag between flows in the KVK and sea-level it is unclear to what extent low frequency flows in the KVK are driven by remotely forced sea-level.

It is proposed that the longer lag time in the Kill van Kull is due to the fact that the local wind forcing in the Kill van Kull tends to oppose the pressure-gradient driven flows. Sub-tidal sea-level in the New York Bight responds to winds that blow along the axis of Long Island (Wong, 1994), with westerly winds tending to drop sea-level and easterly winds tending to raise sea-level. Because sea-level drops more rapidly in the shallow Raritan Bay than in the Upper New York Bay this drives flow into the Kill van Kull that is against the local wind forcing that drives fluid to the east and out of the Kill van Kull. Consequently, local wind forcing in the Kill van Kull competes with the pressure gradient driven flow. In contrast, the Arthur Kill is primarily orientated north/south and thus normal to the wind forcing. This would explain both the decreased correlation and increased time-lag between sea level and currents in the Kill van Kull relative to the Arthur Kill.

9. Suspended Sediment

The field work for this project involved the calibration of the ADP backscatter data with suspended sediment concentrations in the water column. This calibration was performed on October 29, 2003. The calibration process involved deploying the standard Newark Bay mooring at Station NB1 on October 28, and performing an 8-hour anchor station over the mooring on October 29, during which time approximately 100 1-Liter water samples were collected while profiling with a CTD/LISST/OBS package. Water samples were taken from the surface to the bottom at 2-meter intervals, with CTD/LISST/OBS profiles taken approximately every 15 minutes.

The objective of this calibration work was to relate the acoustic backscatter from the ADP to suspended sediment (SS) concentrations (mg/L). Since the ADP also reports current velocity at the same location that the SS estimates are made, it is simple use the ADP profiles of acoustic backscatter and current velocity to calculate estimates of sediment flux.

Figure 17 presents the results of the calibration. Note that because the acoustic backscatter is reported in decibels, a logarithmic scale, we plot the acoustic backscatter against the SS on a logarithmic scale to linearize the relationship. These results are very encouraging, showing a clear trend of increasing SS with increasing acoustic backscatter ($r^2 = 0.77$). The slope of the line is 0.10252 and the y-intercept is -4.7 . Since this is plotted on a logarithmic scale there is more scatter for the low values of SS because, for example, a 2 mg/L error in the estimate of SS produces more scatter in the 5 mg/L range than in the 30 mg/L range. Therefore, with this calibration, SS is estimated based on the ABS backscatter data by the following equation:

$$SS = e^{0.10252 * abs - 4.7}$$

Based on this calibration, estimates of the suspended sediment load in the water column can be made. For example, the average SS concentrations was calculated as a function of depth and tidal phase for spring tide conditions during the first 2002 mooring deployment in the Kill Van Kull (initiated March 7, 2002; Figure 18). Despite similar near bottom tidal current speeds on the flood and ebb tides, there is a clear tidal asymmetry in the suspended load. Suspended sediment exceeds 20 mg/L in the bottom

third of the water column during the flood tide, while during the ebb tide SS tends to be 15 mg/L or less in the lower third of the water column. Thus, although sediments are transported in both directions through the Kill Van Kull, this results in a net transport of sediment into the Newark Bay complex from Upper New York Bay. In fact, for both mooring deployments during the drought in 2002, there was significant transport of sediment into Newark Bay.

We calculated the sediment transport flux (stf) through the KVK as:

$$\text{stf}(t) = W \sum_1^{n(t)} v(z, t) * \text{tss}(z, t) * dz$$

where v is the along channel velocity, tss is the suspended sediment concentration obtained with the acoustic backscatter from the ADP, n is the number of velocity bins, W is the width of the Kill van Kull (380 m) and dz is the bin size of the ADP measurements. Note that n is time dependent because the number of good bins varies over the tidal cycle due to the changing water column depth.

During the first deployment in 2002 (initiated March 7, 2002) the daily net sediment transport into Newark Bay from the Kill van Kull was 344 metric tons, while for the second deployment (initiated April 5, 2002), it was 547 metric tons per day. Note that these estimates are crude because they assume that there is no variability in the cross-section of the Kill van Kull. Nevertheless, these values correspond to 120,000 metric tons/year and 200,000 metric tons/year, respectively, of sediment that flows from Upper New York Bay into Newark Bay. This value is of the order of the discrepancy between the amount of sediment supplied to Newark Bay by the Passaic River (30,000 metric

tons) and the 100,000-150,000 metric tons that is dredged from the system each year (Lowe *et al.*, 2005).

However, during the mooring deployments in 2001 there was essentially no net transport of suspended sediment, with a mean value of 33 metric tons a day flowing from Newark Bay into Upper New York Bay during the first deployment (day 60-92) and 96 metric tons per day flowing from the Upper New York Bay into Newark Bay during the second 2001 deployment (day 95-125). There appear to be two possible explanations for this. The first is that it could represent lateral variability, with the transport of suspended sediment primarily occurring on the southern side of the channel. If this were the case the cross-sectionally averaged transport of suspended sediment into Newark Bay would be somewhat reduced from the estimates made during 2002, but would still likely be in the range of the flux needed to balance the dredging records.

A second possibility is that the difference between the sediment flux in the 2001 and 2002 deployments may represent temporal variability associated with changing river flow. Under this scenario, during the time of high Passaic River flow (as was the case during most of the 2001 mooring deployments), the outward transport of Passaic River suspended sediment is equal to the inflow of sediment from the Upper New York Bay. This results in a weak net sediment flux out of Newark Bay (note, however, that this does not mean that there may not be a net flux of some particulate contaminants, because it is likely that the suspended sediment flowing from Newark Bay is more contaminated than that in the Upper New York Bay). In contrast, when the Passaic River discharge is low and supplies little sediment to the system, the transport of sediment is primarily from Upper New York Bay into Newark Bay. This scenario would also result in a reduced

annual mean transport of suspended sediment, as inferred from the 2002 mooring data. However, if the reduction of net suspended sediment transport is limited to the times of high Passaic River discharge, which occurs about 25% of the time, the estimates from 2002 would also only be reduced by approximately 25%. In either case, however, we suggest that there is an annual mean net suspended sediment flux on the order of 100,000 metric tons per year from Upper New York Bay into Newark Bay.

Similar estimates made at Station AK1 during the 2002 deployment indicate a weak flow of suspended sediments out of Newark Bay and into the Arthur Kill. However, the magnitudes of these estimates are significantly smaller and probably not statistically different than zero. Thus, it is concluded that the Kill van Kull represents the major pathway of sediment transport into Newark Bay.

The upper Hudson River dominates the input of sediment into Upper New York Bay, with a loading of approximately one million metric tons per year (Geyer *et al.*, 2001). During the spring, most of this sediment is temporarily stored in the lower Hudson River and Upper New York Bay, in the vicinity of the Kill van Kull. The estimates made in this study of the annual mean transport of sediment through the Kill van Kull require that approximately 10 percent of this sediment be deposited in Newark Bay. This fraction does not seem unreasonable given the cross-channel section of the KVK compared to the cross-channel areas of other pathways, such as the East River, the Hudson River, and the Verrazano Narrows.

10. Summary and Conclusions

Using long-term mooring data, various aspects of the circulation patterns and suspended sediment transport in the Newark Bay-Kills system have been characterized. These moored observations are by far the most extensive made to date in this economically important estuary.

Detailed characterizations of the tidal motion have shown that **there is significant spring/neap tide variability in the vertical structure of the semidiurnal motion, even during times of low Passaic River discharge.** The vertical structure was strongest where salinity stratification is strongest, at Stations NB1 (Upper Newark Bay) and PA1 (lower Arthur Kill), and weakest at Stations KVK1 (western Kill van Kull) and AK1 (upper Arthur Kill), where strong tidal currents appear to provide sufficient energy to mix the water column during these low flow conditions.

Salinity is seen to respond rapidly to the Passaic River discharge and to the spring/neap tidal cycle. The response is evident in Newark Bay and the Kills. Spring/neap tidal variability is evident at Stations KVK1 and NB3 (lower Newark Bay), even during times of low Passaic River flow. This was most evident during the second 2002 deployment (days 95-125) when the salinity at Stations KVK1 and NB3 rose significantly during the neap tide on days 95 and 110. This suggests that the well documented spring/neap tidal variability in New York Harbor (Geyer *et al.*, 2000) penetrates into Newark Bay through the Kills system. Thus, to accurately model this system, the spring/neap tidal variability in salinity in New York Harbor must be accounted for in the model.

Subtidal flow exhibited a persistent northerly flow in the main navigational channel in Newark Bay. This northward flow was strongest at the bottom of the water column, consistent with gravitational circulation, but also contained a significant depth averaged component. **This is suggestive of a mean depth-averaged inflow in the main navigation channel in Newark Bay, and an outflow along the channel flanks.** This flow structure is consistent with theory and observations in other systems (Friedrichs *et al.*, 1992). The vertical structure of subtidal flows was most pronounced at Stations NB1 and PA1, and weakest at Stations KVK1 and AK1, showing the same spatial structure as the tidal period motion.

Strong depth-averaged subtidal flows were evident in the Kills. These flows were characterized by a flow-through mode, with the flow entering (leaving) the southern Arthur Kill while it is leaving (entering) the eastern Kill van Kull. This flow pattern is most pronounced when sea level drops in response to north-westerly winds. This condition drives a strong southerly flow through the Arthur Kill that at times can overcome tidal period motion, resulting in depth-averaged currents that ebb continuously for several tidal cycles. Depth-averaged flows in the Kills have the highest correlation with sea-level, suggesting that they are driven by remote meteorological forcing.

Finally, calibration of ADP acoustic backscatter data with SS data suggests that the ADPs can be used to estimate suspended sediment fluxes. **An initial estimate of suspended sediment flux through the Kill van Kull using this method indicates that approximately 100,000 metric tons of suspended sediment (net) are transported**

from Upper New York Bay into Newark Bay each year. The Kill van Kull represents the major pathway of sediment transport into Newark Bay.

11. Suggested Future Work

A shortcoming of the 2001-2002 field effort was that it occurred largely during drought conditions. In order to fully characterize the hydrodynamics of this system, there needs to be additional mooring deployments during high flow Passaic River conditions. Future mooring deployments must also include measurements of surface salinity.

More detailed estimates of sediment fluxes should be made in the Kill van Kull, Newark Bay, and the Arthur Kill. This would require extensive calibration of ADP acoustic backscatter data with water column suspended sediment samples. Furthermore, high temporal resolution water column chemical samples should also be taken to develop relationships between the character of suspended matter and the contaminant load. While the comprehensive chemical analyses completed during Phase One of the NJTRWP that included the full spectrum of organic contaminants are not needed, a closer coupling between the temporal scales of chemical and physical properties would yield important insights into contaminant transport pathways.

In summary, future field studies in this system should attempt to estimate fluxes of suspended sediment and associated contaminants. Field work by others has successfully estimated sediment fluxes in the Hudson River (Geyer *et al.*, 2001). To estimate contaminant fluxes between Newark Bay and Upper New York Bay would require measuring contaminant concentrations at relatively high spatial and temporal scales. Experimental design should require hourly estimates of surface and bottom

contaminant concentrations over several tidal cycles, coincident with observations of currents, salinity, and suspended sediment. Since it is possible to measure metals at this frequency (due to relatively low analytical costs), metals are a logical choice to estimate contaminant transport. Furthermore, insofar as metals may be correlated with organic contaminants such as PCBs and dioxins, such an experiment may also shed light on net transport of those compounds between the Newark Bay and the Upper New York Bay.

12. References

Blumberg, A.F., Khan, L.A., and John, J.P.S., 1999. Hydrodynamic model of New York Harbor region. *Journal of Hydraulic Engineering*, **125**, 799-816.

Chant, R. J., 2002. Secondary flows in a region of flow curvature: relationship with tidal forcing and river discharge. *Journal of Geophysical Research (C Oceans)*, **10.1023/2001JC001082**, 21 September.

Caplow, T., Schlosser, P., Ho, D.T., and N. Santella, 2003. Transport dynamics in a sheltered estuary and connecting tidal straits: SF₆ tracer study in New York harbor. *Environmental Science Technology* **37**, 5116-5126.

Emery, W. J. a. R. E. T., 1998. *Data analysis methods in physical oceanography*. Pergamon, 634 pp.

Friedrichs, C. T. and J. M. Hamrick, 1996. Effects of channel geometry on cross sectional variations in along channel velocity in partially stratified estuaries. *Coastal and Estuarine Studies*, **53**, 283-300.

Friedrichs, C. T. and A. Valle-Levinson, 1998. Transverse circulation associated with lateral shear in tidal estuaries. 9th Biennial International Conference on the Physics of Estuaries and Coastal Seas, p. 15.

Friedrichs, C. T., D. R. Lynch, and D. G. Aubrey, 1992. Velocity asymmetries in frictionally-dominated tidal embayments: longitudinal and lateral variability. *Coastal and Estuarine Studies, Dynamics and exchanges in estuaries and the coastal zone*, D. Prandle, Ed., American Geophysical Union, 277-312.

- Geyer, W. R., Trowbridge, J.H., and M. M. Bowen, 2000. The dynamics of a partially mixed estuary. *Journal of Physical Oceanography*, **30**, 2035-2048.
- Geyer, W. R., Woodruff, J.D., and P. Traykovski, 2001. Sediment transport and trapping in the Hudson River estuary. *Estuaries*, **24**, 670-679.
- Knauss, J., 1996. *Introduction to Physical Oceanography: Second Edition*. Prentice Hall, 306 pp.
- Loew, S., Abood, J.Ko, and T. Wakeman, 2005. A Sediment Budget Analysis of Newark Bay. *Journal of Marine Science and Environment*, **Part C(3)**, 37-44.
- New Jersey Department of Environmental Protection, 2001a. New Jersey Toxics Reduction Workplan, Volume I, Revised/Version 2 – February 2, 2001.
- New Jersey Department of Environmental Protection, 2001b. Stevens Institute of Technology and Rutgers University Project Plan, Quality Assurance Plan, and Standard Operating Procedures for Study IE, New Jersey Toxics Reduction Workplan: Newark Bay, Kill Van Kull, and Arthur Kill, February 23, 2001.
- Oey, L.Y., Mellor, G.L., and R. Hires. 1985. A Three Dimensional Simulation of the Hudson-Raritan Estuary Part I: Description of the Model and Model Simulations. *Journal of Physical Oceanography*, **15(12)**, 1676-1692.
- Pence, A.M., Bruno, M.S., Blumberg, A.F., Fullerton, B.J., and T.O. Herrington, 2006. The Hydrodynamics of the Newark Bay-Kills System, Stevens Institute of Technology Technical Report SIT-DL-05-9-2840, April 2006.
- Seim, H.E. and M.C. Gregg, 1997. The importance of aspiration and channel curvature in producing strong vertical mixing over a sill. *Journal of Geophysical Research*, **102(C2)**, 3451-3462.
- Wong, K.-C., 1994. On the nature of transverse variability in a coastal plain estuary. *Journal of Geophysical Research*. **99(C7)**, 14,209-14,222.

Estuarine Dynamics

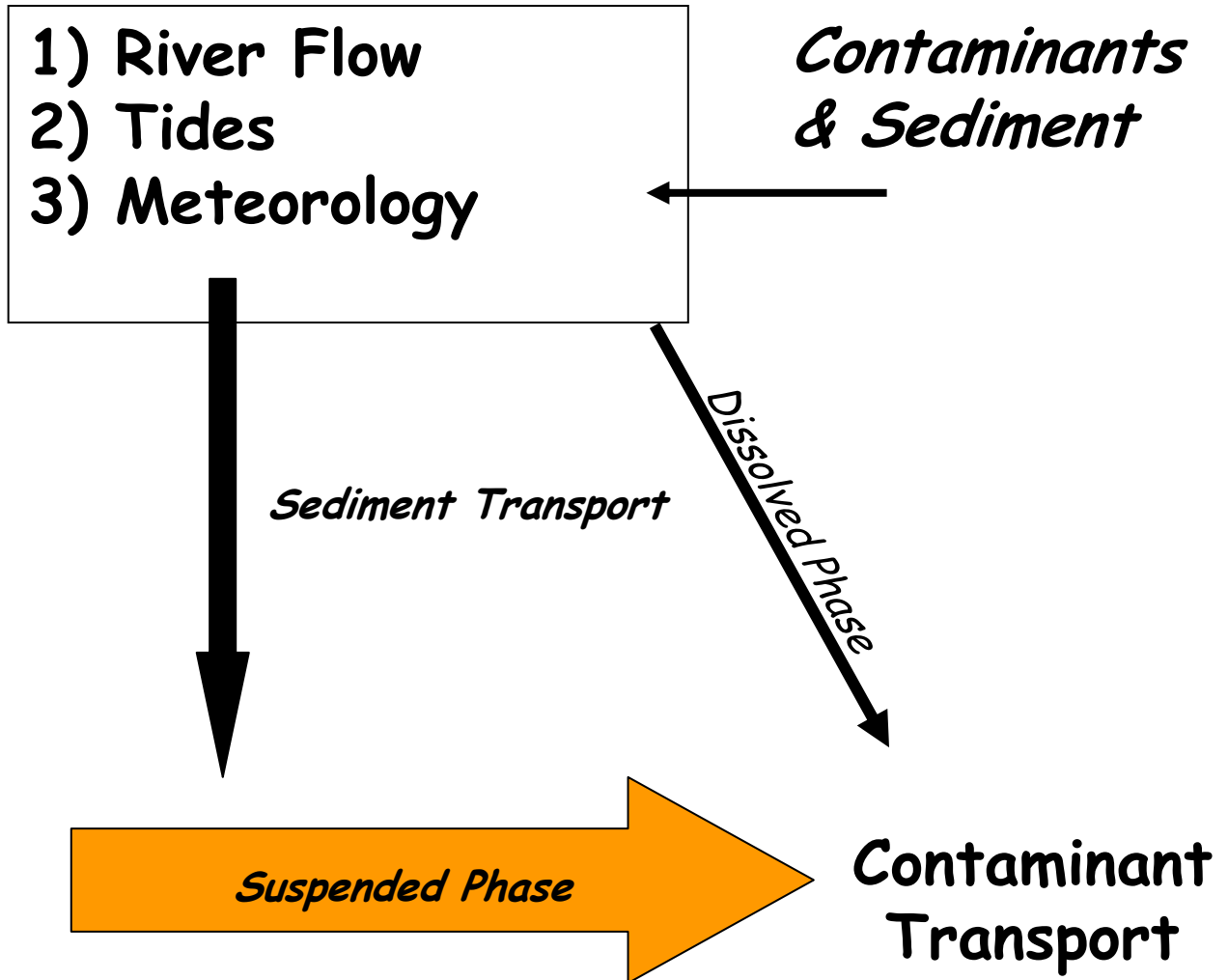


Figure 1. Schematic diagram depicting the processes that drive estuarine sediment and contaminant transport. This report describes processes in the box that represent estuarine dynamics and the response of this system to variations in river flow, and tidal and meteorological forcing.

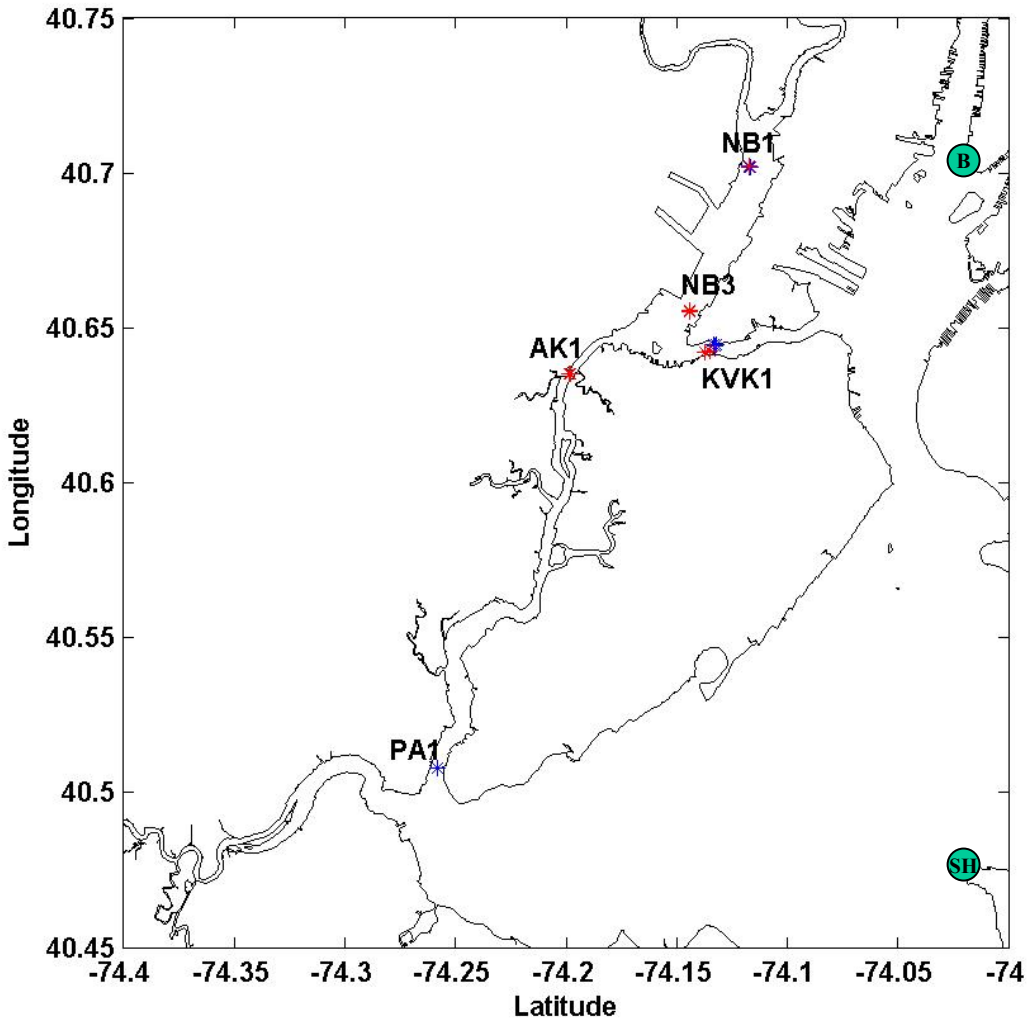


Figure 2a. Long-term mooring locations. Black stars indicate the mooring locations for 2000, blue stars are for 2001, and red stars are for 2002. Due to dredging operations, the mooring location at KVK varied between deployments. [Figure 2b](#) shows the locations of each mooring deployment in the KVK. The green dots show the locations of NOAA tide gauges at Sandy Hook (SH) and The Battery (B).

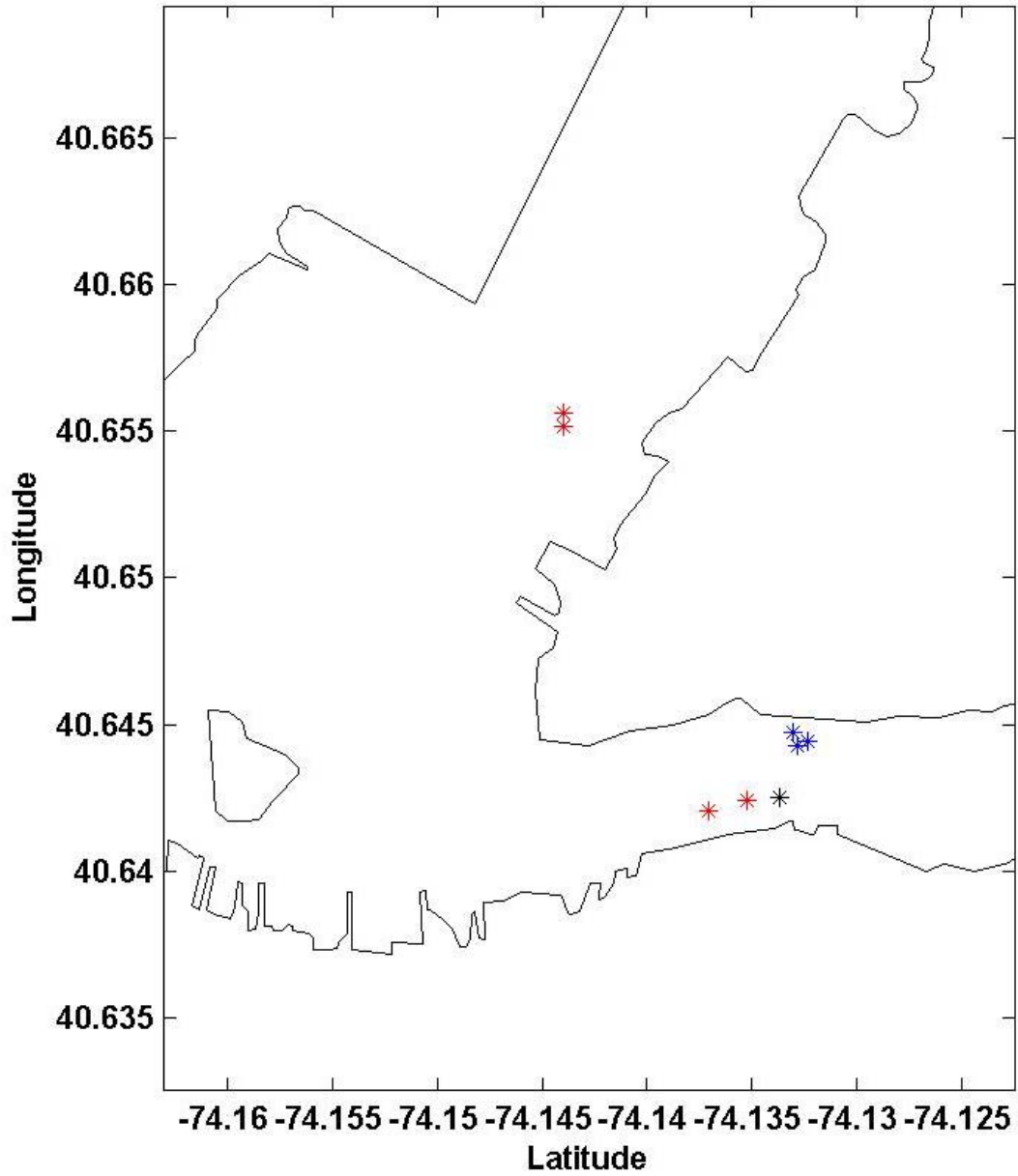


Figure 2b. Mooring locations at in the Kill Van Kull for 2000 (black stars), 2001 (blue stars), and 2002 (red stars).

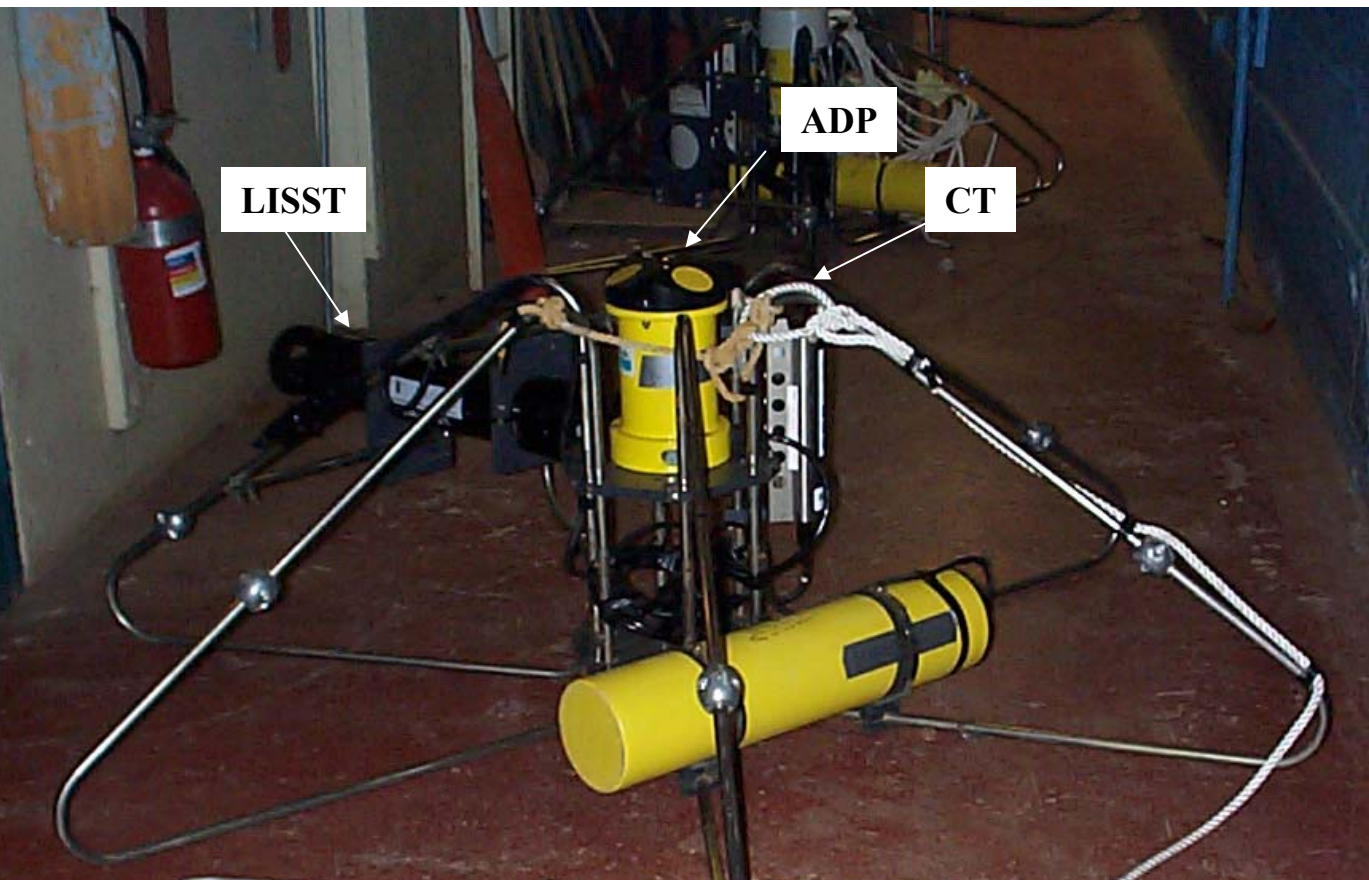


Figure 3. Mooring frame and instrumentation (the OBS mounted on the CT sensor is not visible in this photo).

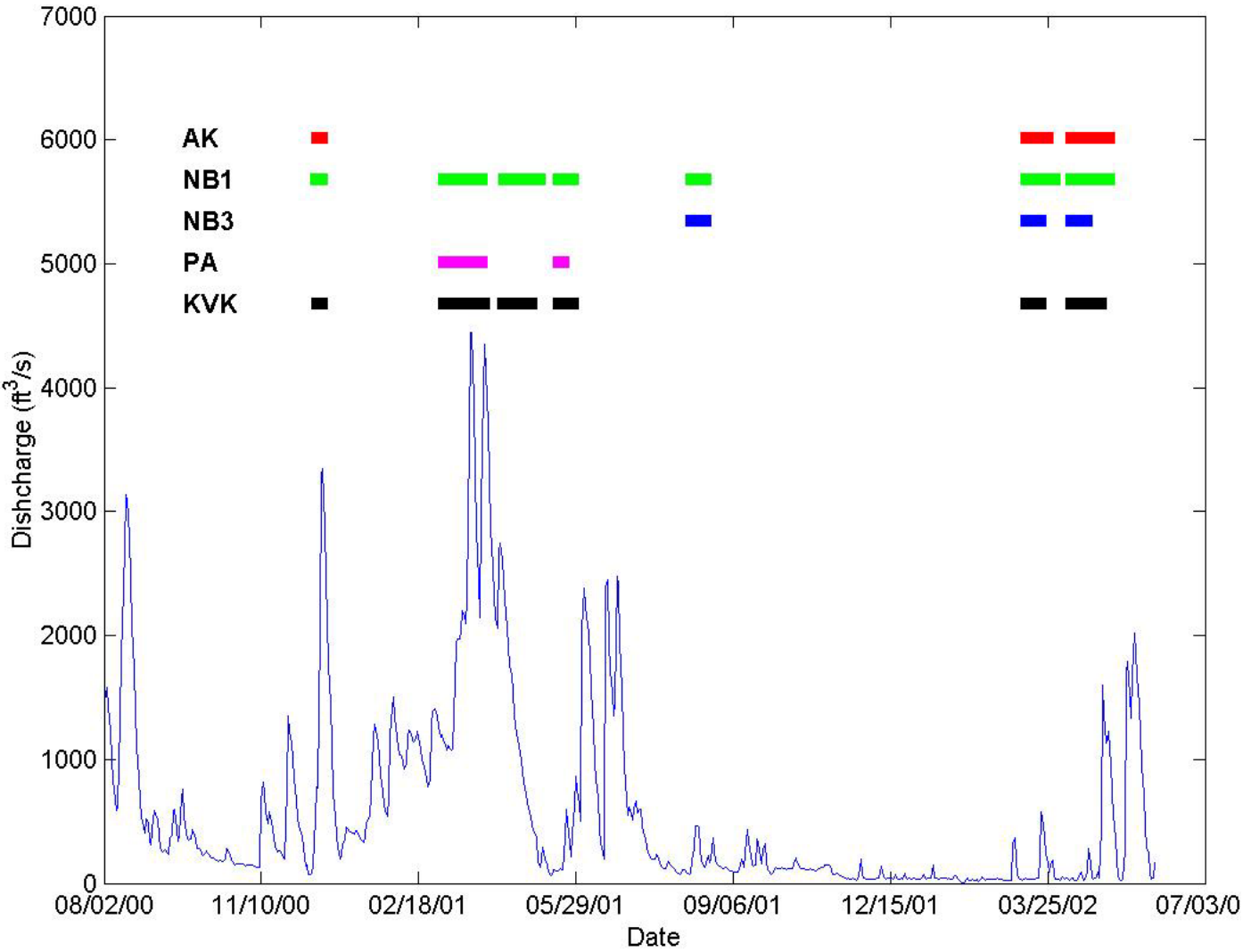


Figure 4. Passaic River discharge (in cubic feet per second) and timing of mooring deployments (colored bars).

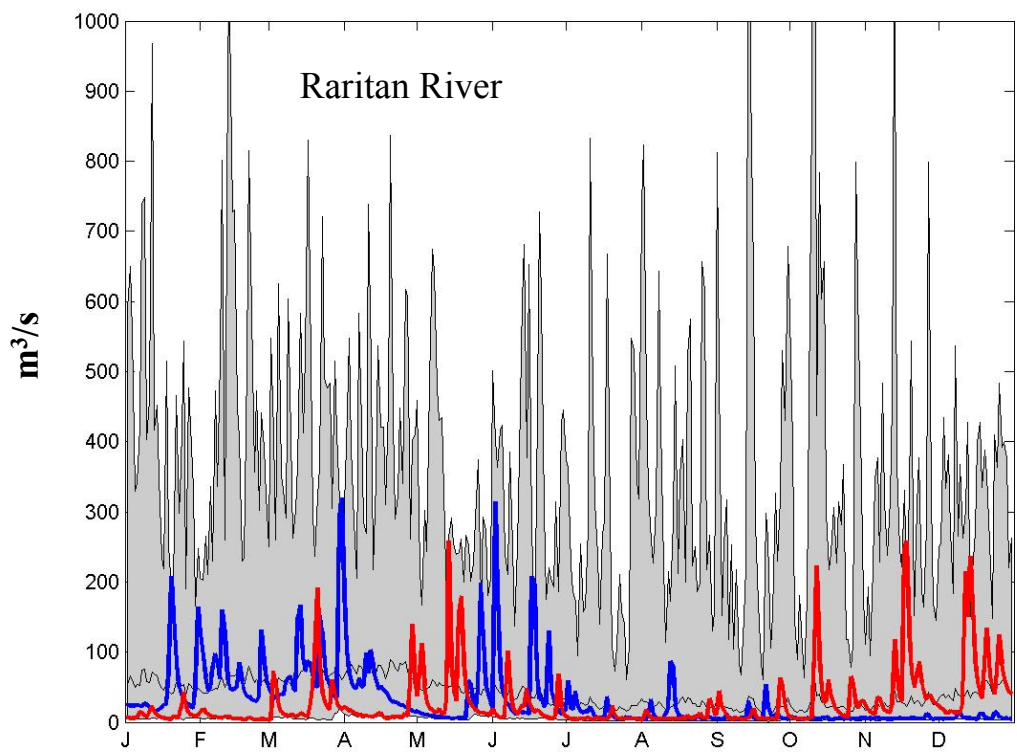
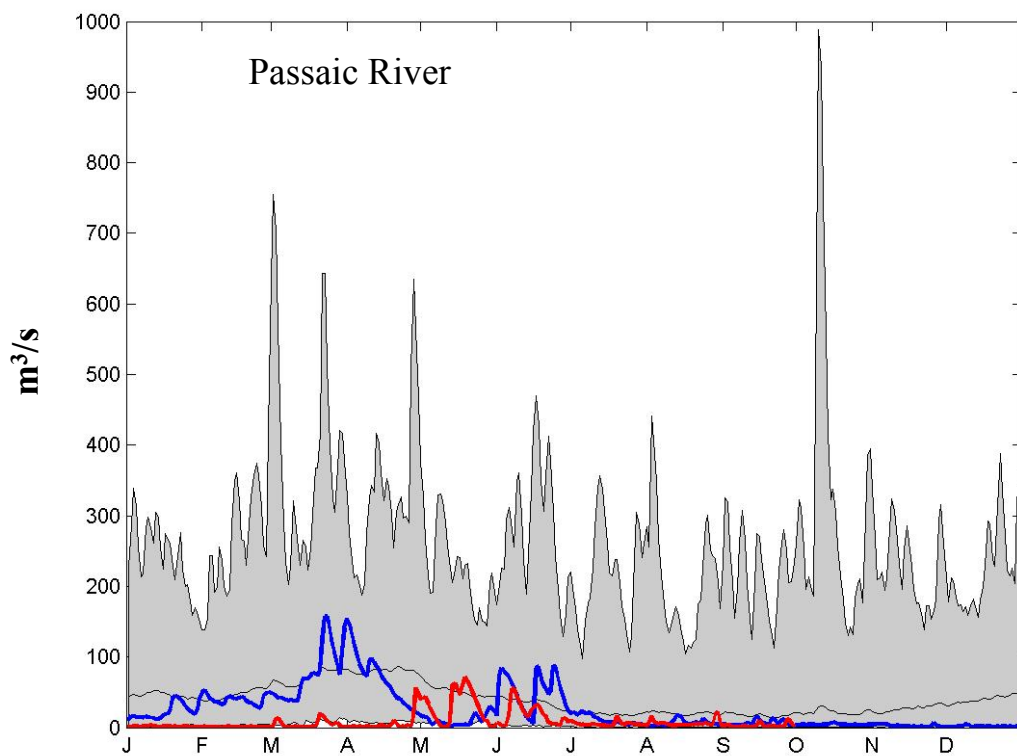


Figure 5. Discharge for the Passaic (upper panel) and Raritan (lower panel) Rivers. The grey envelope shows the daily record discharge for the entire record available from the USGS web site; the black line shows the daily mean based on this record. The blue line is the discharge for 2001, and the red line shows the discharge for 2002.

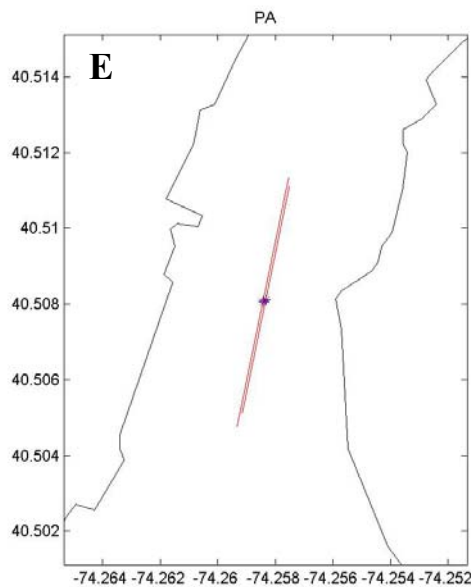
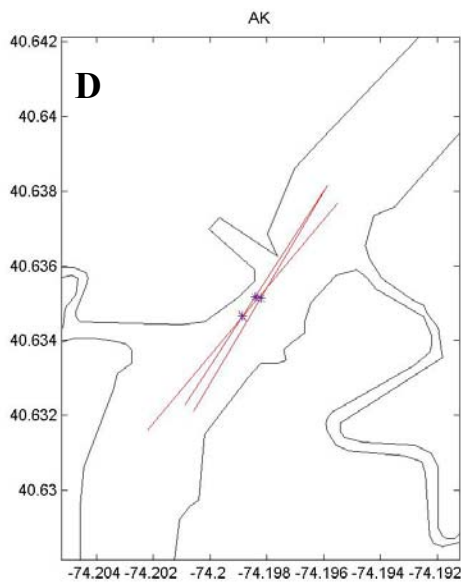
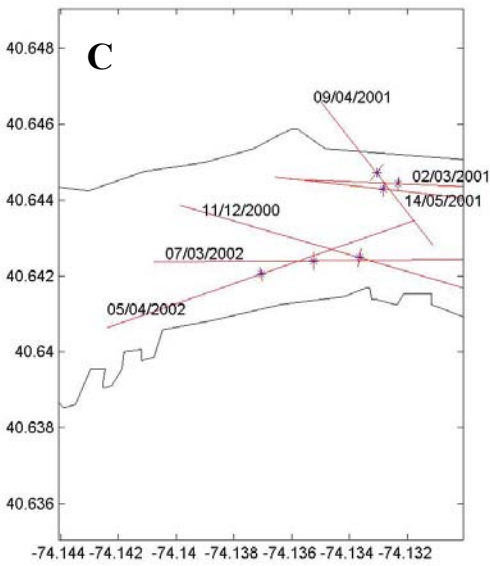
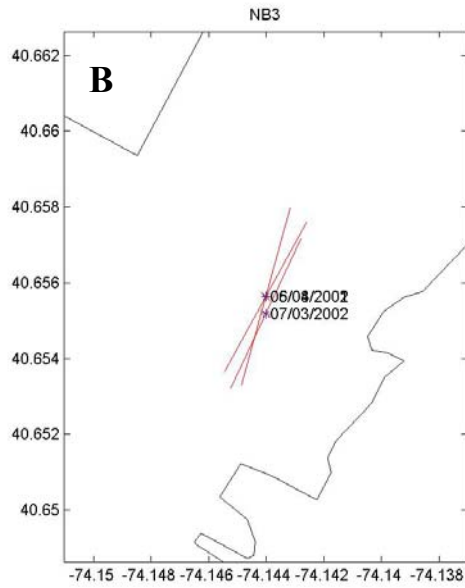
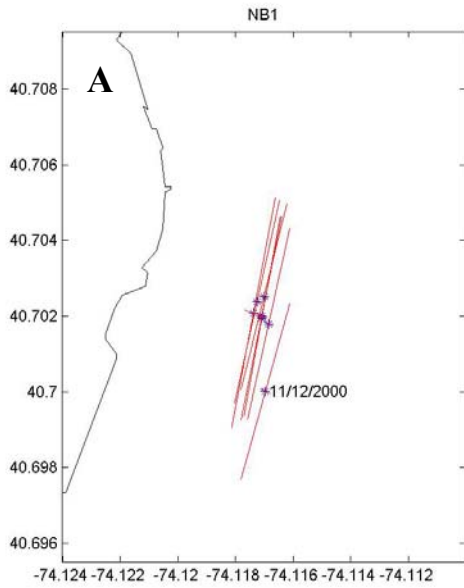


Figure 6. The semidiurnal (M2) tidal ellipse for each mooring deployment at Stations (a) NB1, (b) NB3, (c) KVK, (d) AK1, and (e) PA1. The magnitude of the ellipse can be inferred from the data in Table 2.

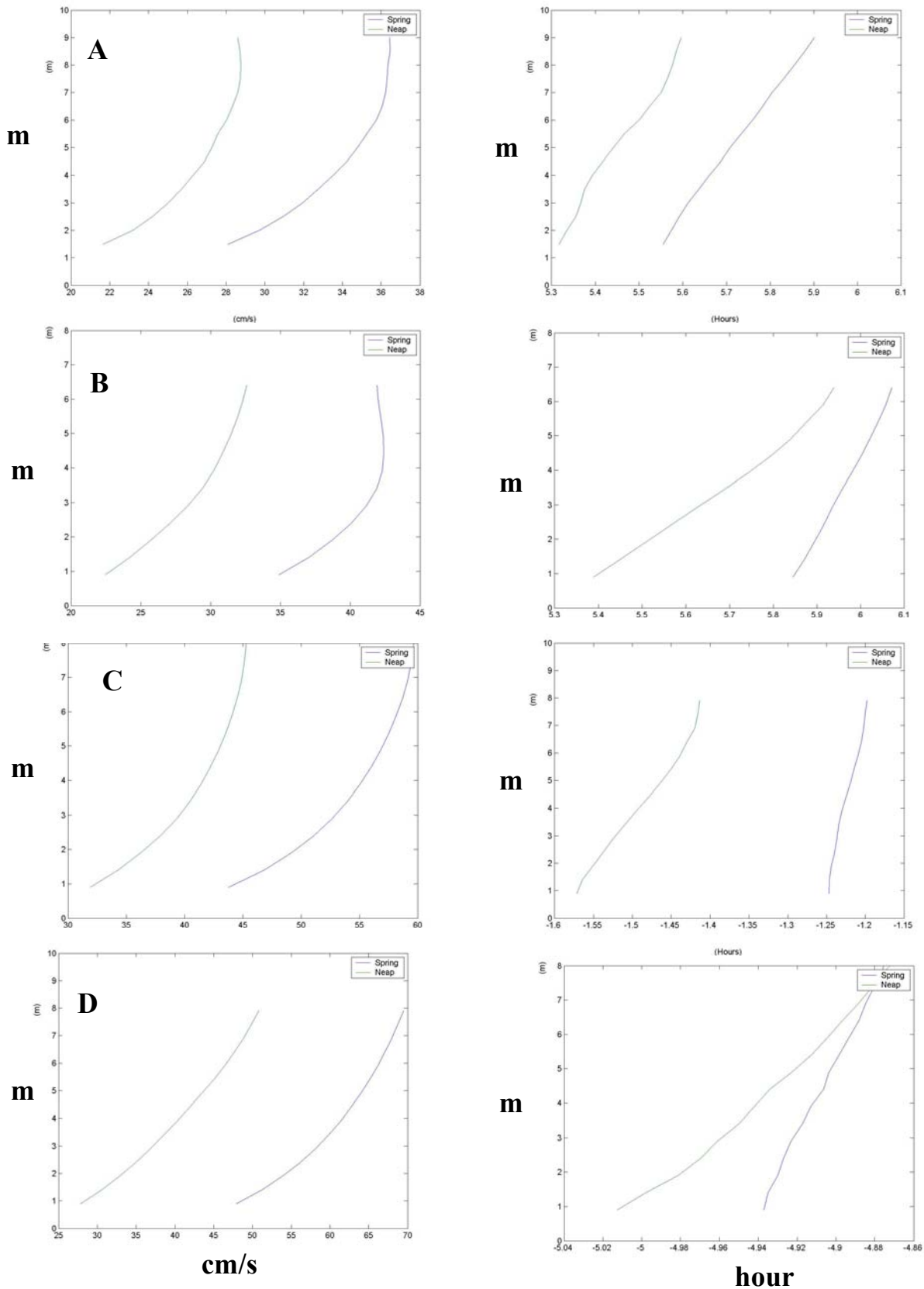


Figure 7. Vertical structure of the semidiurnal tidal (M2) motion at each mooring location. Left panel shows tidal current speed, right panel shows tidal current phase during neap tide and spring tide conditions. Depth is in meters above the bottom. Station (A) NB1, (B) NB3, (C) KVK1 (D) AK1 and (E) PA1.

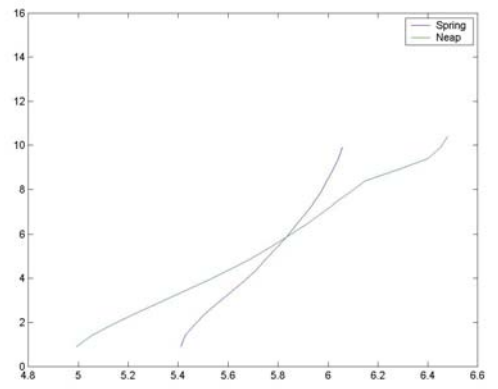
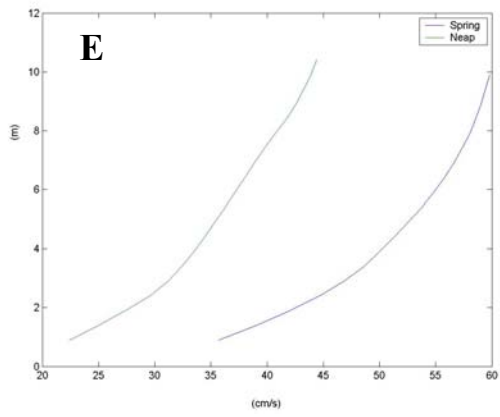


Figure 7. Continued.

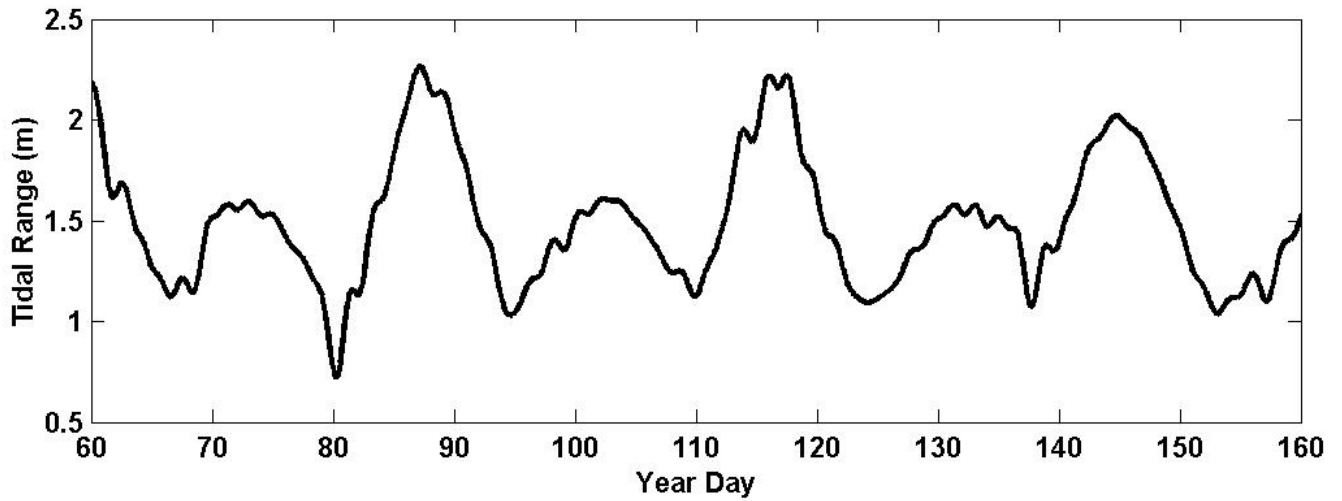
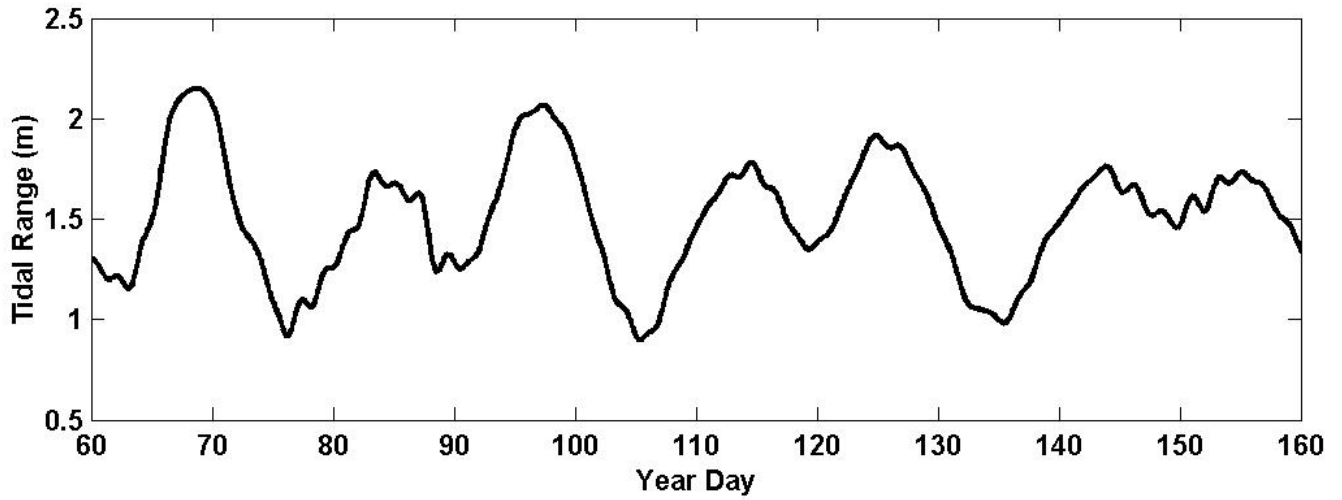


Figure 8. Tidal range at Bergen Point during mooring deployments for the years 2001(upper panel) and 2002 (lower panel).

Crosses show locations of CTD casts taken during ebbing tides on March 14, 2001.

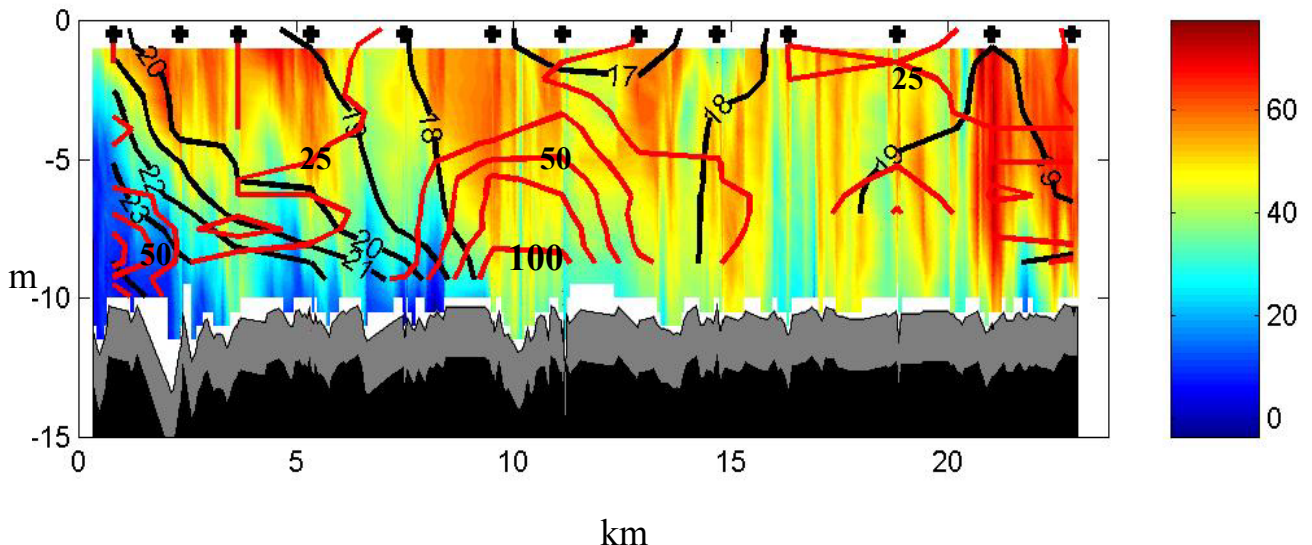
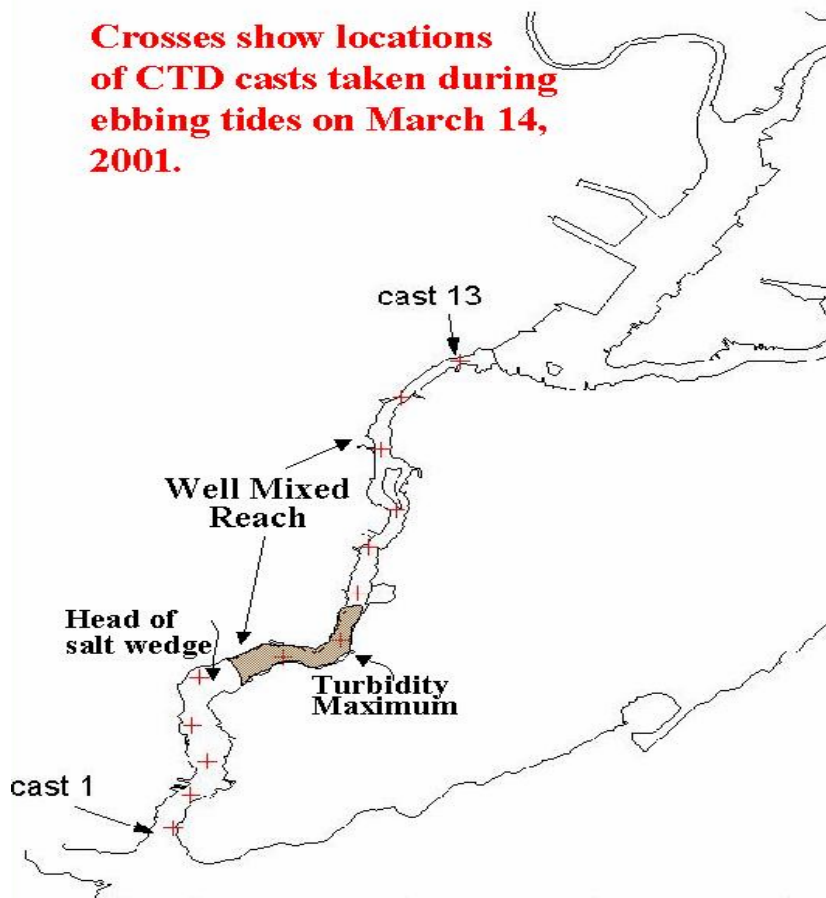


Figure 9. Location of the turbidity maximum in the Arthur Kill. **upper panel** – the crosses show the locations of CTD casts; grey area shows the location of turbidity maximum. **Lower panel** - CTD/ADCP section from Perth Amboy to Newark Bay. The colors show along-channel velocity (cm/sec) during the ebb; red is flow towards Raritan Bay. The black contours show salinity (psu). Note that the ebb velocities are reduced behind the salt front defined by the 20 psu isohaline. The red contours show the OBS derived SS estimates (mg/l).

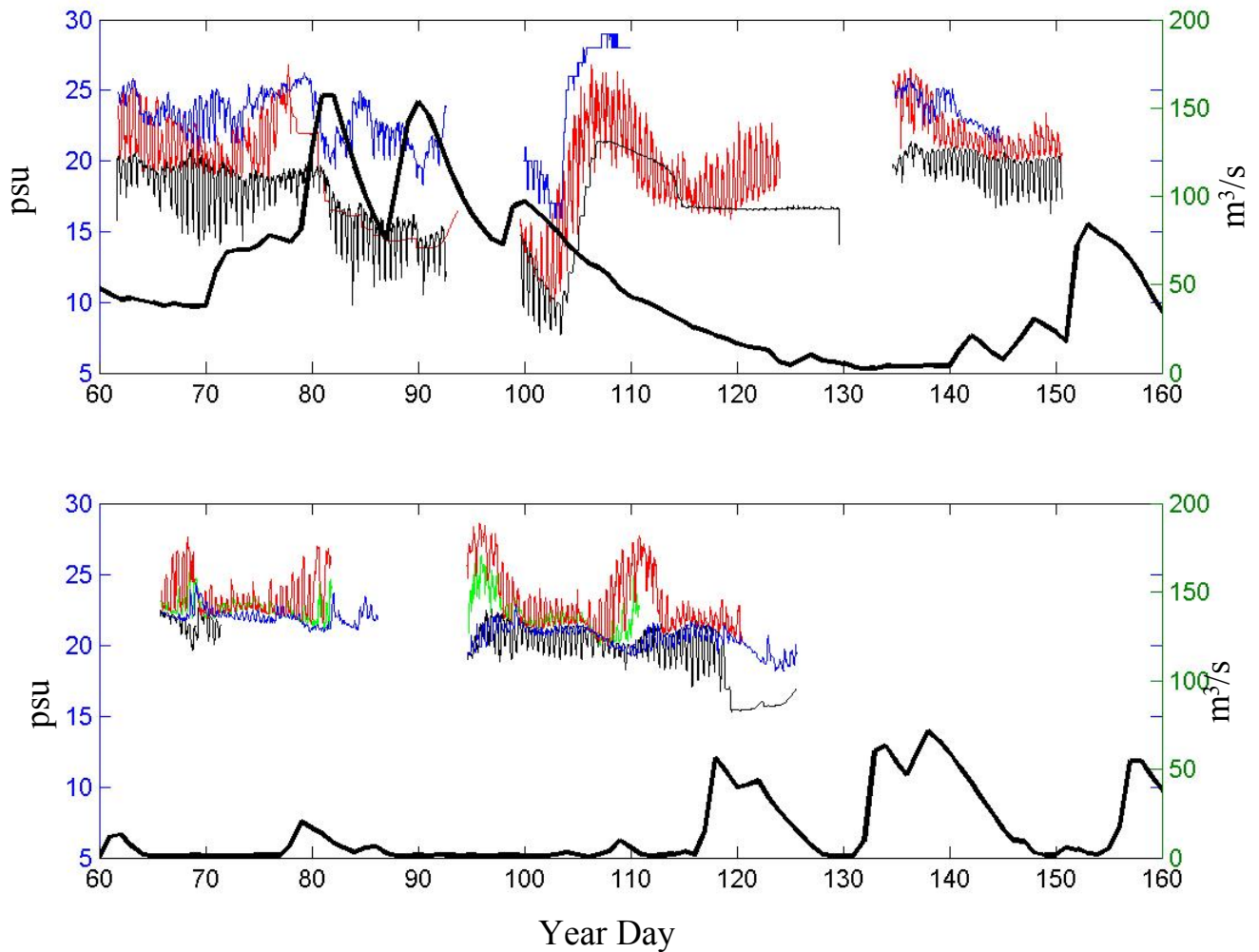


Figure 10. Near-bottom salinity at each mooring location and the Passaic River discharge during 2001 (upper panel) and 2002 (lower panel). The thick black line is the Passaic River discharge. In the upper panel, the thin black line is salinity at NB1, the red line is salinity at KVK1, and the blue line is salinity at PA1. In the lower panel, the black line is salinity at NB1, the red line is salinity at KVK1, the green line is salinity at NB3, and the blue line is salinity at AK1.

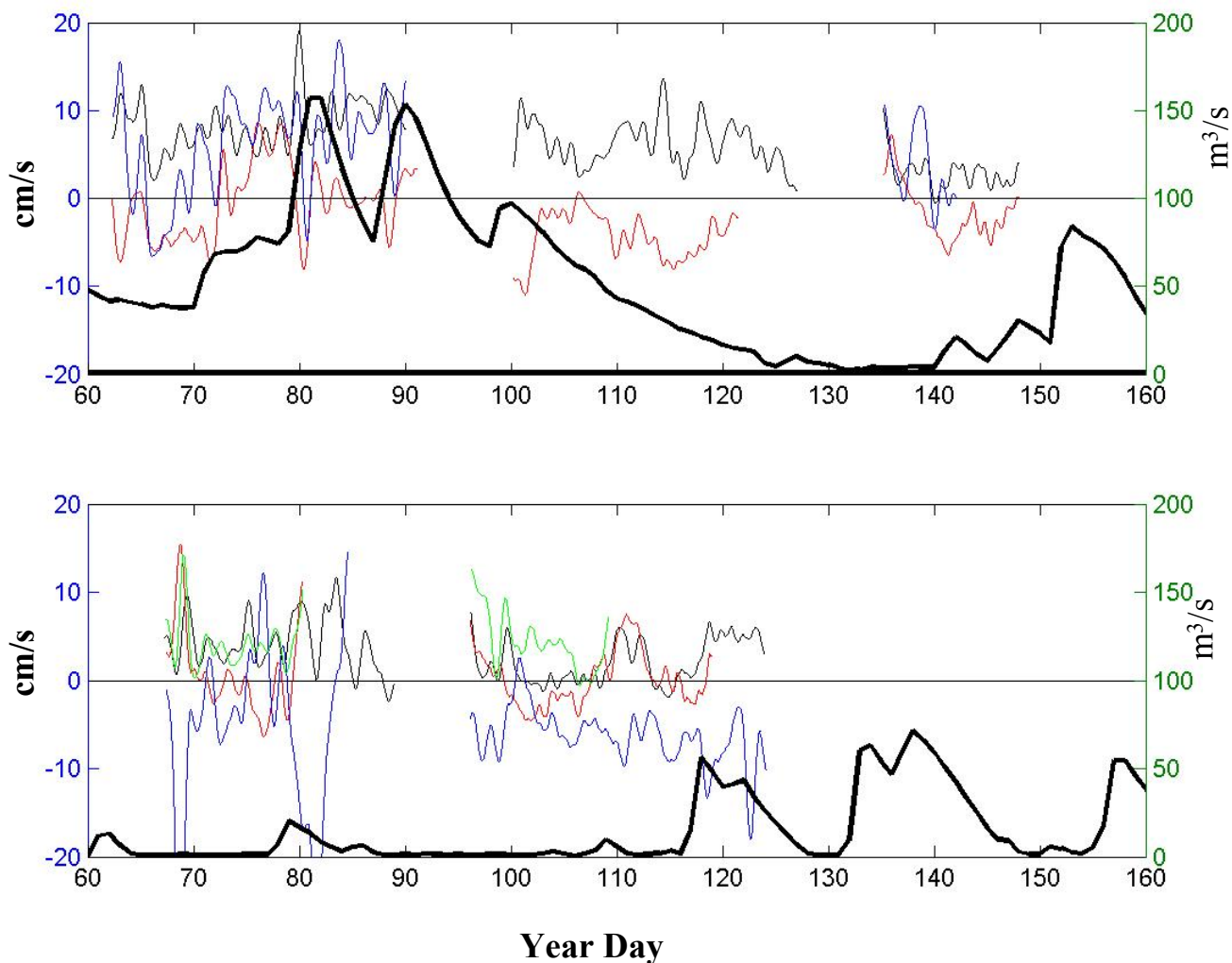


Figure 11. Near-bottom sub-tidal currents at each mooring location and the Passaic River discharge during 2001 (upper panel) and 2002 (lower panel). The thick black line is the Passaic River discharge. In the upper panel, the thin black line is the current at Station NB1, KVK1 (red line), and PA1 (blue line). In the lower panel the black line is the current at Station NB1, KVK1 (red line), NB3 (green line), and AK1 (blue line).

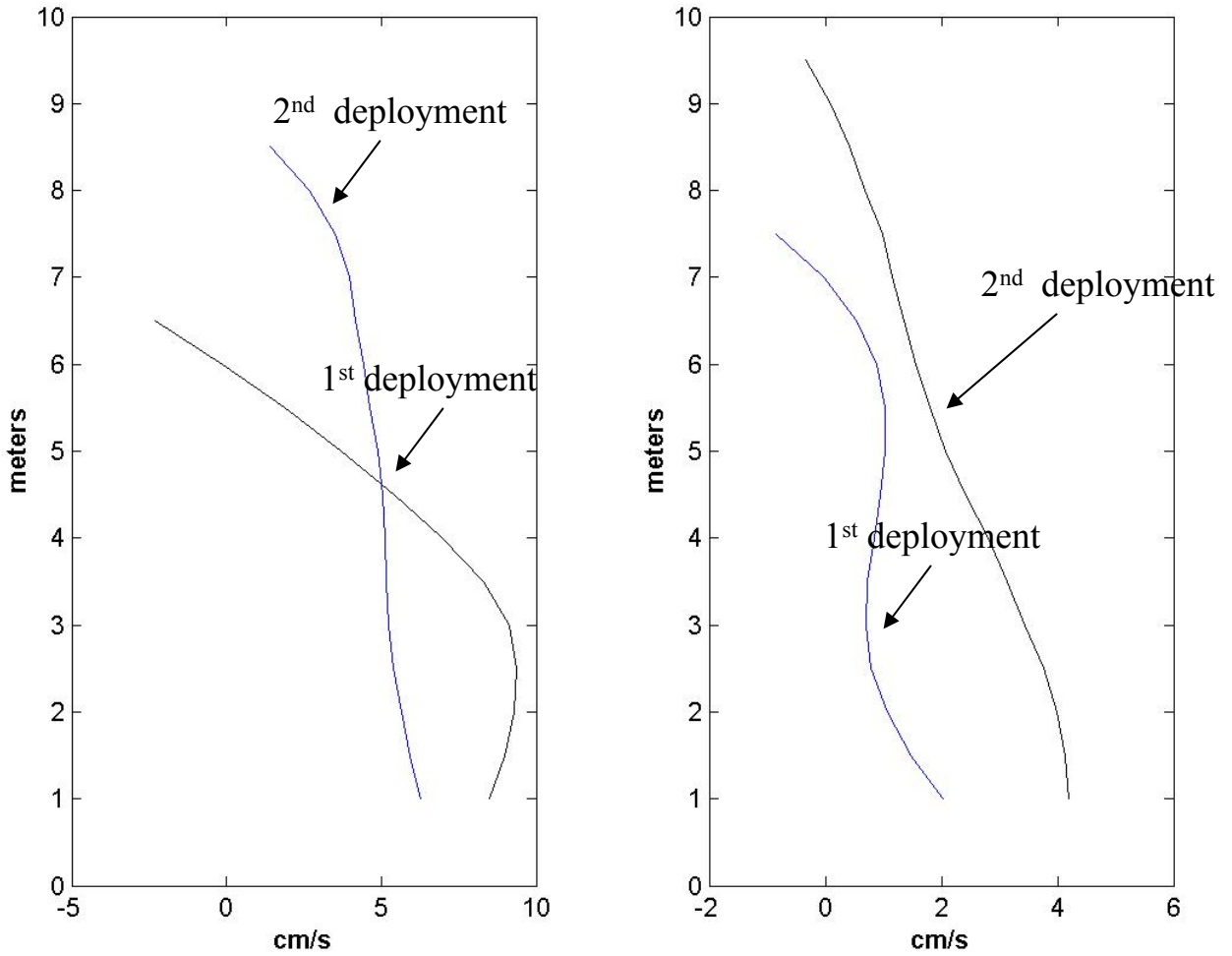


Figure 12. Depth-dependent mean flow at Station NB1 for 2001 (left panel) and 2002 (right panel). In both panels the black line is for the first deployment and the blue line is for the second deployment. Depth is in meters above the bottom. Upstream velocities are positive.

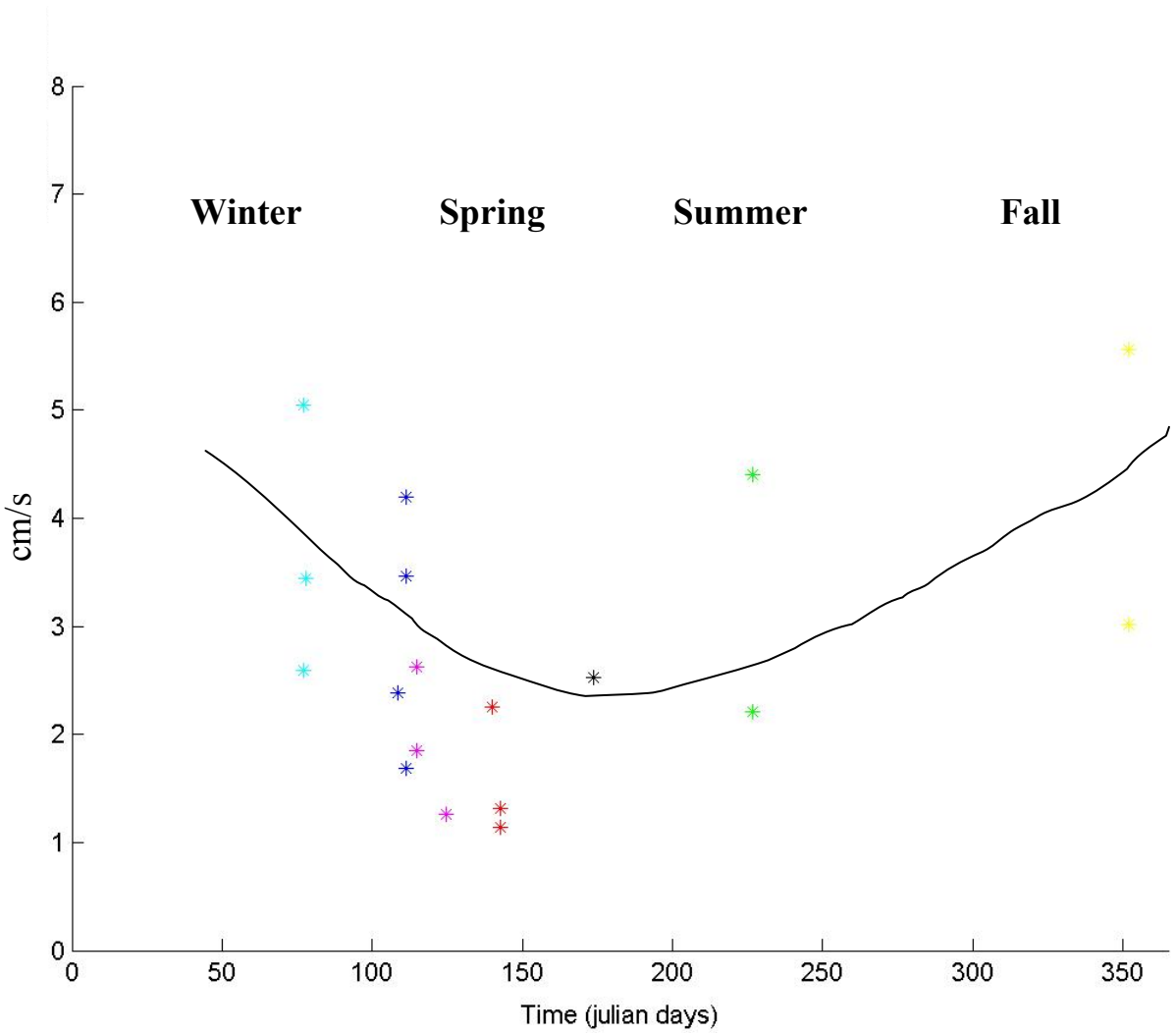


Figure 13. Root mean square (rms) of subtidal velocity for all mooring deployments as a function of season. Black curve depicts seasonal trend showing weaker subtidal rms velocity during summer months relative to winter and fall.

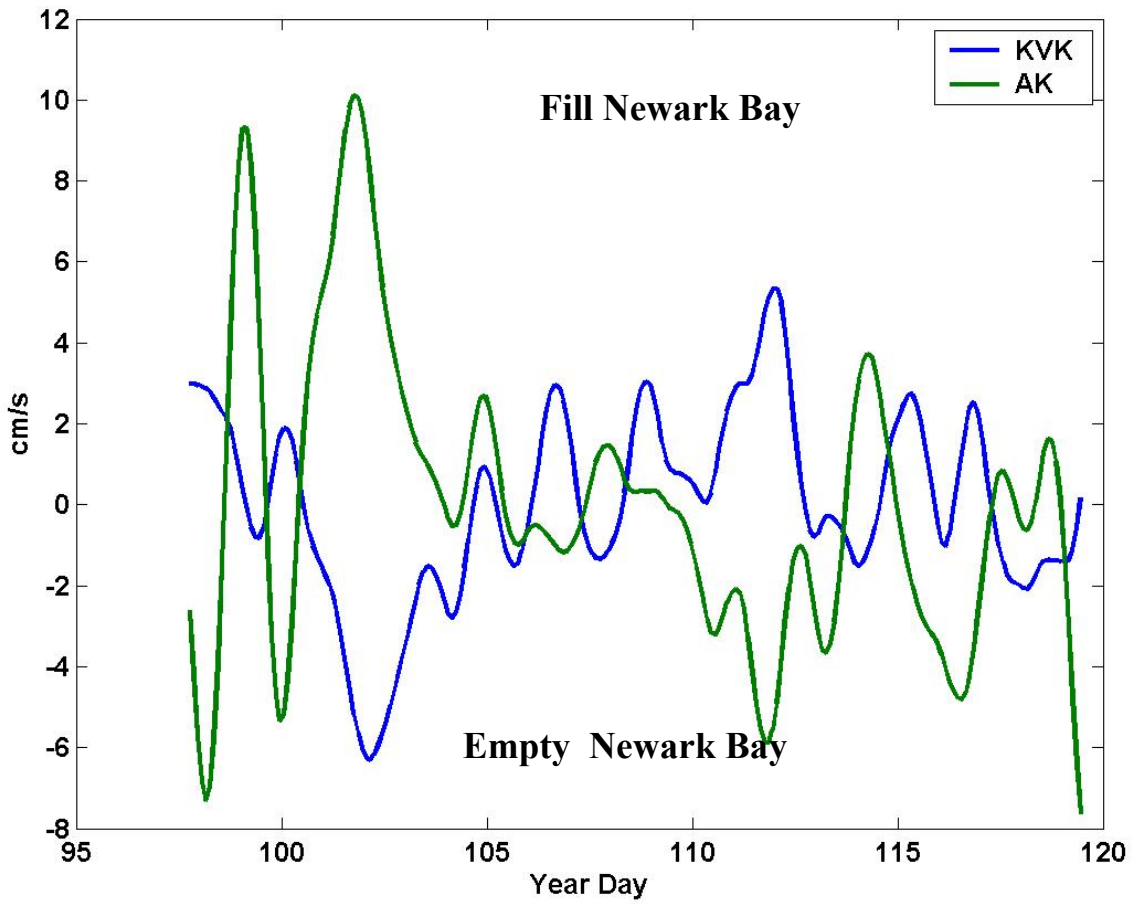


Figure 14a. Depth-averaged currents at Stations KVK and AK1 in 2002.



Figure 14b. Depiction of depth-averaged currents (red arrows) in response to a north-westerly wind (large green arrow).

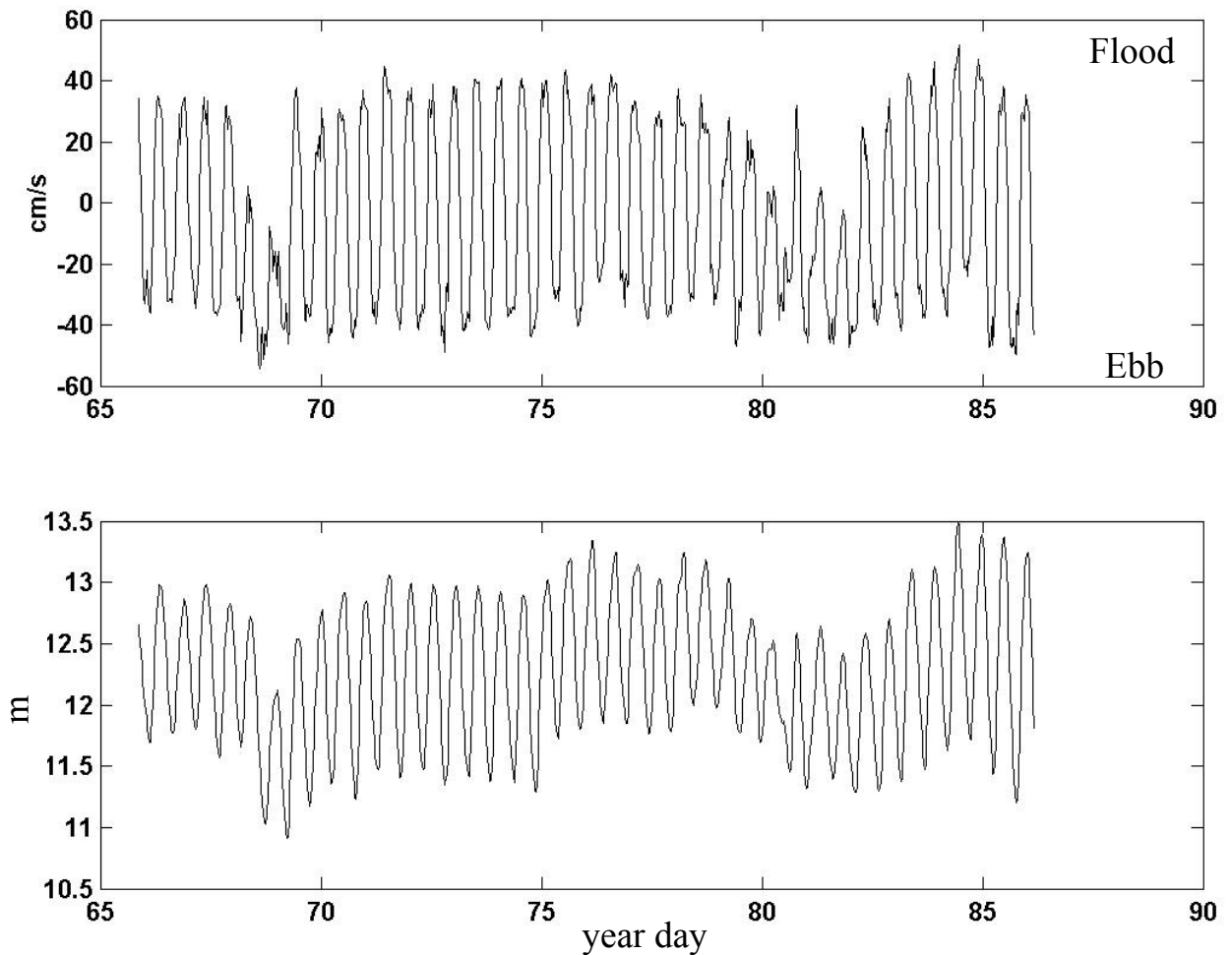


Figure 15. Along channel currents (upper panel) and pressure (lower panel) at Station AK in 2002. Flooding currents are positive. Note that during sea-level set down on days 68 and 82 currents at Station AK1 never flood.

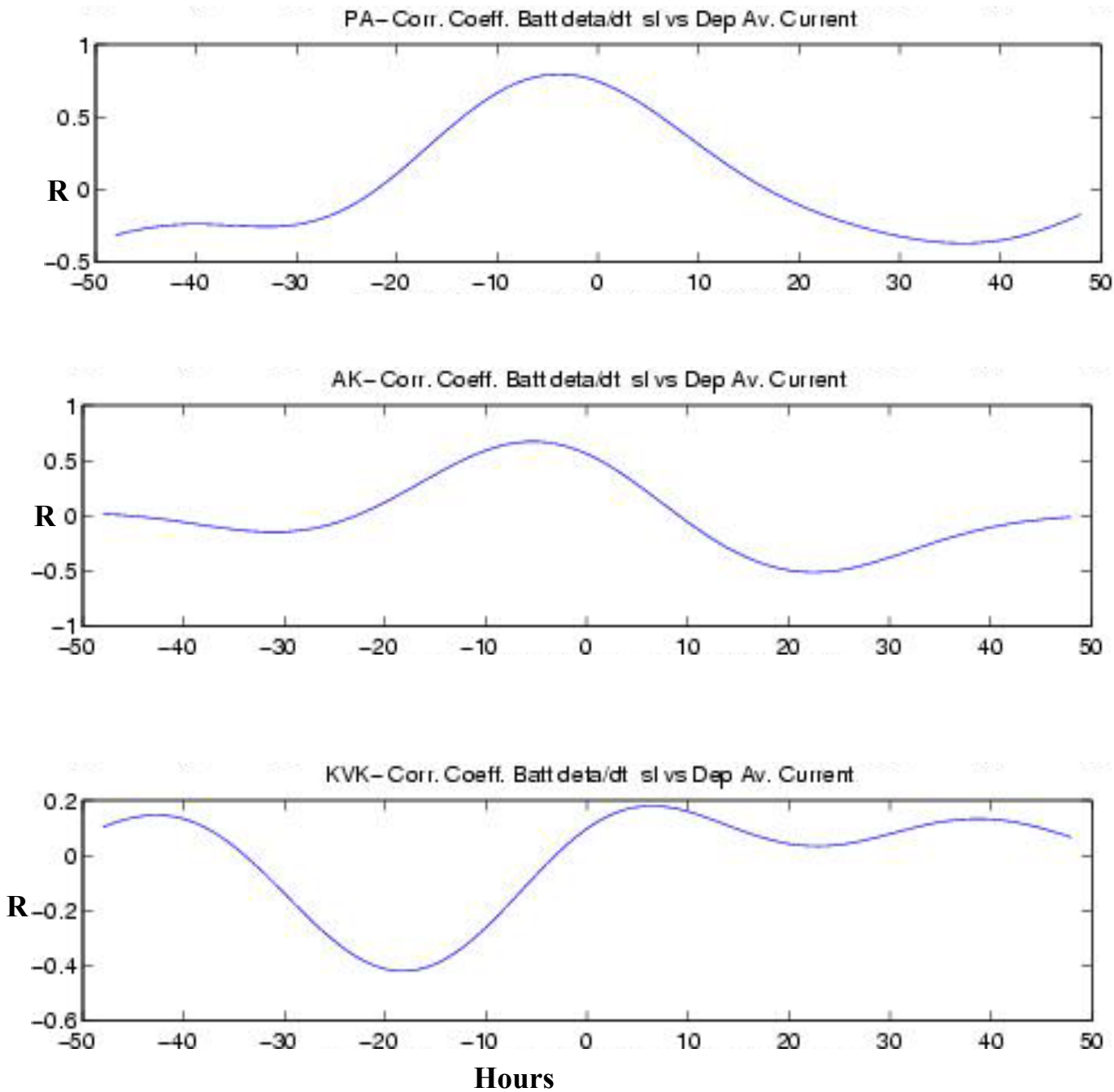


Figure 16. Time-lagged correlation analysis between the time rate of change of subtidal sea level at Sandy Hook ($\partial\eta/\partial t$) and low frequency depth-averaged flow at Stations PA1 (upper panel), AK1 (middle panel), and KVK (lower panel).

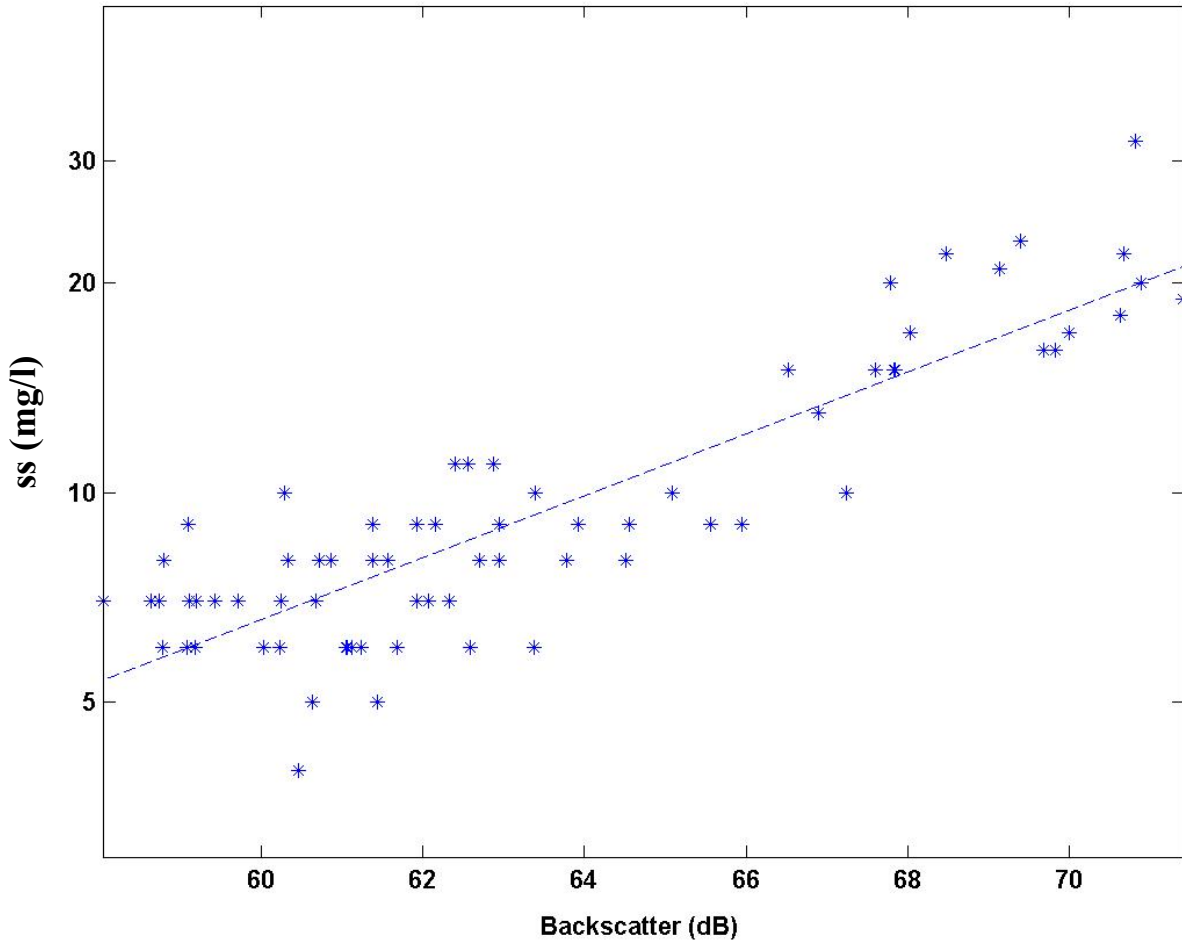


Figure 17. Scatter plot between measured SS and acoustic backscatter from the Sontek ADP; October 29, 2003 calibration experiment.

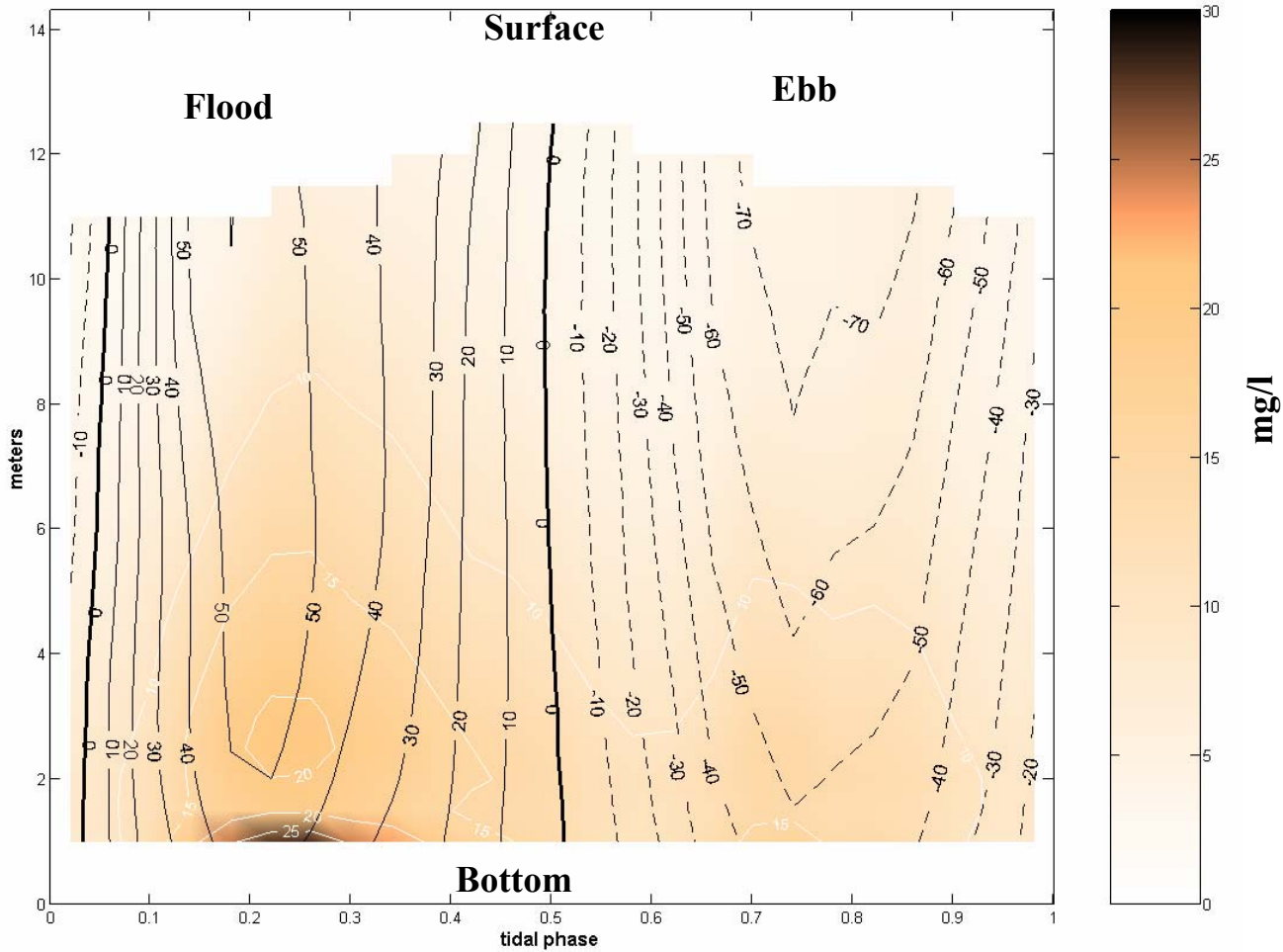


Figure 18. Current speed (black contours) and suspended sediment concentration (brown color and white contours, in mg/l) during spring tide conditions at Station KVK during deployment 2 in 2002. Note higher SS values during the flood tide.

Table 1: Mooring location, time of deployment, and mean depths.

| Site Name | Deployed | Recovered | Latitude | Longitude | Depth (m) |
|------------------|-----------------|------------------|-----------------|------------------|------------------|
| NB1 | 12/11/2000 | 12/21/2000 | 40.7000 | 74.117 | 10.5 |
| NB1 | 03/02/2001 | 04/02/2001 | 40.7018 | 74.1168 | 9.07 |
| NB1 | 04/09/2001 | 05/09/2001 | 40.7019 | 74.1171 | 11.5 |
| NB1 | 05/14/2001 | 05/30/2001 | 40.7020 | 74.1171 | 10.2 |
| NB1 | 08/06/2001 | 08/23/2001 | 40.7021 | 74.1145 | 12.0 |
| NB1 | 09/28/2001 | 10/05/2001 | 40.7021 | 74.1145 | 11.0 |
| NB1 | 10/12/2001 | 10/30/2001 | 40.7021 | 74.1145 | 11.5 |
| NB1 | 11/02/2001 | 11/19/2001 | 40.7021 | 74.1145 | 11 |
| NB1 | 03/07/2002 | 04/01/2002 | 40.7024 | 74.1172 | 12.5 |
| NB1 | 04/05/2002 | 05/06/2002 | 40.7025 | 74.1170 | 10.1 |
| NB3 | 08/06/2001 | 08/23/2001 | 40.6556 | 74.1440 | 12.3 |
| NB3 | 03/07/2002 | 04/01/2002 | 40.6552 | 74.1440 | 13.4 |
| NB3 | 04/05/2002 | 05/06/2002 | 40.6556 | 74.1440 | 13.3 |
| KVK1 | 12/11/2000 | 12/21/2000 | 40.6425 | 74.1337 | 14.8 |
| KVK1 | 03/02/2001 | 04/02/2001 | 40.6444 | 74.1323 | 14.3 |
| KVK1 | 04/09/2001 | 05/09/2001 | 40.6447 | 74.1331 | 10.6 |
| KVK1 | 05/14/2001 | 05/30/2001 | 40.6433 | 74.1328 | 13.4 |
| KVK1 | 09/28/2001 | 10/05/2001 | | | |
| KVK1 | 10/12/2001 | 10/30/2001 | | | |
| KVK1 | 11/02/2001 | 11/19/2001 | | | |
| KVK1 | 03/07/2002 | 04/01/2002 | 40.6424 | 74.1352 | 15.0 |
| KVK1 | 04/05/2002 | 05/06/2002 | 40.6420 | 74.1371 | 15.6 |
| AK1 | 12/11/2000 | 12/21/2000 | 40.6347 | 74.1988 | 12.5 |
| AK1 | 03/07/2002 | 04/01/2002 | 40.6352 | 74.1984 | 12.3 |
| AK1 | 04/05/2002 | 05/06/2002 | 40.6351 | 74.1982 | 12.7 |
| PA | 03/02/2001 | 04/02/2001 | 40.5080 | 74.2584 | 13.4 |
| PA | 04/09/2001 | 05/09/2001 | 40.5080 | 74.2584 | |
| PA | 05/14/2001 | 05/30/2001 | 40.5080 | 74.2584 | 13.3 |
| PA | 09/28/2001 | 10/05/2001 | 40.5080 | 74.2584 | |
| PA | 10/12/2001 | 10/30/2001 | 40.5080 | 74.2584 | |
| PA | 11/02/2001 | 11/19/2001 | 40.5080 | 74.2584 | |

Table 2: Calculated Tidal Constituents at the Mooring Locations

Major Tidal Constituents NB1 (Currents)

| | <u>K1</u> | <u>M2</u> | <u>M4</u> | <u>M6</u> |
|-------------|-----------|-----------|-----------|-----------|
| Major(cm/s) | 1.97 | 34.93 | 3.07 | 2.99 |
| Minor(cm/s) | 0.05 | -0.20 | -0.15 | 0.07 |
| Phase(hrs) | -3.2 | -0.31 | 0.25 | 0.62 |
| Oren(deg) | -104.5 | -106.12 | -95.53 | 76.22 |

Major Tidal Constituents NB1 (Sea Level)

| | <u>K1</u> | <u>M2</u> | <u>M4</u> | <u>M6</u> |
|--------------|-----------|-----------|-----------|-----------|
| Magnitude(m) | 0.08 | 0.75 | 0.036 | 0.026 |
| Phase(hrs) | -9.52 | -4.04 | 0.23 | 1.344 |

Major Tidal Constituents KVK1 (Currents)

| | <u>K1</u> | <u>M2</u> | <u>M4</u> | <u>M6</u> |
|-------------|-----------|-----------|-----------|-----------|
| Major(cm/s) | 3.58 | 52.22 | 2.90 | 4.15 |
| Minor(cm/s) | 0.19 | 1.58 | 0.08 | 0.55 |
| Phase(m) | -4.08 | -1.29 | 0.740 | 0.01 |
| Oren(deg) | -3.33 | -3.37 | -12.58 | 176.72 |

Major Tidal Constituents KVK1 (Sea Level)

| | <u>K1</u> | <u>M2</u> | <u>M4</u> | <u>M6</u> |
|--------------|-----------|-----------|-----------|-----------|
| Magnitude(m) | 0.095 | 0.691 | 0.032 | 0.017 |
| Phase(hrs) | -9.447 | -4.27 | 0.349 | 0.991 |

Table 2: Calculated Tidal Constituents (continued)

Major Tidal Constituents PA1 (Currents)

| | <u>K1</u> | <u>M2</u> | <u>M4</u> | <u>M6</u> |
|-------------|-----------|-----------|-----------|-----------|
| Major(cm/s) | 2.81 | 42.88 | 1.17 | 2.60 |
| Minor(cm/s) | -0.05 | -0.57 | -0.04 | -0.09 |
| Phase(hrs) | -2.90 | -0.44 | 0.21 | 0.22 |
| Oren(deg) | -105.33 | -105.28 | -105.20 | 70.84 |

Major Tidal Constituents PA1 (Sea Level)

| | <u>K1</u> | <u>M2</u> | <u>M4</u> | <u>M6</u> |
|-------------------|-----------|-----------|-----------|-----------|
| Magnitude(m) 0.08 | | 0.71 | 0.021 | 0.02 |
| Phase(hrs) | -10.37 | -4.73 | -0.33 | 0.37 |

Major Tidal Constituents AK1 (Currents)

| | | | | |
|-------------|--------|-------|--------|------|
| Major(cm/s) | 1.82 | 48.29 | 1.95 | 4.98 |
| Minor(cm/s) | -0.04 | 0.39 | 0.01 | 0.15 |
| Phase(hrs) | 0.09 | -4.88 | 1.59 | 1.26 |
| Oren(deg) | 177.18 | 0.10 | -13.19 | 1.03 |

Major Tidal Constituents AK1 (Sea Level)

| | <u>K1</u> | <u>M2</u> | <u>M4</u> | <u>M6</u> |
|-------------------|-----------|-----------|-----------|-----------|
| Magnitude(m) 0.08 | | 0.71 | 0.03 | 0.02 |
| Phase(hrs) | -8.54 | -4.00 | 0.38 | 1.19 |

Estuarine Dynamics

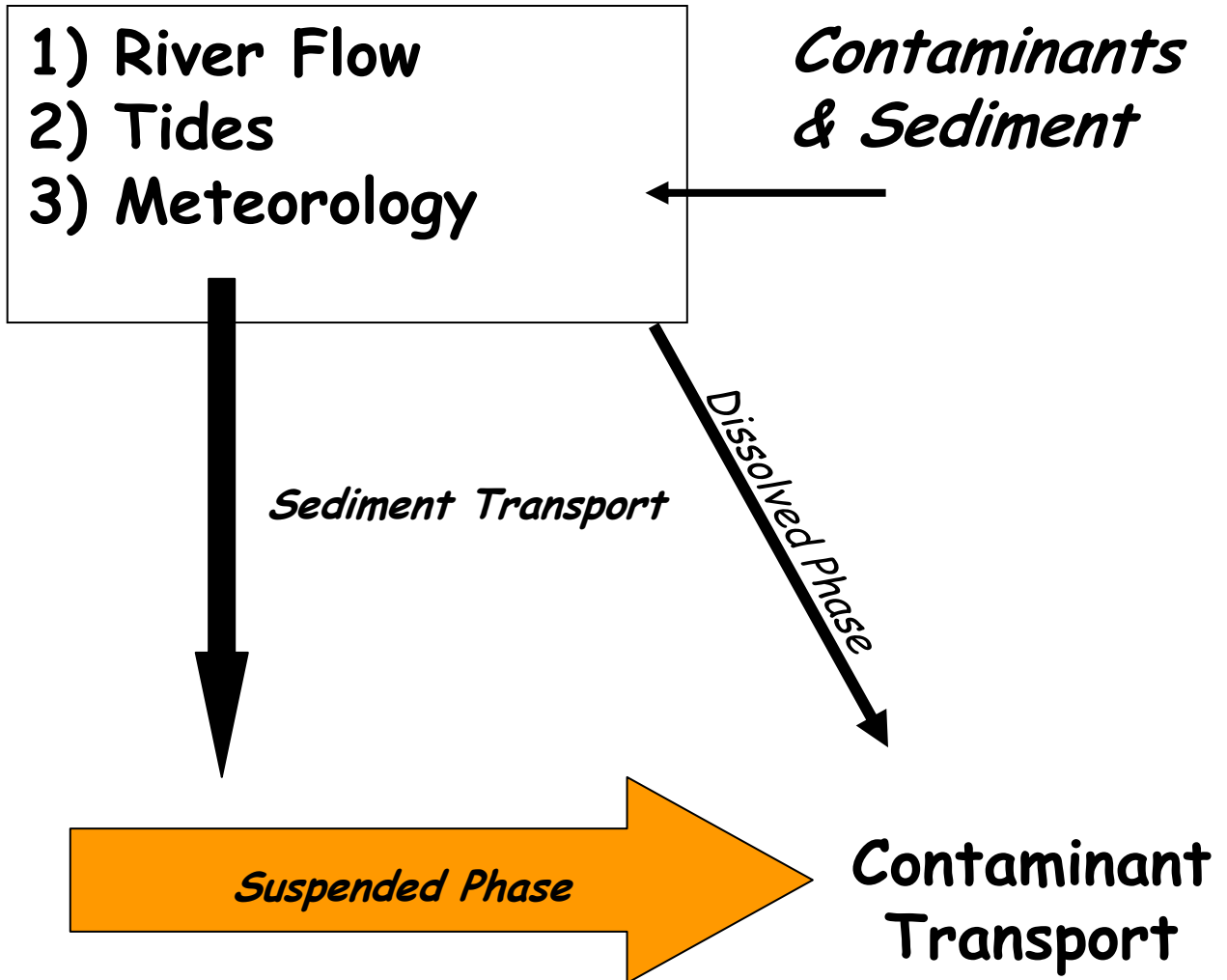


Figure 1 Schematic diagram depicting processes that drive estuarine sediment and contaminant transport. This report describes processes in the box that represent estuarine dynamics and the response of this system to variations in river flow and tidal and meteorological forcing.

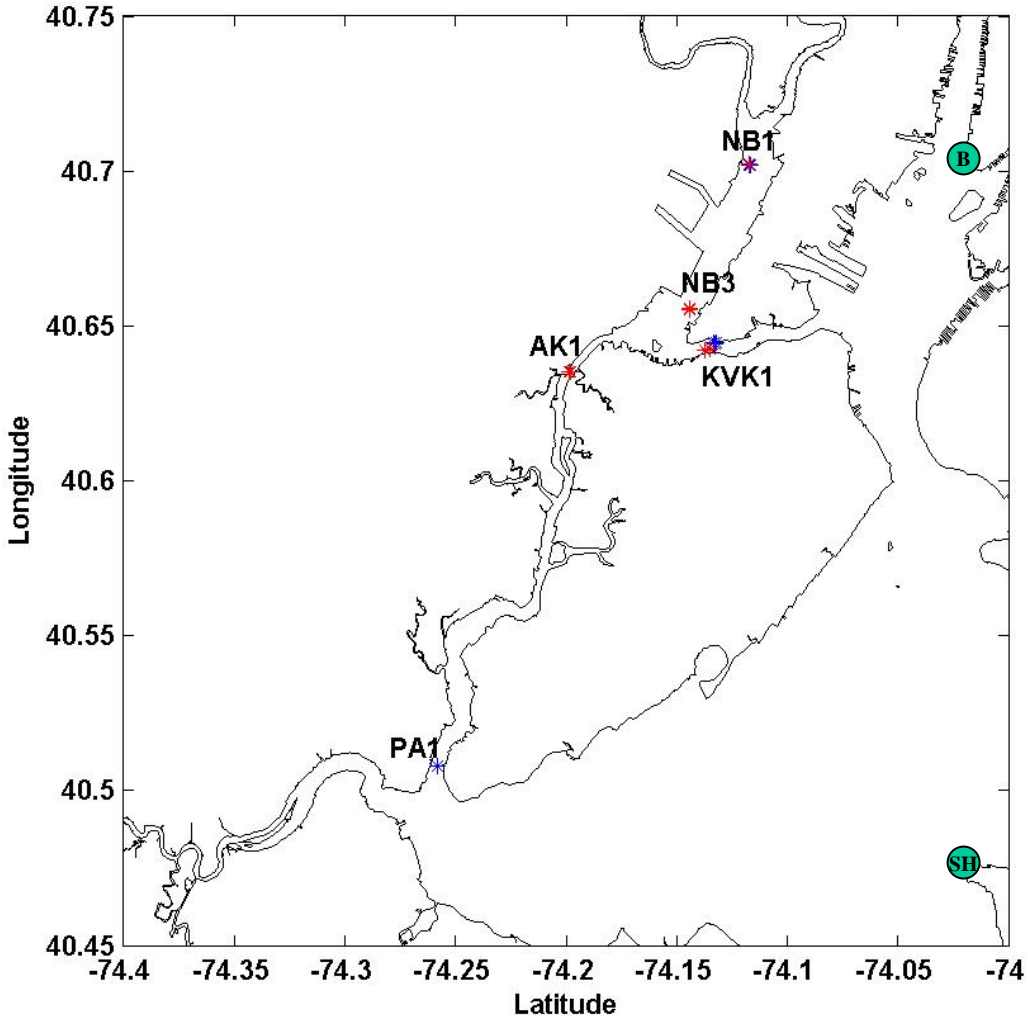


Figure 2a Long-term mooring locations. Black stars indicate mooring locations for 2000, blue stars are for 2001, and red stars are 2002. Due to dredging operations the mooring location at KVK varied between deployments. Figure 2b shows location of each deployment in the KVK. The green dots show the locations of NOAA tide gauges at Sandy Hook (SH) and The Battery (B).

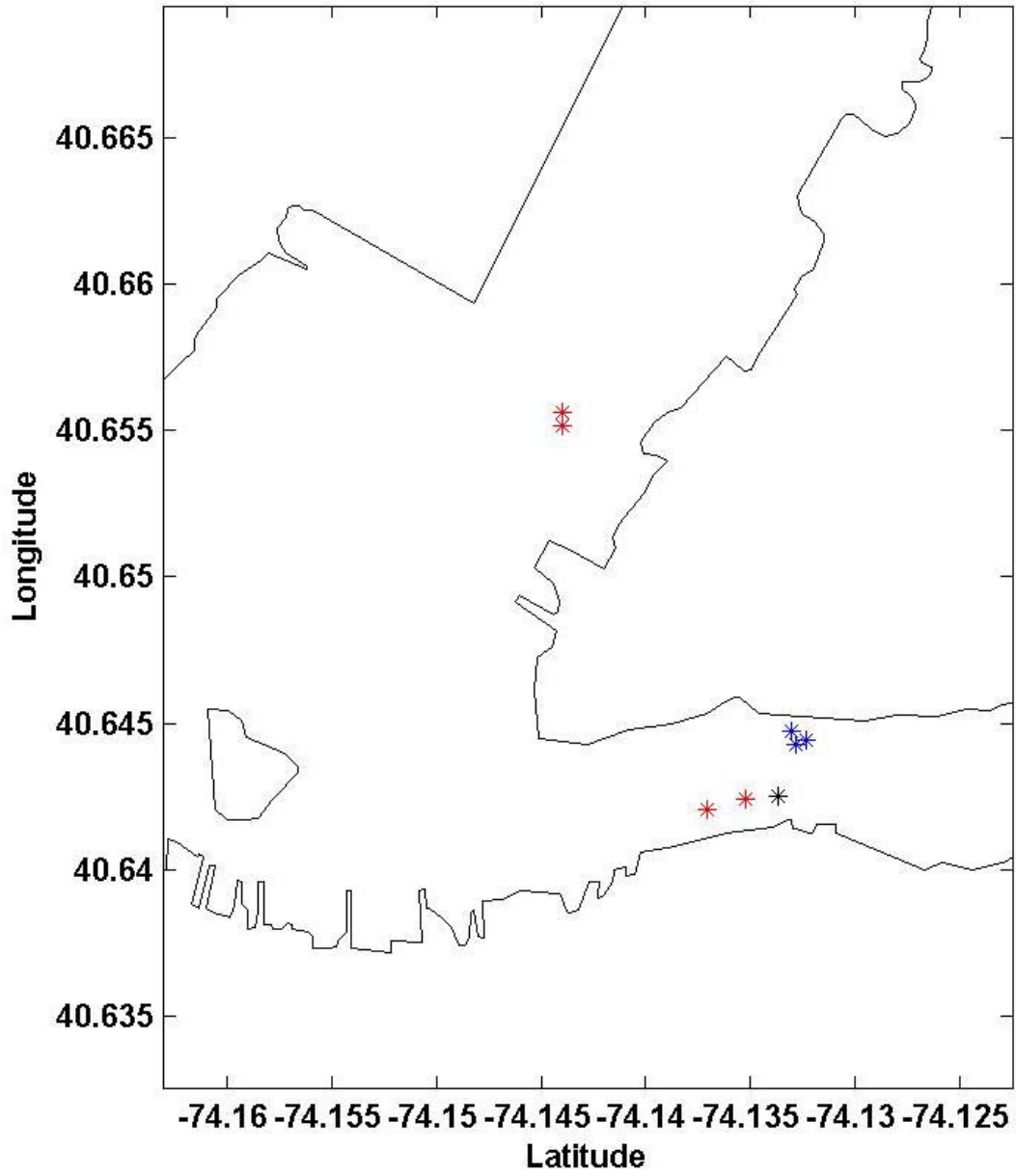


Figure 2b Mooring locations at station KVK site for 2000 (black), 2001 (blue), and 2002 (red).

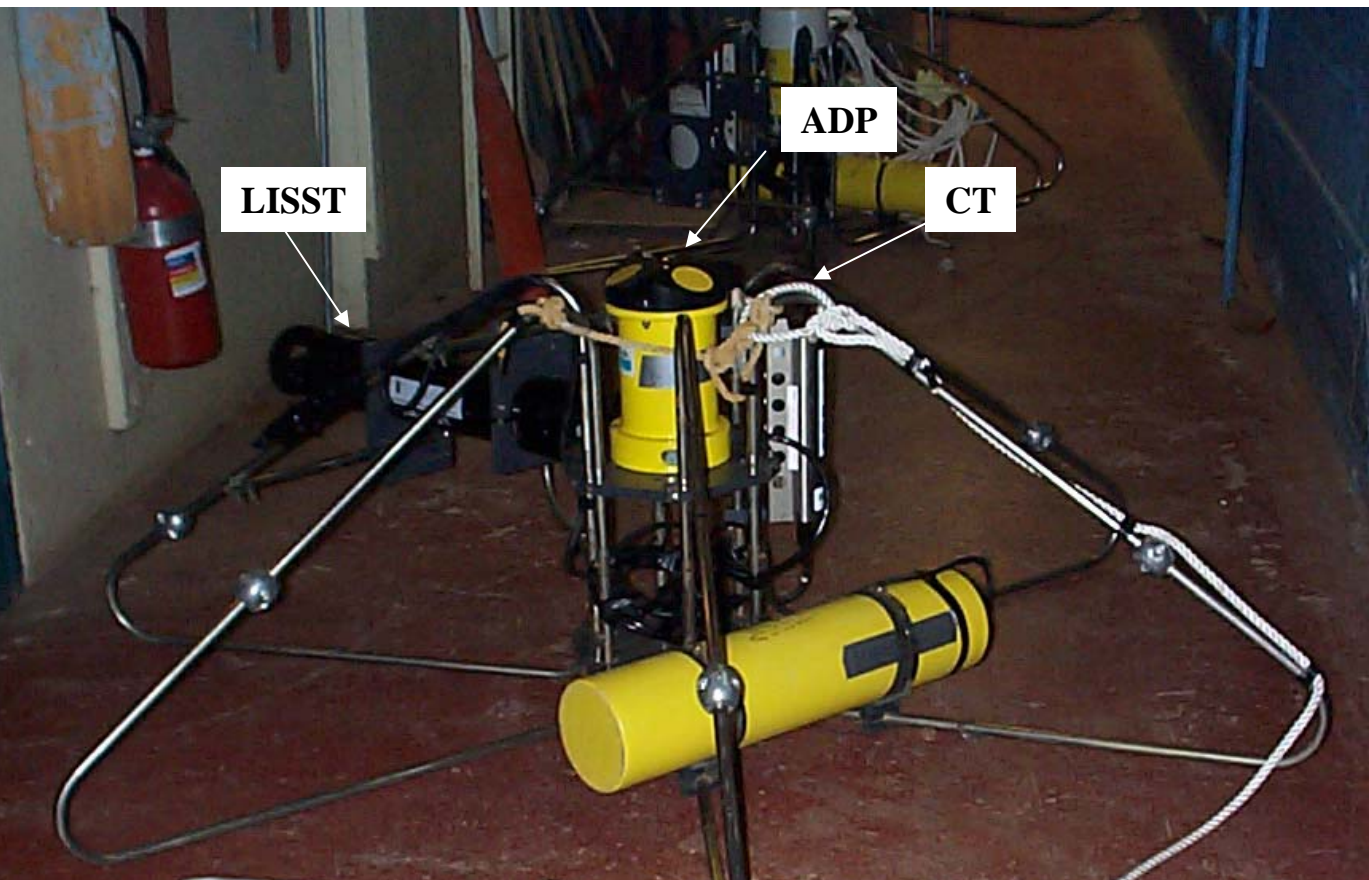


Figure 3 Mooring frame and instrumentation (OBS mounted on CT sensor not visible in this photo).

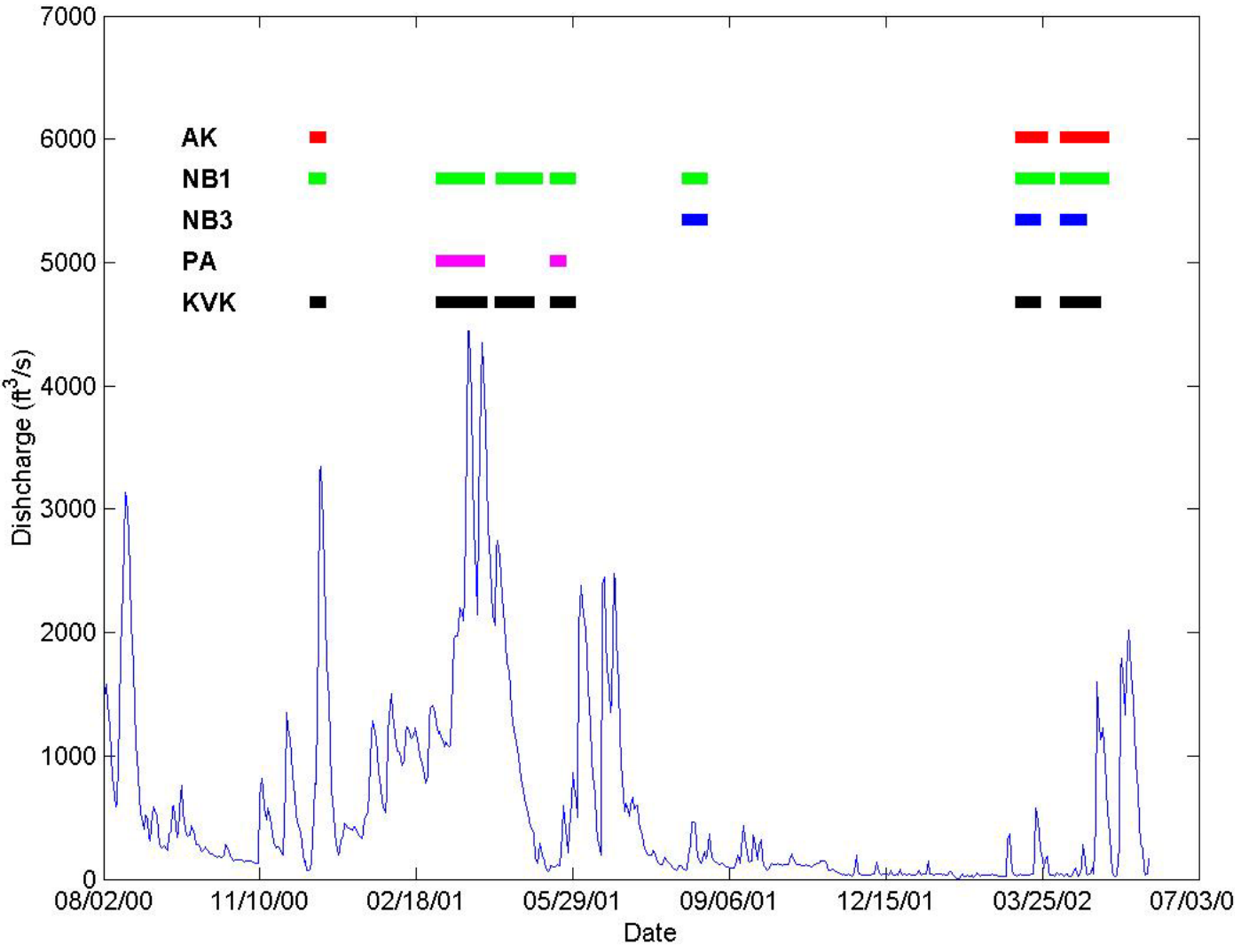


Figure 4 Passaic River discharge (in cubic feet per second) and with timing of mooring deployments (color bars).

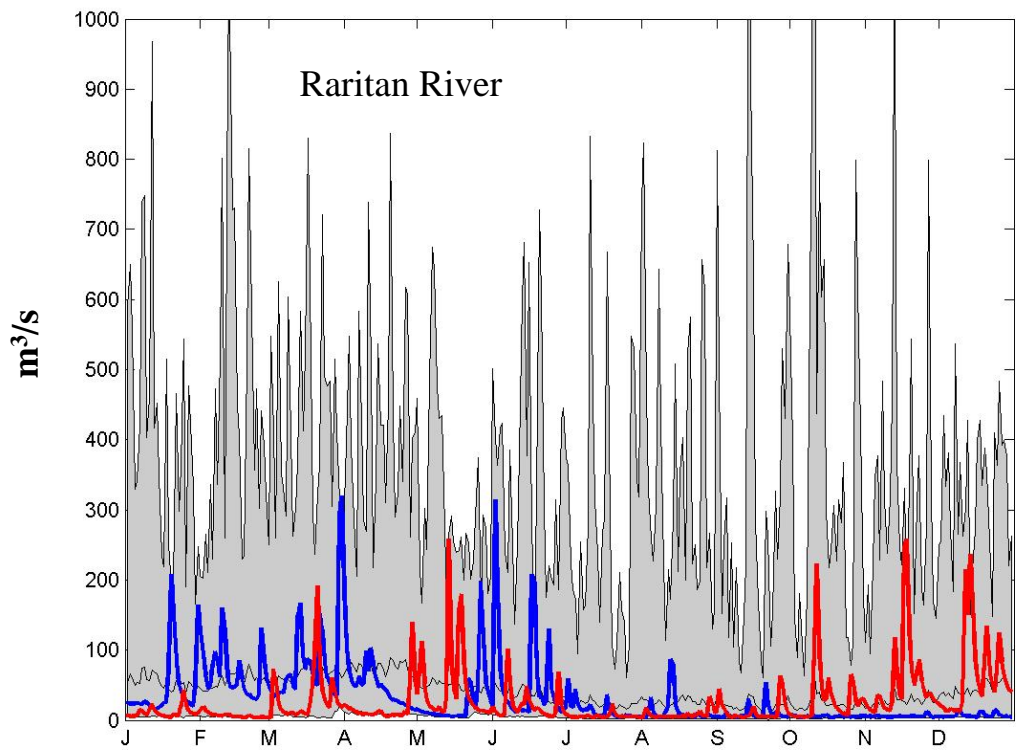
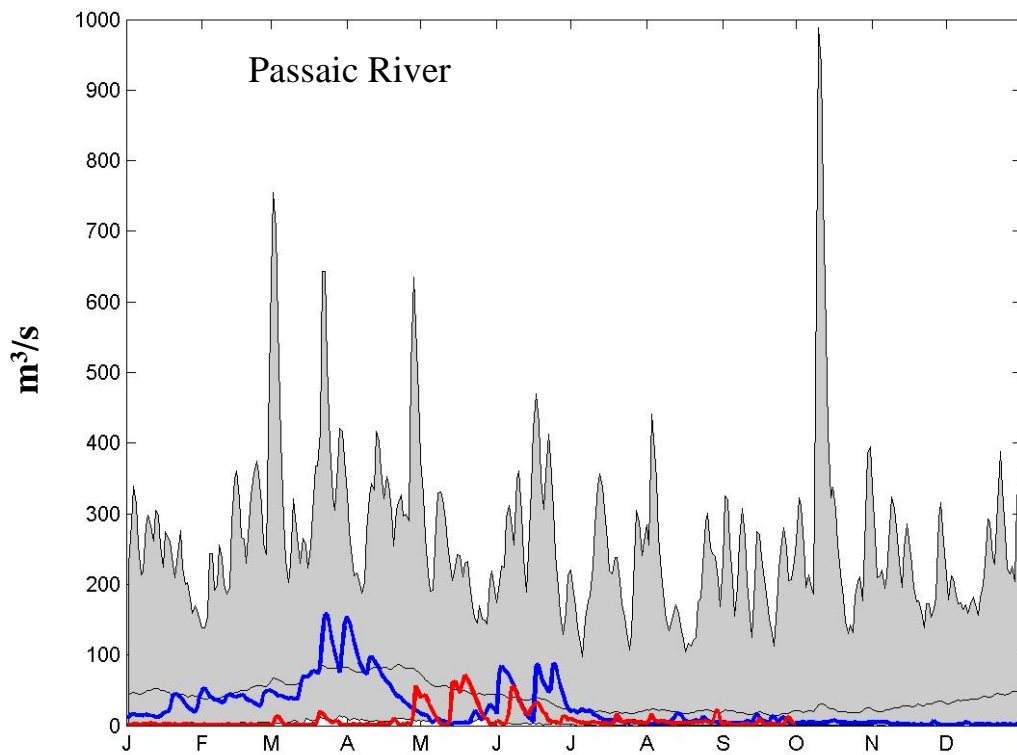


Figure 5 Discharge for the Passaic (upper panel) and Raritan (lower panel) rivers. Grey envelop shows daily record discharge for the entire record available from the USGS web site. Black line shows daily mean based on this record. Blue line shows discharge for 2001 and red line shows discharge for 2002.

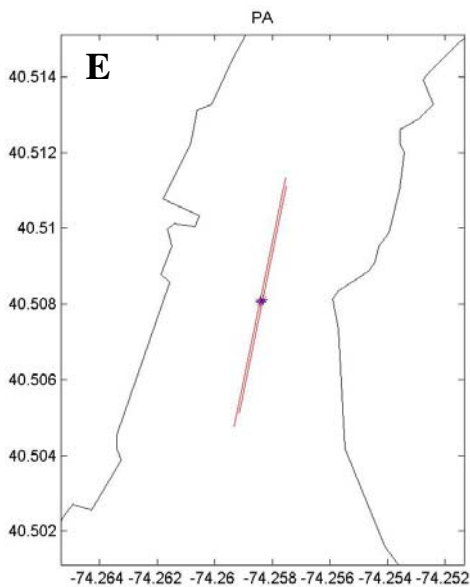
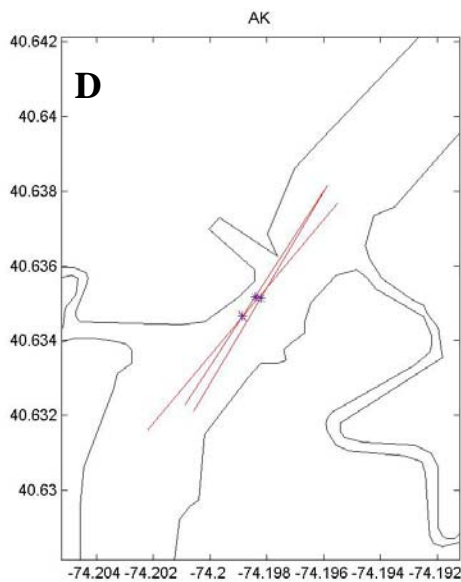
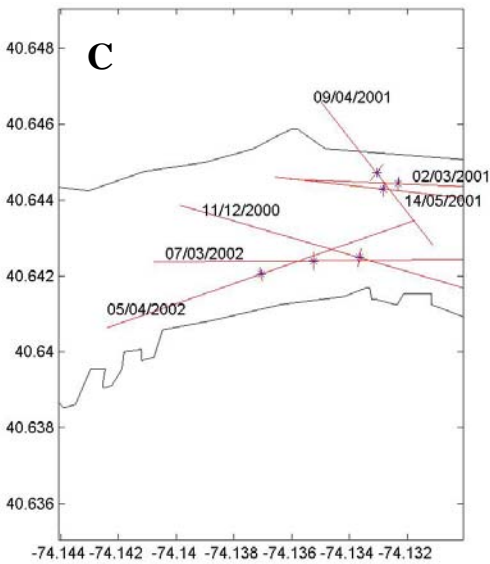
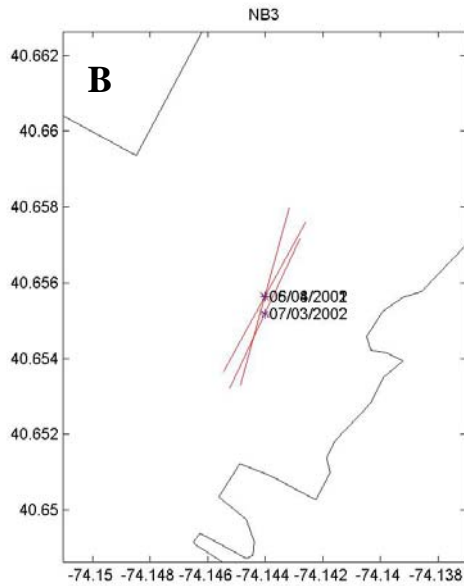
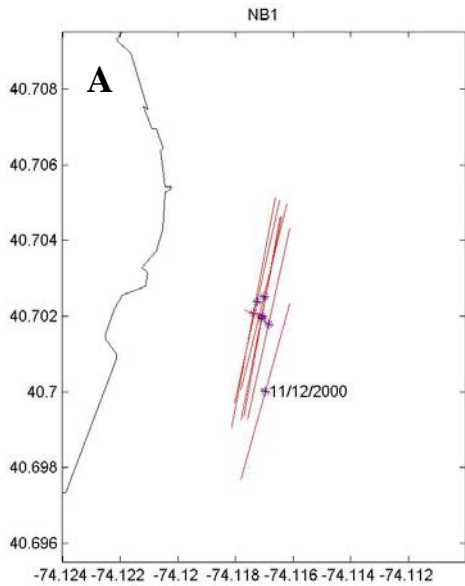


Figure 6 Semidiurnal (M2) tidal ellipse for each mooring deployment at stations a) NB1, b) NB3, c) KVK, d) AK1, e) PA1. The magnitude of the ellipse can be inferred from Table 2

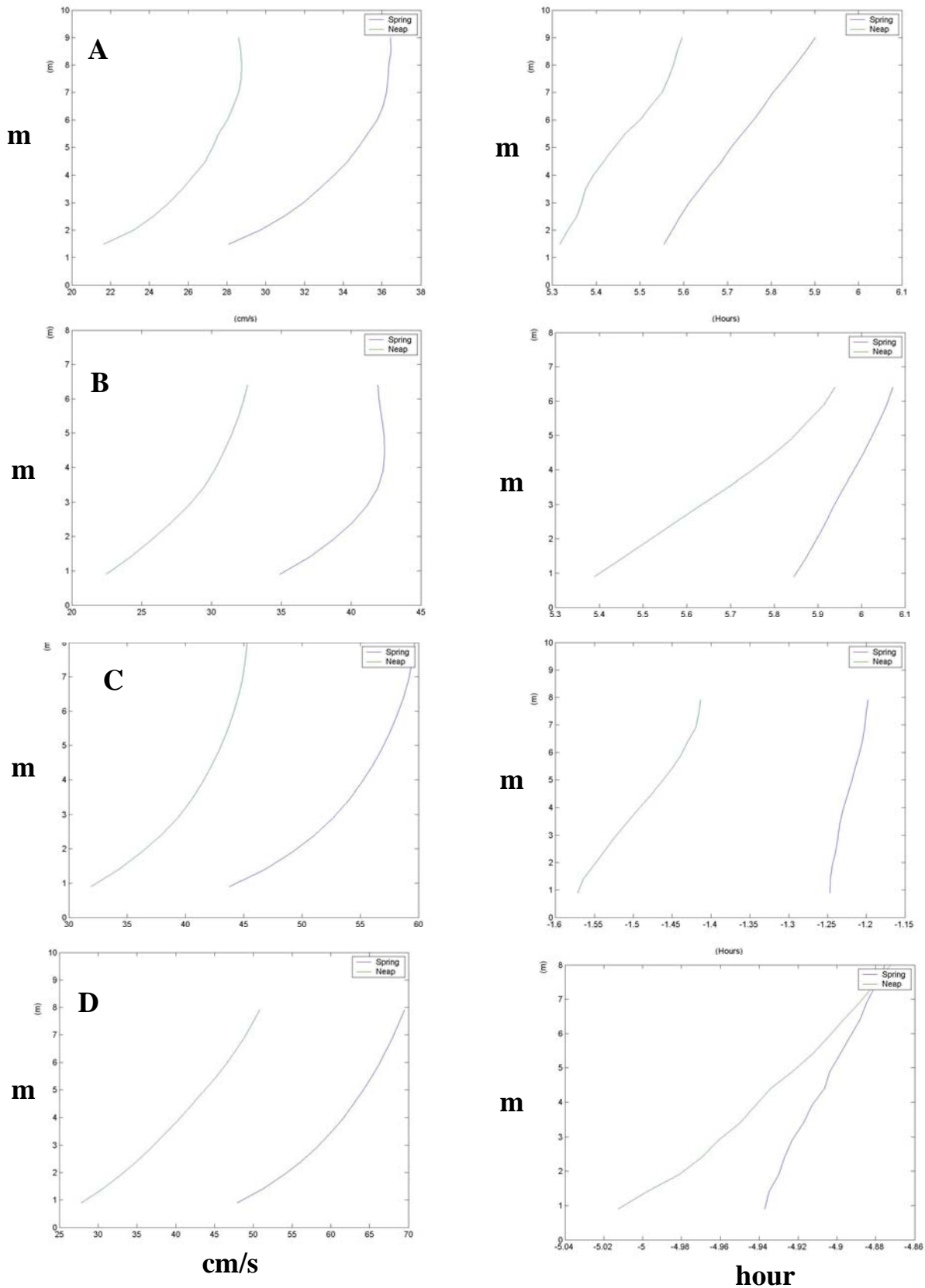


Figure 7 Vertical structure of the semidiurnal tidal (M2) motion at each mooring location. Left panels show tidal current speed, right panel shows tidal current phase during neap tide and spring tide conditions. Depth is in meters above the bottom. Station A) NB1, B) NB3, C) KVK1 D) AK1 E) PA1

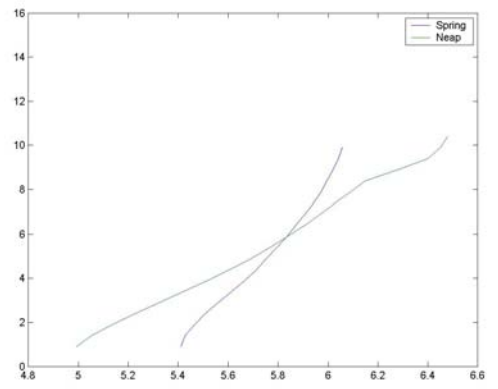
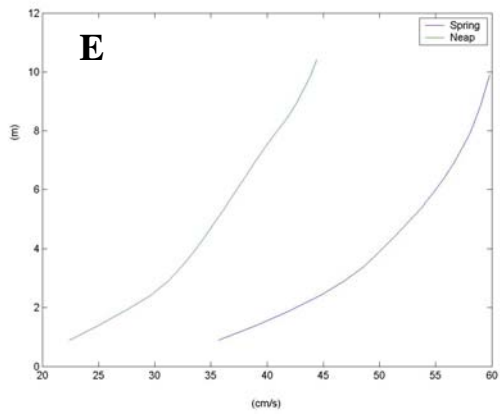


Figure 7 Continued

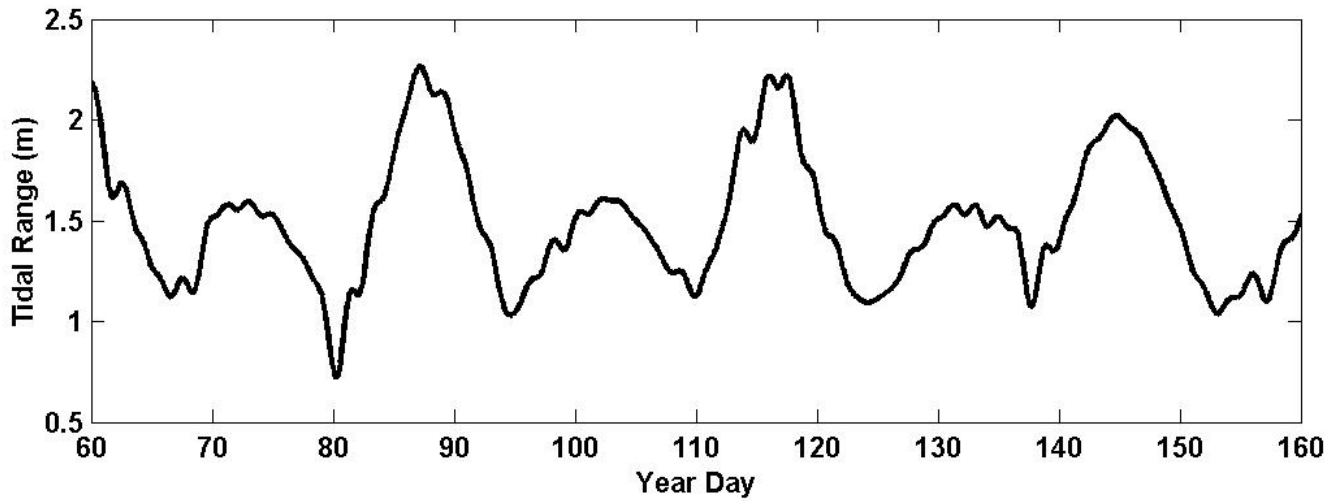
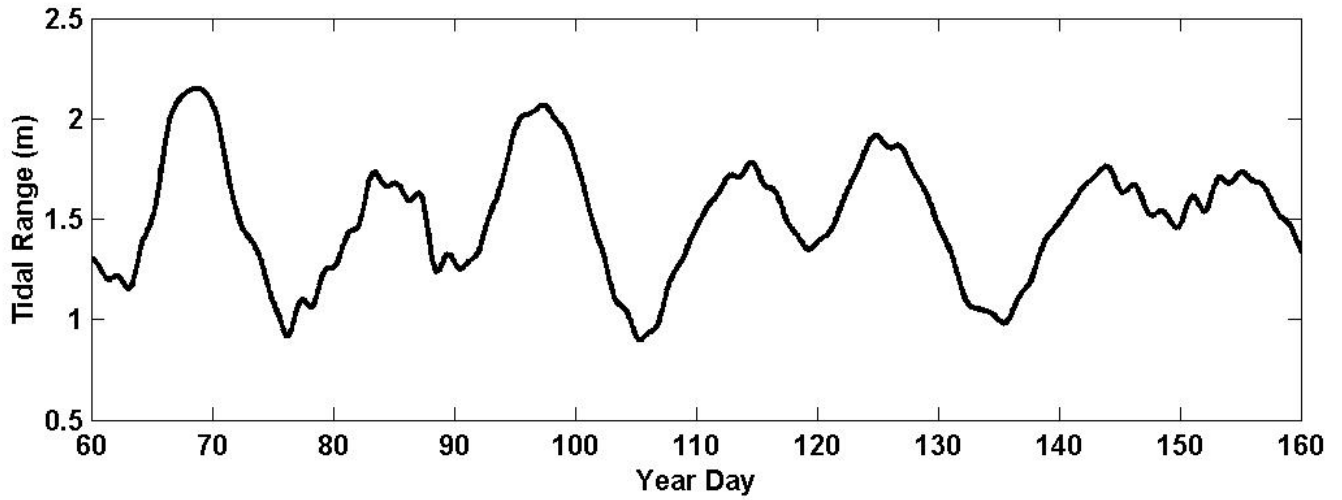


Figure 8 Tidal range at Bergen Point during mooring deployments for 2001(upper panel) and 2002 (lower panel).

**Crosses show locations
of CTD casts taken during
ebbing tides on March 14,
2001.**

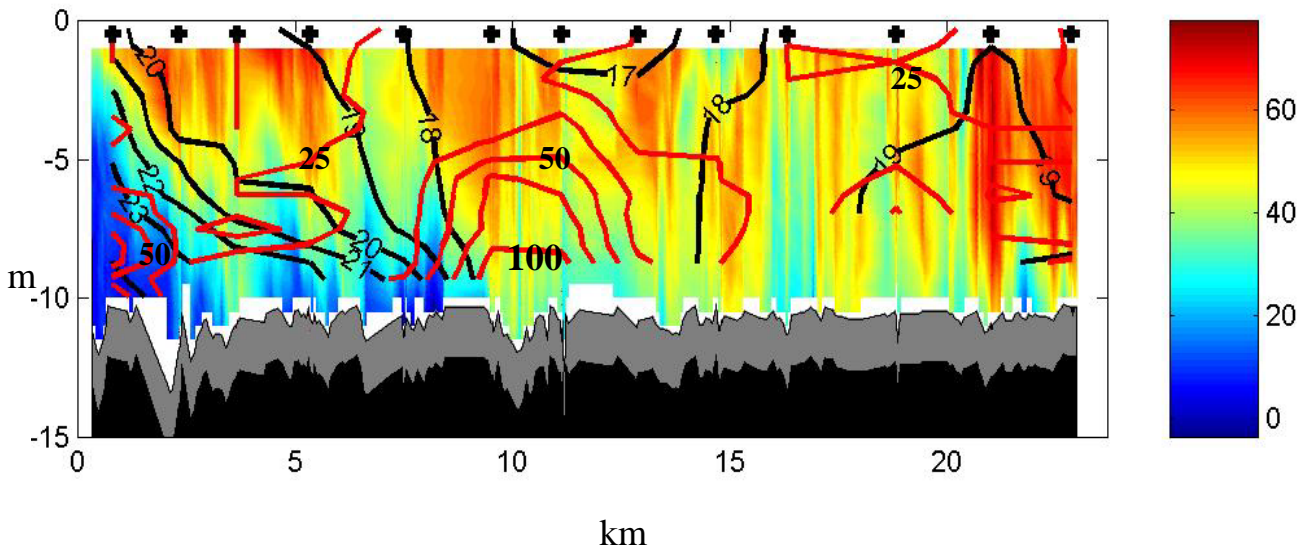
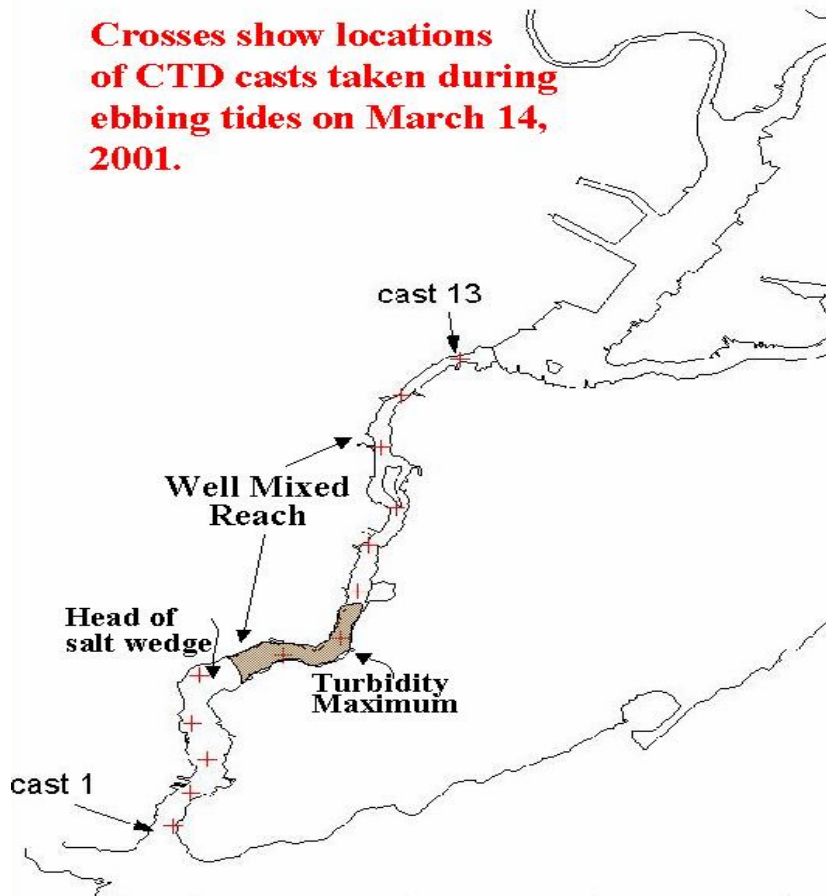


Figure 9. Upper panel. Crosses show locations of CTD casts. Grey area shows location of turbidity maximum. Lower panel. CTD/ADCP section from Perth Amboy to Newark Bay. Colors show along channel velocity during the ebb. Red is flow towards Raritan Bay. Black Contours show Salinity. Note that ebb velocities are reduced behind salt front defined by 20 psu isohaline. Red contours show OBS derived TSS estimates (mg/l).

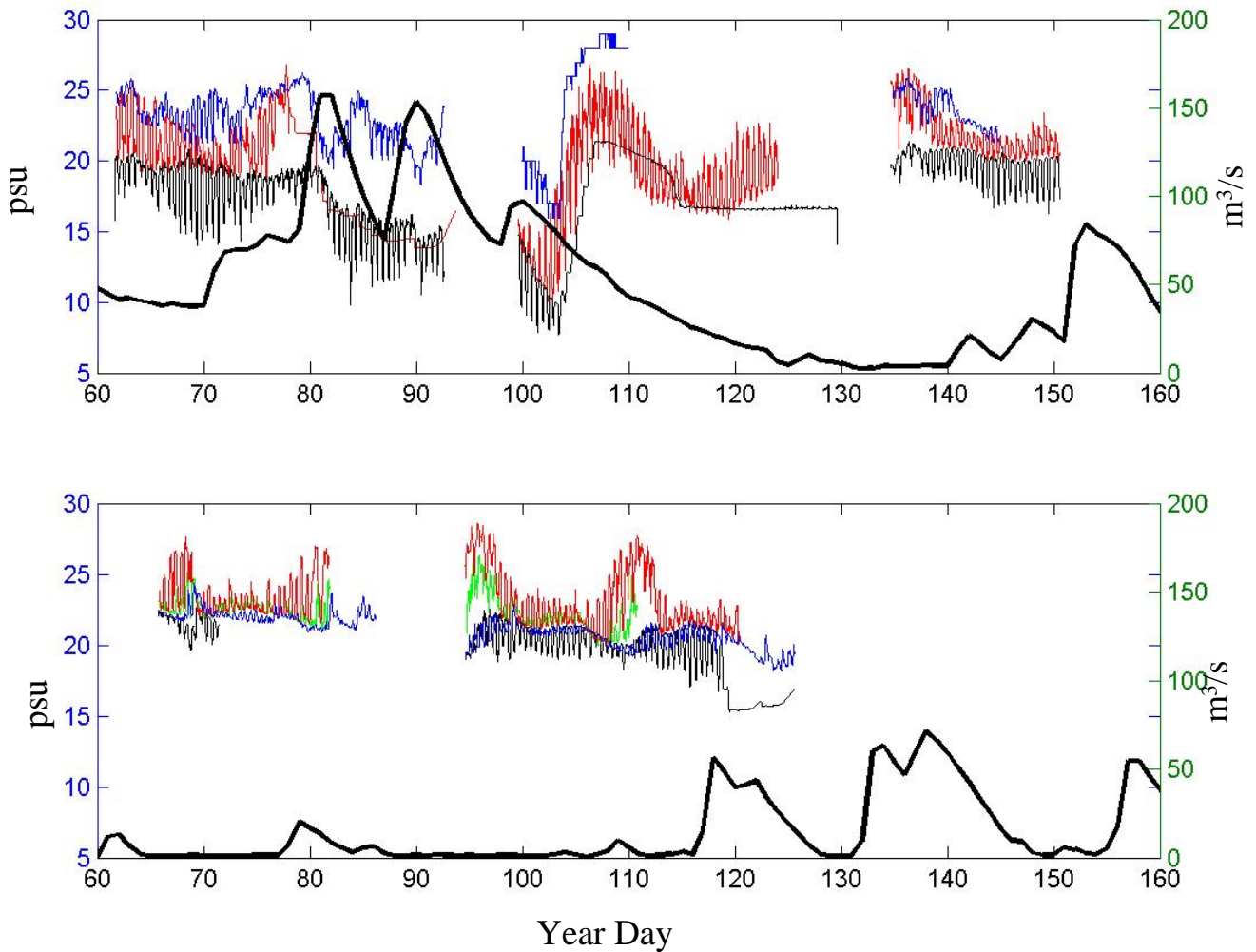


Figure 10 Near-bottom salinity at each mooring location and Passaic River discharge during 2001 (upper panel) and 2002 (lower panel) Thick black line is the Passaic River discharge. In upper panel, thin black line is salinity at NB1, red line is salinity at KVK1, and blue is salinity at PA1. In lower panel, black line is NB1, red KVK1, green NB3, and blue AK1.

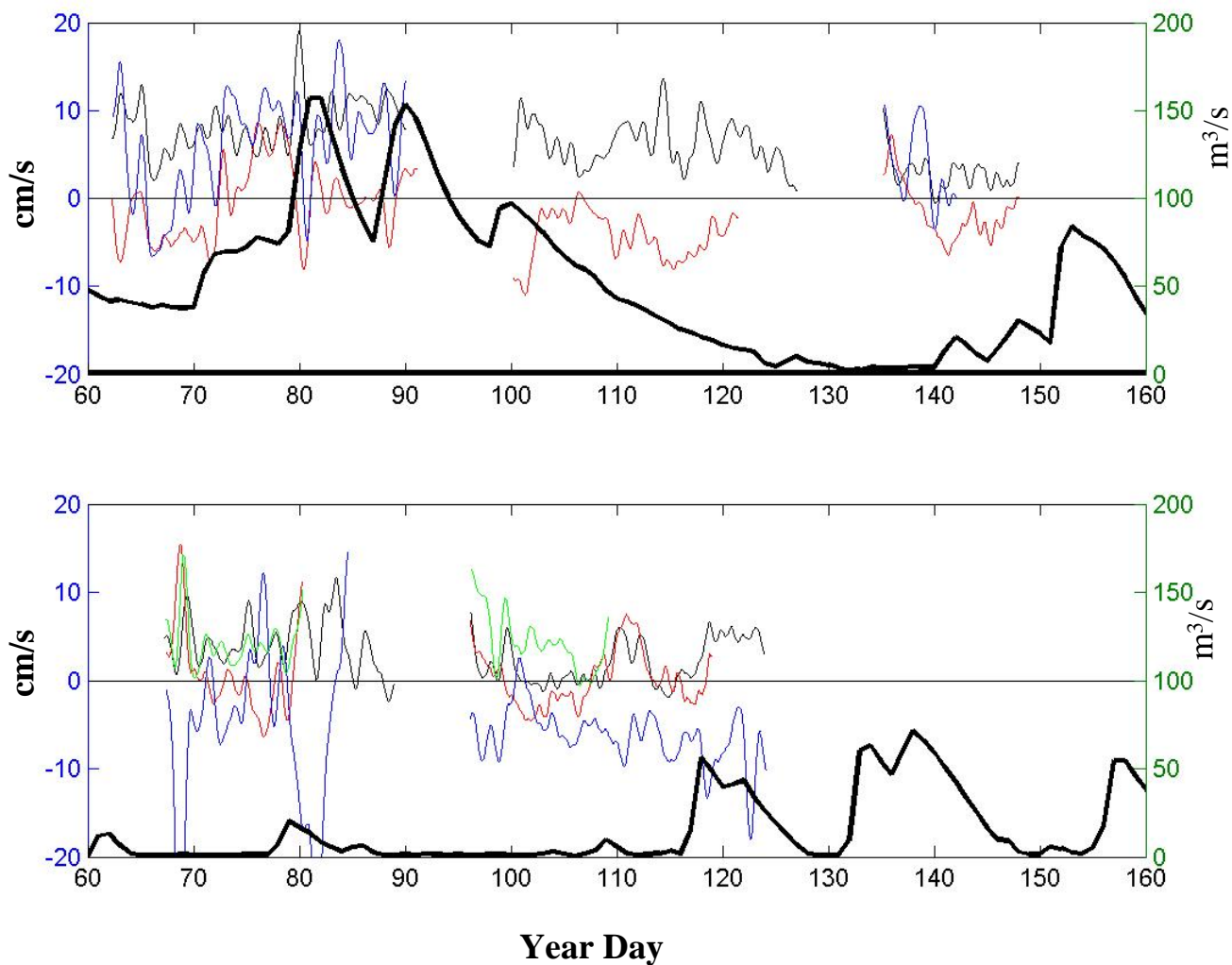


Figure 11 Near bottom sub-tidal currents at each mooring location and Passaic River discharge during 2001 (upper panel) and 2002 (lower panel). Thick black line is Passaic River discharge. In upper panel thin black line is current at station NB1, KVK1 (red) and PA1 (blue). In the lower panel black line is current at NB1, KVK1 (red), NB3 (green) and AK1 (Blue).

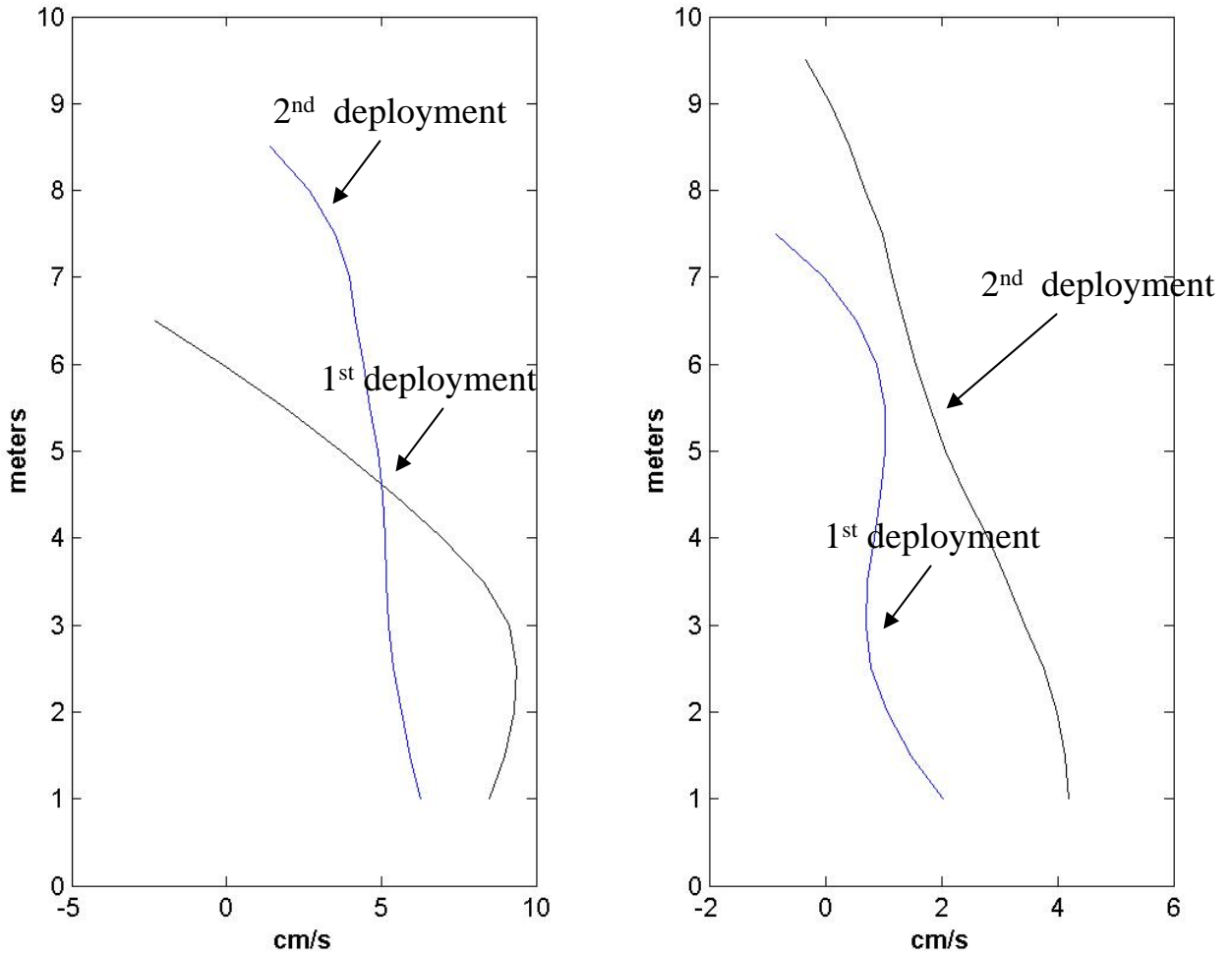


Figure 12 Depth dependent mean flow at station NB1 for 2001 (left panel) and 2002 (right panel). In both panels the black line is for the first deployment and the blue line is for the second deployment. Depth is in meters above the bottom. Upstream velocities are positive.

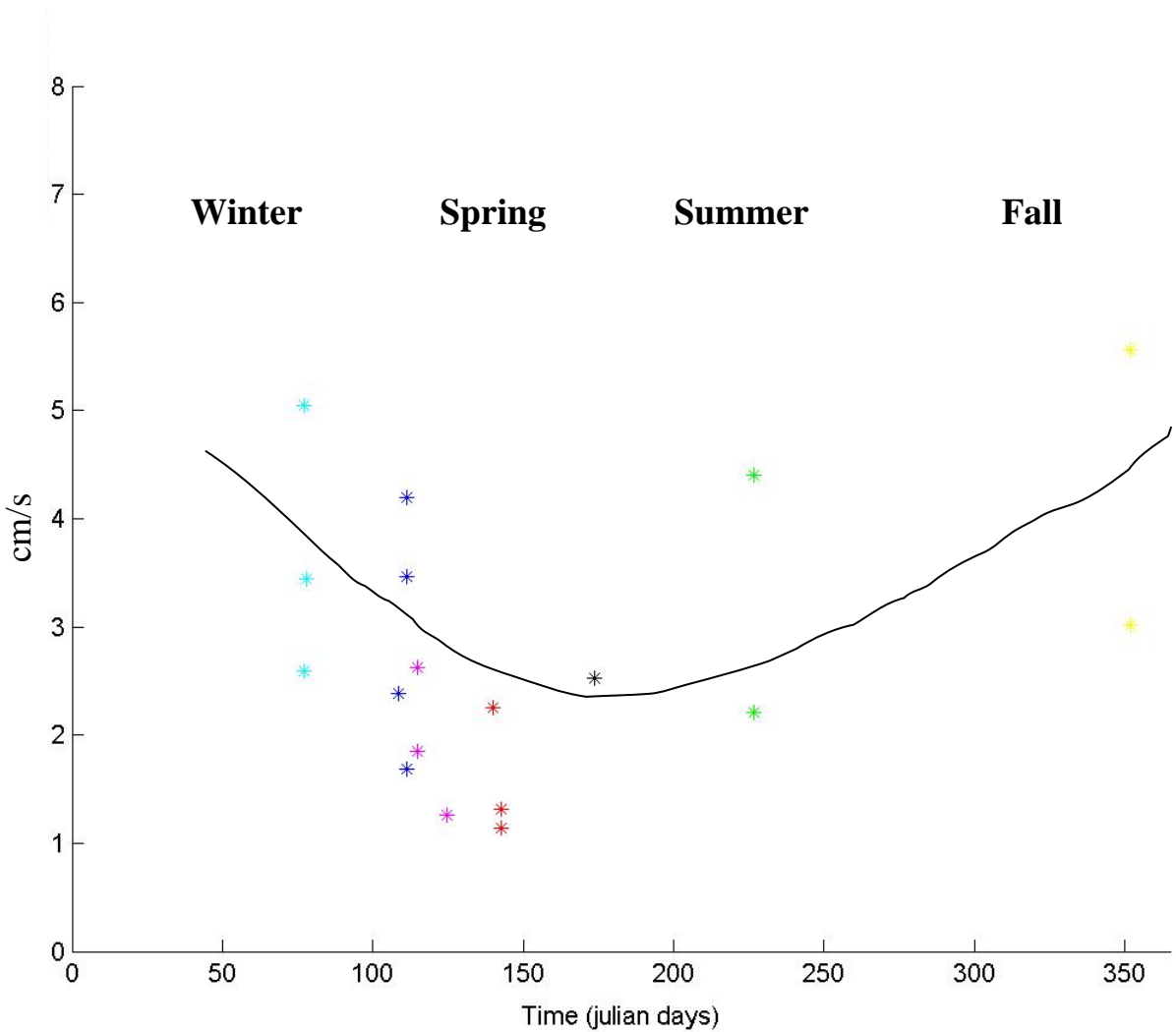


Figure 13 Root mean square (rms) of subtidal velocity for all mooring deployments as a function of season. Black curve depicts seasonal trend showing weaker subtidal rms velocity during summer months relative to winter and Fall.

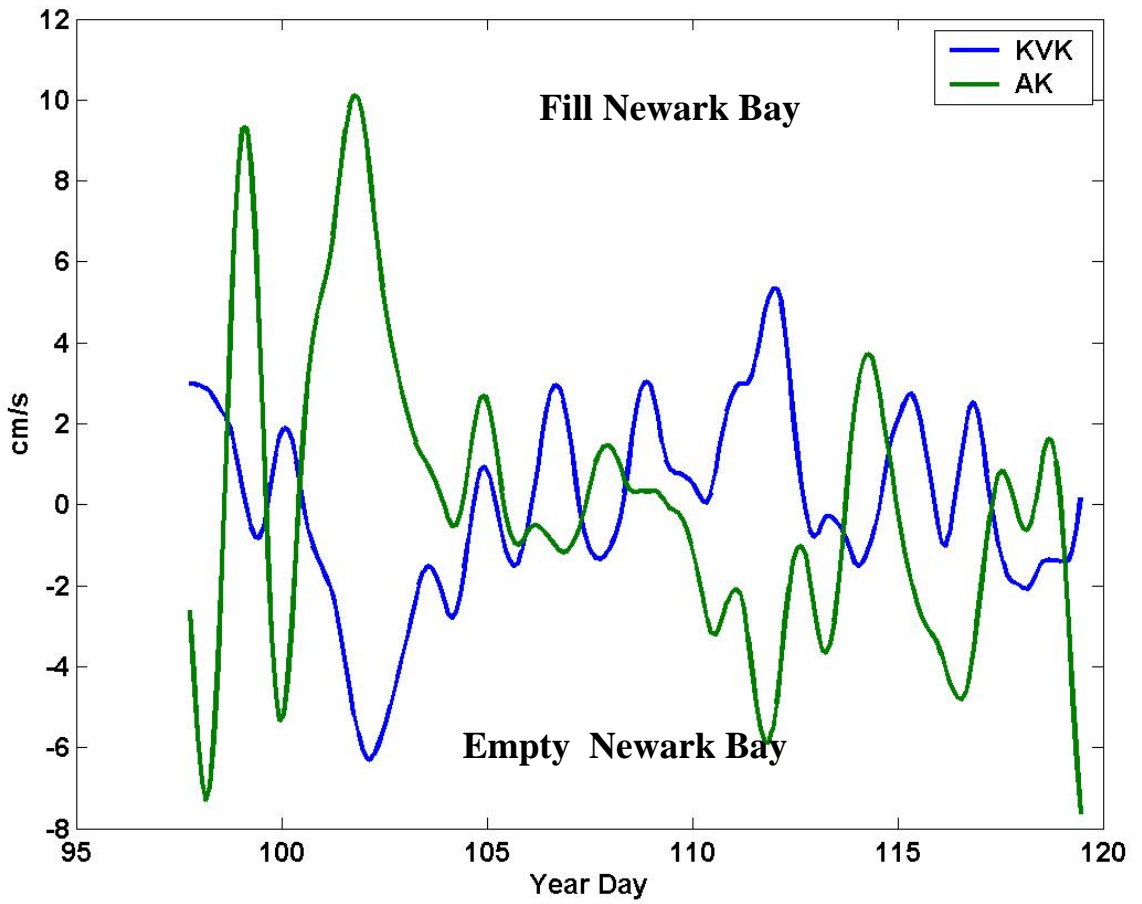


Figure 14a Depth averaged currents at stations KVK and AK1 in 2002.



Figure 14b. Depiction of depth averaged currents (red arrows) in response to a north-westerly wind (large green arrow).

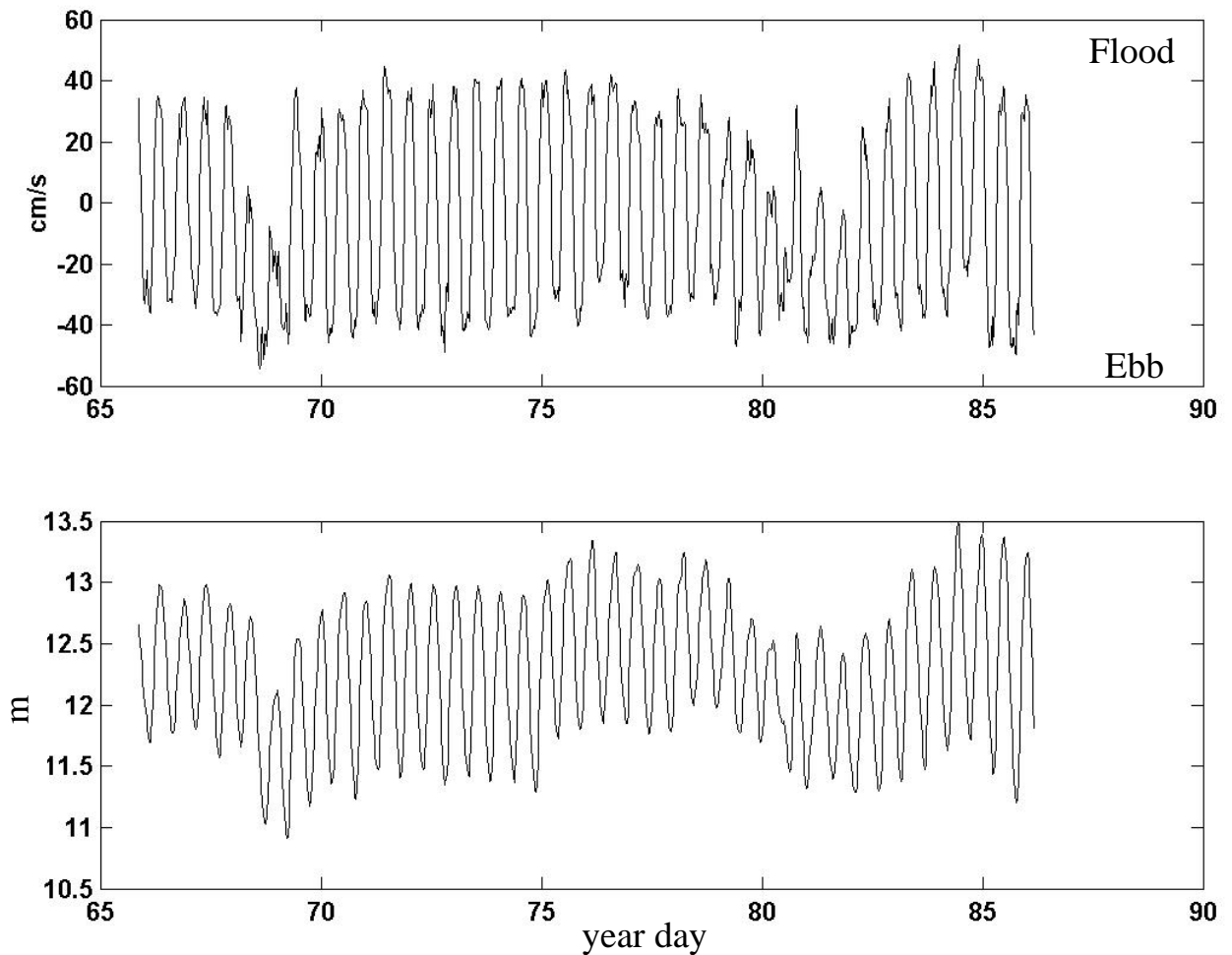


Figure 15 Along channel currents (upper panel) and pressure (lower panel) at station AK in 2002. Flooding currents are positive. Note that during sea-level set down on days 68 and 82 currents at station AK1 never flood.

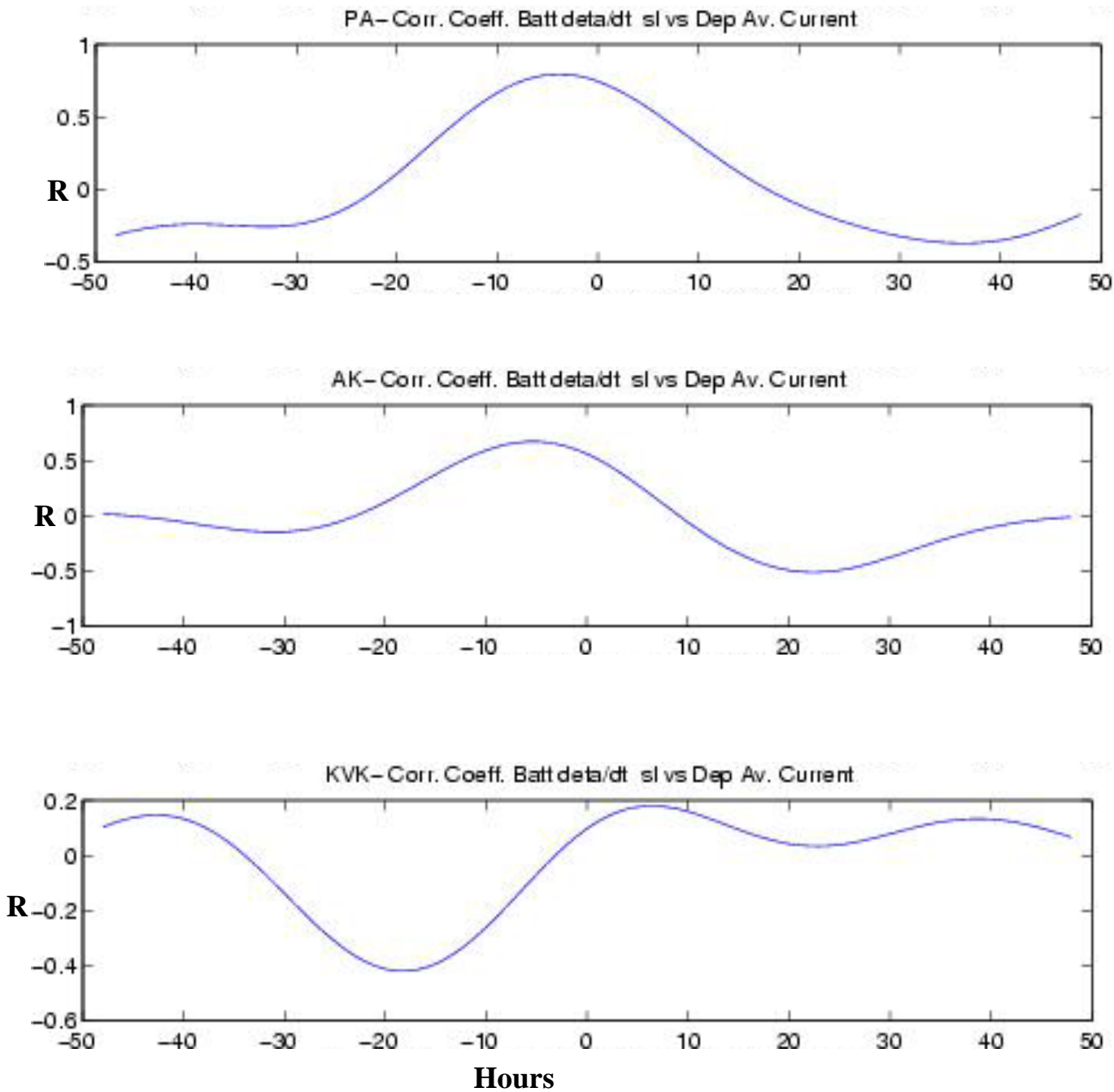


Figure 16 Time lagged correlation between the time rate of change of subtidal sealevel at Sandy Hook ($\partial\eta/\partial t$) and low frequency depth averaged flow at station PA1 (upper panel), AK1 (middle panel), and KVK (lower panel).

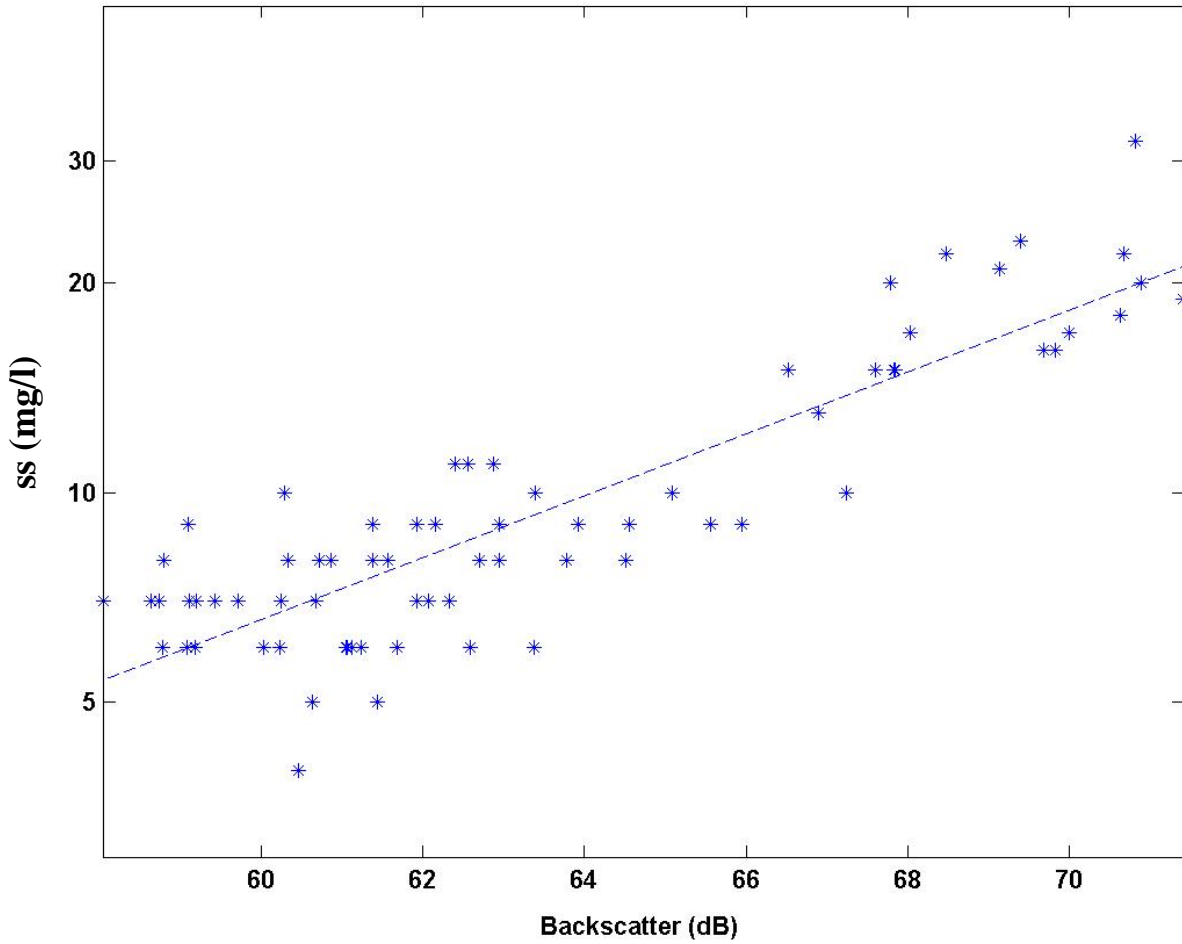


Figure 17 Scatter plot between measured SS and acoustic backscatter from the Sontek ADP; October 29, 2003 calibration experiment.

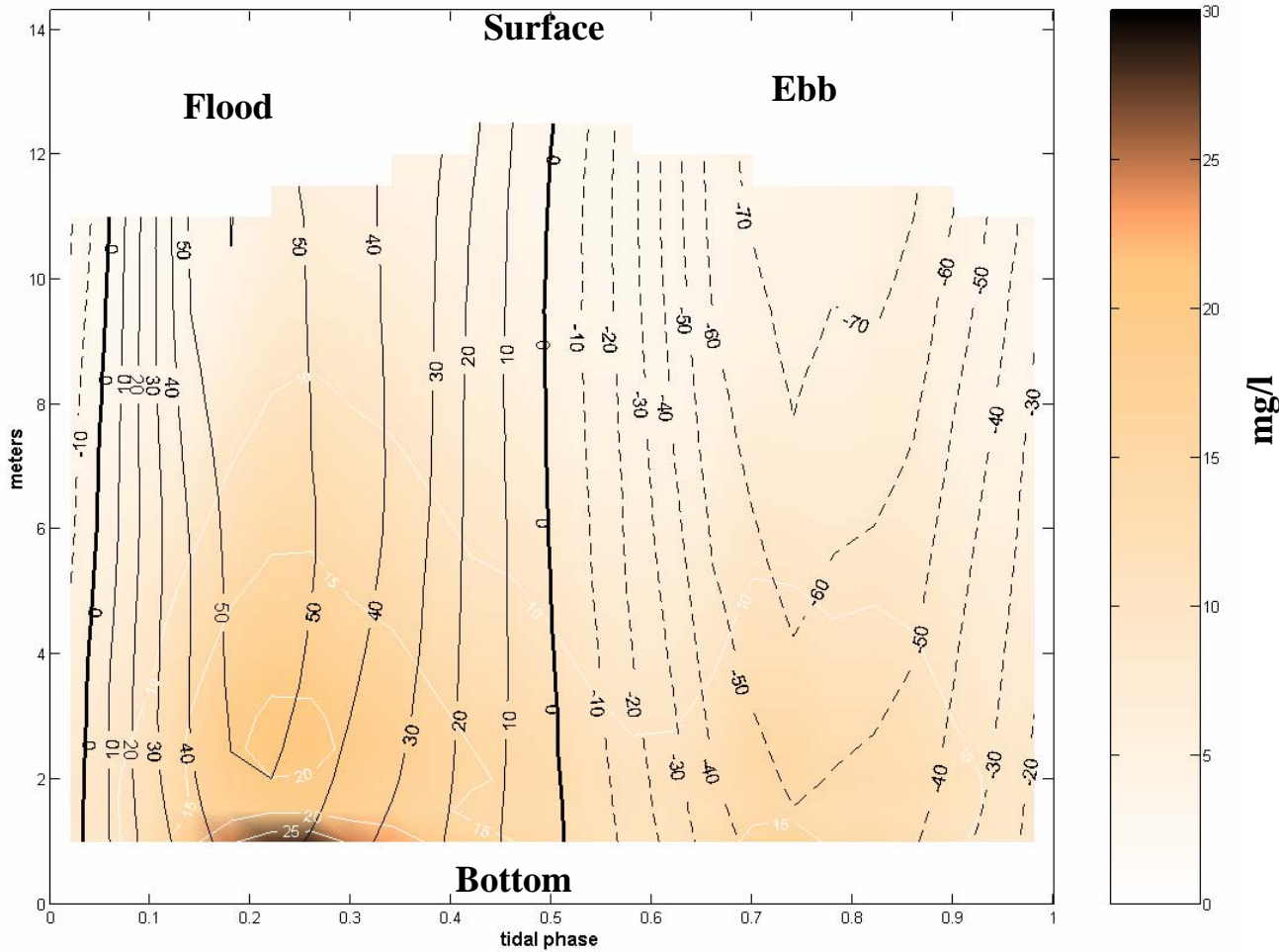


Figure 18 Current speed (black contours) and suspended sediment concentration (brown color and white contours, in mg/l) during spring tide conditions at station KVK during deployment 2 in 2002. Note higher SS values during the flood tide.

Table 1: Mooring location, time of deployment, and mean depths

| Site Name | Deployed | Recovered | Latitude | Longitude | Depth (m) |
|-----------|------------|------------|----------|-----------|-----------|
| NB1 | 12/11/2000 | 12/21/2001 | 40.7000 | 74.117 | 10.5 |
| NB1 | 03/02/2001 | 04/02/2001 | 40.7018 | 74.1168 | 9.07 |
| NB1 | 04/09/2001 | 05/09/2001 | 40.7019 | 74.1171 | 11.5 |
| NB1 | 05/14/2001 | 05/30/2001 | 40.7020 | 74.1171 | 10.2 |
| NB1 | 08/06/2001 | 08/22/2001 | 40.7021 | 74.1145 | 12.0 |
| NB1 | 09/27/2001 | 10/05/2001 | 40.7021 | 74.1145 | 11.0 |
| NB1 | 10/12/2001 | 10/30/2001 | 40.7021 | 74.1145 | 11.5 |
| NB1 | 11/02/2001 | 11/19/2001 | 40.7021 | 74.1145 | 11 |
| NB1 | 03/07/2002 | 04/01/2002 | 40.7024 | 74.1172 | 12.5 |
| NB1 | 04/05/2002 | 05/06/2002 | 40.7025 | 74.1170 | 10.1 |
| NB3 | 08/06/2001 | 08/22/2001 | 40.6556 | 74.1440 | 12.3 |
| NB3 | 03/07/2002 | 03/23/2002 | 40.6552 | 74.1440 | 13.4 |
| NB3 | 04/05/2002 | 04/21/2002 | 40.6556 | 74.1440 | 13.3 |
| KVK | 12/11/2000 | 12/21/2000 | 40.6425 | 74.1337 | 14.8 |
| KVK | 03/02/2001 | 04/03/2001 | 40.6444 | 74.1323 | 14.3 |
| KVK | 04/09/2001 | 05/03/2001 | 40.6447 | 74.1331 | 10.6 |
| KVK | 05/14/2001 | 05/30/2001 | 40.6433 | 74.1328 | 13.4 |
| KVK | 03/07/2002 | 03/23/2002 | 40.6424 | 74.1352 | 15.0 |
| KVK | 04/05/2002 | 05/01/2002 | 40.6420 | 74.1371 | 15.6 |
| AK | 12/11/2000 | 12/21/2000 | 40.6347 | 74.1988 | 12.5 |
| AK | 03/02/2001 | 04/02/2001 | 40.6347 | 74.1988 | 12 |
| AK | 04/09/2001 | 05/09/2001 | 40.6347 | 74.1988 | 12 |
| AK | 05/14/2001 | 05/24/2001 | 40.6347 | 74.1988 | 12 |
| AK | 09/29/2001 | 10/03/2001 | 40.6347 | 74.1988 | 12 |
| AK | 11/02/2001 | 11/19/2001 | 40.6347 | 74.1988 | 12 |
| AK | 04/08/2001 | 05/09/2001 | 40.6347 | 74.1988 | 12 |
| AK | 03/07/2002 | 03/28/2002 | 40.6352 | 74.1984 | 12.3 |
| AK | 04/05/2002 | 05/06/2002 | 40.6351 | 74.1982 | 12.7 |
| PA | 03/02/2001 | 04/02/2001 | 40.5080 | 74.2584 | 13.4 |
| PA | 05/14/2004 | 05/25/2005 | 40.5081 | 74.2583 | 13.3 |

Table 2: Calculated Tidal Constituents at the mooring location

Major Tidal Constituents NB1 (Current)

| | K1 | M2 | M4 | M6 |
|-------------|--------|---------|--------|-------|
| Major(cm/s) | 1.97 | 34.93 | 3.07 | 2.99 |
| Minor(cm/s) | 0.05 | -0.20 | -0.15 | 0.07 |
| Phase(hrs) | -3.2 | -0.31 | 0.25 | 0.62 |
| Oren(deg) | -104.5 | -106.12 | -95.53 | 76.22 |

Major Tidal Constituents NB1 (Sea Level)

| | K1 | M2 | M4 | M6 |
|--------------|-------|-------|-------|-------|
| Magnitude(m) | 0.08 | 0.75 | 0.036 | 0.026 |
| Phase(hrs) | -9.52 | -4.04 | 0.23 | 1.344 |

Major Tidal Constituents KVK1 (Current)

| | K1 | M2 | M4 | M6 |
|-------------|-------|-------|--------|--------|
| Major(cm/s) | 3.58 | 52.22 | 2.90 | 4.15 |
| Minor(cm/s) | 0.19 | 1.58 | 0.08 | 0.55 |
| Phase(m) | -4.08 | -1.29 | 0.740 | 0.01 |
| Oren(deg) | -3.33 | -3.37 | -12.58 | 176.72 |

Major Tidal Constituents KVK1 (Sea Level)

| | K1 | M2 | M4 | M6 |
|--------------|--------|-------|-------|-------|
| Magnitude(m) | 0.095 | 0.691 | 0.032 | 0.017 |
| Phase(hrs) | -9.447 | -4.27 | 0.349 | 0.991 |

Table 2: Tidal Constituents (continued)**Major Tidal Constituents PA1 (Current)**

| | K1 | M2 | M4 | M6 |
|-------------|---------|---------|---------|-------|
| Major(cm/s) | 2.81 | 42.88 | 1.17 | 2.60 |
| Minor(cm/s) | -0.05 | -0.57 | -0.04 | -0.09 |
| Phase(hrs) | -2.90 | -0.44 | 0.21 | 0.22 |
| Oren(deg) | -105.33 | -105.28 | -105.20 | 70.84 |

Major Tidal Constituents PA1 (Sea Level)

| | K1 | M2 | M4 | M6 |
|-------------------|--------|-------|-------|------|
| Magnitude(m) 0.08 | | 0.71 | 0.021 | 0.02 |
| Phase(hrs) | -10.37 | -4.73 | -0.33 | 0.37 |

Major Tidal Constituents AK1 (Current)

| | | | | |
|-------------|--------|-------|--------|------|
| Major(cm/s) | 1.82 | 48.29 | 1.95 | 4.98 |
| Minor(cm/s) | -0.04 | 0.39 | 0.01 | 0.15 |
| Phase(hrs) | 0.09 | -4.88 | 1.59 | 1.26 |
| Oren(deg) | 177.18 | 0.10 | -13.19 | 1.03 |

Major Tidal Constituents AK1 (Sea Level)

| | K1 | M2 | M4 | M6 |
|-------------------|-------|-------|------|------|
| Magnitude(m) 0.08 | | 0.71 | 0.03 | 0.02 |
| Phase(hrs) | -8.54 | -4.00 | 0.38 | 1.19 |